AD_____

Award Number: W81XWH-08-1-0415

TITLE: Prostate-Specific Membrane Antigen Regulation of Prostate Tumor Growth, Angiogenesis, and Integrin Signal Transduction

PRINCIPAL INVESTIGATOR: Dr. Linda Shapiro

CONTRACTING ORGANIZATION: University of Connecticut, Farmington, CT 06032

REPORT DATE: July 2012

TYPE OF REPORT: Final

PREPARED FOR: U.S. Army Medical Research and Materiel Command
Fort Detrick, Maryland 21702-5012

DISTRIBUTION STATEMENT: Approved for public release; distribution unlimited

The views, opinions and/or findings contained in this report are those of the author(s) and should not be construed as an official Department of the Army position, policy or decision unless so designated by other documentation.

REPORT DOCUMENTATION PAGE

Form Approved
OMB No. 0704-0188

Public reporting burden for this collection of information is estimated to average 1 hour per response, including the time for reviewing instructions, searching existing data sources, gathering and maintaining the data needed, and completing and reviewing this collection of information. Send comments regarding this burden estimate or any other aspect of this collection of information, including suggestions for reducing this burden to Department of Defense, Washington Headquarters Services, Directorate for Information Operations and Reports (0704-0188), 1215 Jefferson Davis Highway, Suite 1204, Arlington, VA 22202-4302. Respondents should be aware that notwithstanding any other provision of law, no person shall be subject to any penalty for failing to comply with a collection of information if it does not display a currently valid OMB control number. **PLEASE DO NOT RETURN YOUR FORM TO THE ABOVE ADDRESS.**

1. REPORT DATE *(DD-MM-YYYY)*	2. REPORT TYPE	3. DATES COVERED *(From - To)*
01-07-2012	Final	15 JUN 2008-14 JUN 2012

4. TITLE AND SUBTITLE

Prostate-Specific Membrane Antigen Regulation of Prostate Tumor Growth, Angiogenesis,and Integrin Signal Transduction

5a. CONTRACT NUMBER

5b. GRANT NUMBER

W81XWH-08-1-0415

5c. PROGRAM ELEMENT NUMBER

6. AUTHOR(S)

Dr. Linda Shapiro

E-Mail: lshapiro@neuron.uchc.edu

5d. PROJECT NUMBER

5e. TASK NUMBER

5f. WORK UNIT NUMBER

7. PERFORMING ORGANIZATION NAME(S) AND ADDRESS(ES)

University of Connecticut
Farmington, CT 06032

8. PERFORMING ORGANIZATION REPORT NUMBER

9. SPONSORING / MONITORING AGENCY NAME(S) AND ADDRESS(ES)

U.S. Army Medical Research and Materiel Command
Fort Detrick, Maryland 21702-5012

10. SPONSOR/MONITOR'S ACRONYM(S)

11. SPONSOR/MONITOR'S REPORT NUMBER(S)

12. DISTRIBUTION / AVAILABILITY STATEMENT

Approved for Public Release; Distribution Unlimited

13. SUPPLEMENTARY NOTES

14. ABSTRACT

PSMA has been shown to be significantly and universally up-regulated on the vasculature of solid tumors, while it is absent in normal, quiescent vessels suggesting it may play a role in pathologic angiogenesis. Inhibiting the enzymatic activity of PSMA leads to a decrease in endothelial cell adhesion, invasion and migration in vitro, processes which are necessary for angiogenesis. Taken together, these findings suggest that PSMA may play a role in angiogenesis in vivo. We examined tumor initiation, growth and metastasis in a transgenic model of tumor progression in wild-type and PSMA-null animals. We also investigated the relative contribution of tumor vs. endothelial PSMA expression using PSMA positive tumor allografts into wild type or PSMA null mice, and show that PSMA expression on endothelial cells is necessary for tumor angiogenesis. We also showed that PSMA contribution to pathologic angiogenesis was not restricted to tumor angiogenesis, using a mouse model of retinopathy of prematurity to show that PSMA function changes outcome in this model. Understanding the contribution of PSMA to angiogenesis progression will further understanding of diseases involving pathologic blood vessel growth. Better understanding of the molecules regulating this process may lead to new therapies for tumor metastasis and for diseases involving detrimental angiogenesis.

15. SUBJECT TERMS

Prostate cancer, tumor angiogenesis, macular degeneration, retinopathy, endothelial

16. SECURITY CLASSIFICATION OF:			17. LIMITATION OF ABSTRACT	18. NUMBER OF PAGES	19a. NAME OF RESPONSIBLE PERSON
a. REPORT	b. ABSTRACT	c. THIS PAGE			USAMRMC
U	U	U	UU	75	19b. TELEPHONE NUMBER *(include area code)*

Table of Contents

	Page
Introduction…….……..	**4**
Body……..	**4**
Key Research Accomplishments…….……..	**59**
Reportable Outcomes…….	**60**
Conclusion…….	**61**
References…….	**61**
Appendices…….	**66**
Appendix 1- PLoS manuscript.	

INTRODUCTION

The Prostate Specific Membrane Antigen (PSMA) transmembrane peptidase is highly expressed on endothelial cells of tumor vasculature and on epithelial cells in advanced and metastatic prostate carcinoma where its expression correlates with tumor progression. While the expression pattern of PSMA makes it a potentially attractive target for therapeutic development, the precise function of PSMA in either tumor associated endothelium or prostate epithelial cells is not SMA has been shown to be significantly and universally up-regulated on the vasculature of solid tumors, while it is absent in normal, quiescent vessels suggesting it may play a role in pathologic angiogenesis. Inhibiting the enzymatic activity of PSMA leads to a decrease in endothelial cell adhesion, invasion and migration in vitro, processes which are necessary for angiogenesis. Taken together, these findings suggest that PSMA may play a role in angiogenesis in vivo. We examined tumor initiation, growth and metastasis in a transgenic model of tumor progression in wild-type and PSMA-null animals. We also investigated the relative contribution of tumor vs. endothelial PSMA expression using PSMA positive tumor allografts into wild type or PSMA null mice, and show that PSMA expression on endothelial cells is necessary for tumor angiogenesis. We also showed that PSMA contribution to pathologic angiogenesis was not restricted to tumor angiogenesis, using a mouse model of retinopathy of prematurity to show that PSMA function changes outcome in this model. Understanding the contribution of PSMA to angiogenesis progression will further understanding of diseases involving pathologic blood vessel growth. While angiogenesis occurs during normal development and in healing wounds, it is also involved in processes which involve the growth of new blood vessels, such as tumor growth and metastasis and the pathologic overgrowth of vessels into the eye which often results in blindness. Better understanding of the molecules regulating this process may lead to new therapies for tumor metastasis and for diseases involving detrimental angiogenesis.

BODY:

Experimental Design

Pathologic neovascularization plays a critical role in numerous human diseases including some forms of blindness, chronic inflammation, and cancer growth and metastasis. Expression of Prostate Specific Membrane Antigen (PSMA) is potently induced on the vasculature of virtually all solid tumors, and on advanced and metastatic prostate cancer, where its expression correlates with poor prognosis. Our published and preliminary studies indicate that PSMA is necessary for pathologic angiogenesis. PSMA has been identified as a potentially attractive therapeutic target; however, a clearer understanding of the molecular mechanisms by which it regulates prostate cancer progression and angiogenic processes would enable the enhancement of current PSMA-directed therapeutic strategies and facilitate the development of new approaches.

To investigate the hypothesis that PSMA functionally contributes to prostate cancer progression and metastasis, and that PSMA expression on endothelial cells is necessary for pathologic angiogenesis, we investigated the following Tasks:

Task 1: To determine the role of PSMA as a regulator of prostate cancer angiogenesis, progression and invasiveness (months 1-24)

- **a)** Breed and accumulate age matched cohorts of TRAMP x wt and TRAMP x PSMA null mice
- **b)** Monitor tumor parameters such as vascularity, incidence, volume, grade, invasiveness
- **c)** Breed and accumulate age matched TRAMP wt mice
- **d)** Treat with GPI 5630 starting at 8 weeks and monitor tumor parameters at 18 and 30 weeks

e) Assess tumor size, vascularity, necrosis, proliferation, apoptosis and relative hypoxia in PSMA expressing tumors from wild type vs. PSMA null animals.
f) Confirm that PSMA is a universal (as opposed to tumor specific) regulator of angiogenesis by assessing the effect of lack of PSMA in a non-tumor model of retinopathy.

Task 2: Analyze candidate PSMA substrates- individual peptides (months 12-36)
a) Synthesize candidate peptides
b) Test candidate peptides for ability to be cleaved by PSMA
c) Test candidate peptides for effects on PSMA dependent adhesion- (+/- antagonist, null cells)
d) Test candidate peptides *in vitro* and *in vivo* for effects on PSMA dependent invasion (null cells *in vitro*, null mice *in vivo*)
e) Test candidate peptides for *in vivo* rescue of tumor angiogenesis
f) Verify that peptide is present in tumor lysates by Western blot analysis
g) Localize peptide in prostate tumors by histopathologic analysis

Task 3: Identify PSMA substrates in laminin 10 by proteomic analysis (months 18-36)
a) Physiologically digest recombinant laminin 10 with proteases present in intact cells
b) Isolate small mw peptide fraction- $\leq$ 3kD (YM-3) and assess adhesion capabilities
c) HPLC fractionate and test peptide fractions for PSMA dependent adhesion
d) Identify peptides in active fraction by mass spectrometer
e) Functionally test individual peptides for angiogenic activity as outlined in Task 2.

Task 1 a,b. To determine the role of PSMA as a regulator of prostate cancer angiogenesis, progression and invasiveness.

Task 1 a,b-1 Rationale.

Although PSMA expression has been shown to be significantly upregulated on advanced, metastatic prostate cancer compared to low grade prostate cancer and benign prostatic disease, its functional contribution to disease progression remains unknown. Expression of PSMA on metastatic disease, but not normal prostate tissue, makes it an attractive therapeutic target. For example, monoclonal antibodies conjugated to chemotherapeutic drugs and to radioisotopes are currently in clinical trial for advanced prostate cancer, and are showing some degree of success. While PSMA is a useful marker for targeting cancer, it is unknown whether PSMA expression contributes to prostate cancer advancement and spread, or if its up-regulation is a by-product of other cell processes involved in disease progression. For example, low grade carcinoma and benign prostate tissue are typically growth restricted by androgen availability. As prostate cancer progresses and loses androgen sensitivity, the cells can grow more quickly. PSMA expression is inversely correlated to androgen receptor expression and activity; therefore PSMA up-regulation may simply be a consequence of decreasing androgen sensitivity. The use of PSMA in human therapies makes a compelling case for further study of the role of PSMA in cancer development and progression.

In contrast to the notion that PSMA is a bystander in cell functions, PSMA has been shown to be functionally involved in signal transduction in endothelial cells and to contribute to cell adhesion to and invasion through the extracellular matrix, both processes necessary for successful neovascularization. Importantly, similar cell processes are required for both angiogenesis and cell metastasis. Our in vitro studies indicate a role for PSMA activity in prostate cancer cells in many cellular processes required for successful tumor cell metastasis, such as cell adhesion to and invasion through an extracellular matrix and anchorage independent cell growth in 3D culture. Therefore, it is reasonable that PSMA may also

directly enhance prostate cancer progression through functional involvement in cell processes necessary to metastasis.

To directly investigate the role of PSMA in prostate cancer progression, we have crossed PSMA null mice with a murine model of prostate cancer, the Transgenic Adenocarcinoma of the Mouse Prostate (TRAMP). While *in vitro* studies can be valuable to dissect cellular mechanisms, it is difficult to evaluate how cells would react in the physiologic environment, with contributions from other cell types and complex architecture. Additionally, while certain *in vivo* studies using animal models are powerful tools to elucidate contributions of molecules to complex biological processes, drawbacks to these studies include artificially induced non-physiologic environments. In contrast to *in vitro* studies or non-physiologic *in vivo* model systems, we can use this model in order to investigate the contribution of PSMA to tumors and tumor vasculature arising in the normal environment in the presence of a physiologic blood supply which is then altered in response to tumor growth and hypoxia, which would be impossible to perform in an *in vitro* or short duration *in vivo* model. This model will enable us to evaluate the role of PSMA in tumor initiation, progression and angiogenesis beginning with the initial transforming event as well as its contribution to metastatic disease.

Task 1 a,b-2 Materials and Methods

2.1 *Breeding Scheme*: TRAMP mice on a C57BL6 background have been described[32] and were obtained from the Jackson Laboratory. C57BL6 PSMA null mice have been described[11] and were a generous donation from Warren Heston at Cleveland Clinic. The TRAMP transgene is maintained as hemizygote in the maternal line. Given poor breeding performance of C57BL6 mice, and the experimental design of WT vs. PSMA null males, mating TRAMP hemizygote PSMA heterozygous females to PSMA heterozygous males as a breeding scheme is unreasonable, and would lead to statistically 1/8 usable experimental animals. Therefore, we used a cohort of animals bred from the same original founders. In this scheme, sibling female TRAMP mice were mated to WT and PSMA-null sibling males. Resultant female TRAMP-hemizygote PSMA-heterozygote females were bred with PSMA-null males to yield TRAMP-hemizygote PSMA-null females (as well as a small number of TRAMP-hemizygote PSMA-null males, were entered into the experiment), which were then bred to produce TRAMP-hemizygote PSMA-null males for the study. At the same time, mice from the original cohort will be bred with WT-PSMA males to obtain TRAMP-hemizygote WT-PSMA males. Overall, male mice from the same cohort of animals (same original founders) hemizygous for the TRAMP transgene, either WT-PSMA or PSMA-null (20 mice per genotype per time-point, total 120 mice), were be bred and held until they reach the desired time-points (8 weeks, 18 weeks, and 30 weeks). Littermate male mice were housed no more than 4 to a cage due to cage density guidelines. Mice showing signs of distress (lethargy, protruding abdomen, over- or under-grooming, abnormal posture or behavior) before the designated time-point were euthanized early and are not included in the final analysis if they are euthanized more than 1 week early. Mice were maintained in the UCHC animal facility and be provided food and water *ad libitum*. All animals were used under animal protocols approved by UCHC Animal Care Committee.

2.2 *Genotype*: Mice were genotyped by isolating DNA from tail biopsies[62] (50mM Tris pH8.8, 1mM EDTA pH8.0, 0.5% Tween20, 3ug Proteinase K, 50C overnight, then 100C x 10'). Genotype for PSMA and the TRAMP transgene has been described[11, 32].

2.3 *Necropsy*- Animals were euthanized by CO_2 asphyxiation, in accordance with the guidelines given by Animal Care Committee of the University of Connecticut Health Center, followed by cervical dislocation to ensure death. Prostate was removed as part of the whole male urogenital system, and then dissected away from non-prostatic tissue and weighed. Periaortic lymph nodes, lungs, liver, and any gross metas*tatic lesions were measured and removed. Weight of total prostate, urogenital system, and any gross tumor metastases were recorded.*

2.4 *Tissue Sample Preparation- Lungs were inflated with 10% phosphate buffered formalin to better visualize tis*sue later. Prostates were be rinsed in PBS, fixed in phosphate buffered 10% formalin at 4C

overnight, then removed to 70% ethanol at 4C for at least overnight and submitted to the university's histology core for paraffin embedding and 5µM sectioning. If the tumor was large enough, a section was embedded in OCT media and snap frozen for frozen sections.

2.5 Histology- Paraffin embedded sections were stained with hematoxylin and eosin (H&E) and scored for g*rade by at least 2 blinded scorers according to Prostate Pathology of Genetically Engineered Mice: Definitions and Classification1 and Pathobiology of autochthonous prostate cancer in a pre-clinical transgenic mouse model2. At least 2 liver sections were examined for the presence of micro-metastasis (defined as 10 or more prostate cancer cells).*

2.6 *Statistics- Statistical significance will be p≤0.05 and determined using one-way ANOVA. Metastatic in*cidence was evaluated by Fisher's exact test.

Task 1 a,b-3 Results and Discussion:

3.1 Prostates isolated from TRAMP hemizygous mice express PSMA.

For the TRAMP model would be appropriate to use in studying PSMA contribution to Prostate Cancer in vivo, the tumors must express PSMA. We isolated tumors from 30 week old wild type and PSMA null TRAMP mice. Tumors showing moderately to poorly differentiated carcinoma were stained for PSMA expression. We find staining consistent with PSMA expression on wild type TRAMP mice but not on PSMA null TRAMP mice, indicating that this model is appropriate for studying the contribution of PSMA to prostate cancer progression (Figure 1.1).

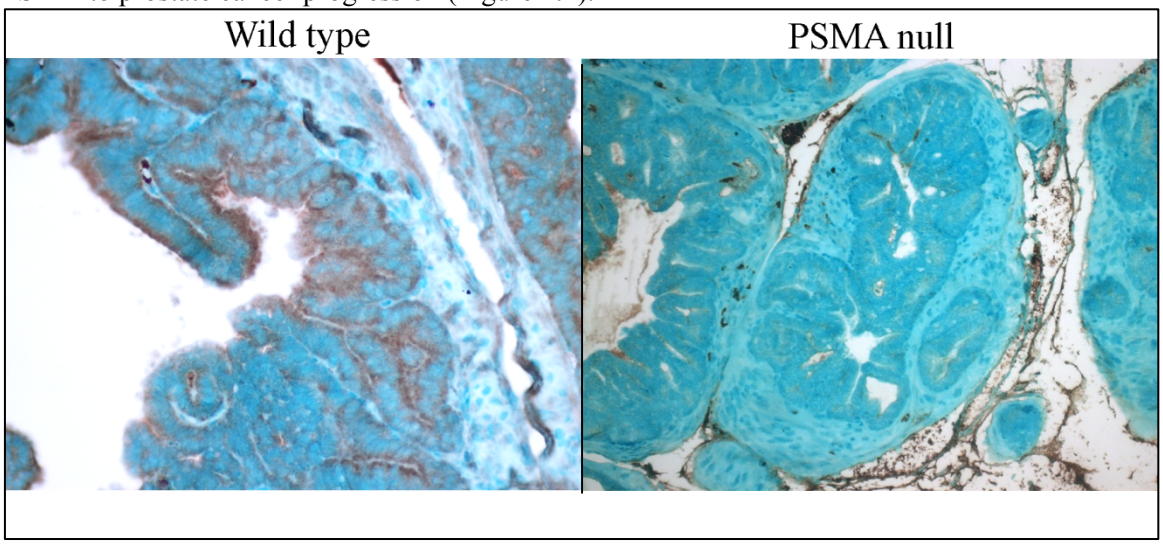

Figure 1.1- Prostate tumors isolated from wild type (left) but not PSMA null (right) TRAMP mice at 30 weeks of age show positive PSMA staining (red-brown), 20x magnification.

3.2 **Overview of TRAMP x PSMA animal models.**

We have accumulated and analyzed the animals as outlined in our experimental plan. Comparison of body weight and prostate weight at the various timepoints indicates that while body weights trended to be lower in the TRAMP-PSMA KO animals, most prominently at 18 weeks, there was not a remarkable difference between the genotypes **(Fig 1-2).** Prostates were weighed at dissection in lieu of measuring tumor volume due to the abnormal shape of the prostate and variations arising from calculating the volume of each prostate lobe. Prostates isolated from wild type and PSMA null did not differ significantly until the 30 week time point where prostate weights were significantly lower in the null animals, which correlates with the less severe phenotype of the tumors in mice lacking PSMA (see below). Because the prostate constitutes a small percentage of the total body weight, these data are internally consistent.

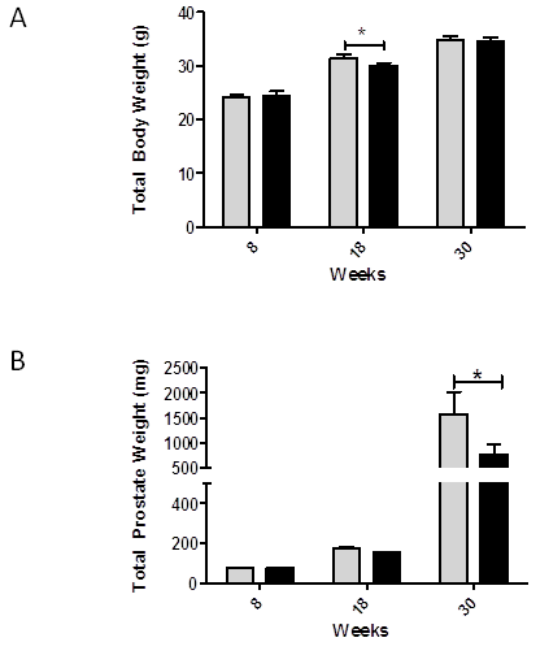

Figure 1-2- Body and prostate weights of wild type and PSMA null animals. Characterization of PSMA +/+ TRAMP +/+ and PSMA-/- TRAMP +/+ mice at 8, 18 and 30 weeks of age. A. Total body weights. B. Total prostate weights. PSMA +/+ TRAMP +/+ (WT) prostates are significantly larger than those of PSMA-/- TRAMP +/+ (KO) at 26-30 weeks. □ = WT ■ = KO. Each value is the mean ± SEM from 10 WT and 10 KO, mice per group. **P* < 0.05 versus control (Student's *t*-test).

3.3 Lack of PSMA does not alter tumor incidence, but tumors are significantly smaller, more necrotic and the vasculature is more 'normalized'.

To determine if PSMA expression was necessary for the initiation of prostate neoplasia, we calculated the incidence of tumor formation (TRAMP positive male mouse with prostatic intraductal neoplasia (PIN) in at least one lobe). As expected, all mice harvested at 30 weeks show at least well differentiated carcinoma in at least 1 lobe, indicating 100% tumor incidence by this time point (data not shown). Hematoxylin and eosin (H&E) staining of sections from wild type and null tumors show that the null tumors are more necrotic when viewed at low magnification (pink areas, arrows, **Fig 1-3, A,B**). Closer inspection indicates that similar to PSMA vasculature in the retina, lack of PSMA produces less tortuous, more normal vasculature (**Fig 1-3)**.

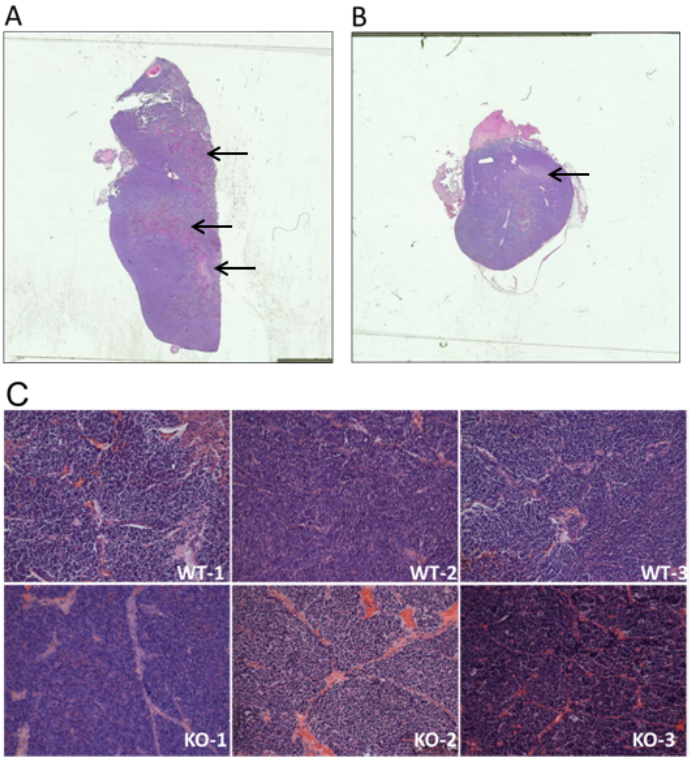

Fig 1-3. PSMA null tumors are more necrotic and the vasculature is more 'normalized'. Gross histological characterization of PSMA +/+ TRAMP + and PSMA-/- TRAMP + mouse tumors at 30 weeks of age. **A.** Hematoxylin–eosin stained whole PSMA + TRAMP + (WT) tumor preparation showing differences in size and necrotic areas than (as indicated by arrows) in comparison to **B**. PSMA-/- TRAMP + (KO). 5x magnification. **C.** Hematoxylin–eosin stained sections of whole PSMA +/+ TRAMP + (WT) tumor preparation showing differences in vascular organization in comparison to PSMA-/- TRAMP + (KO). 40x magnification.

3.4 Lack of PSMA significantly alters tumor grade at early time points but not 30 week old mice. Tumors were harvested from PSMA wild type and PSMA null TRAMP+ mice at 8, 18 and 30 weeks of age. Prostate lobes were dissected and processed for histology. H&E stained sections were analyzed by 3 independent blinded observers to define tumor grade for each lobe. This scoring system includes consideration of tumor localization (focal vs. diffuse) as well as degree of differentiation (PIN to poorly differentiated). Tumor grade was significantly different in all lobes between wild type and PSMA null tumors at 8 and 18 weeks **(Fig 1-4).** However, this difference was not sustained at the 30 week time point, suggesting that these tumors are maximal at this late time point. Therefore, PSMA significantly contributes to prostate tumor progression in this model.

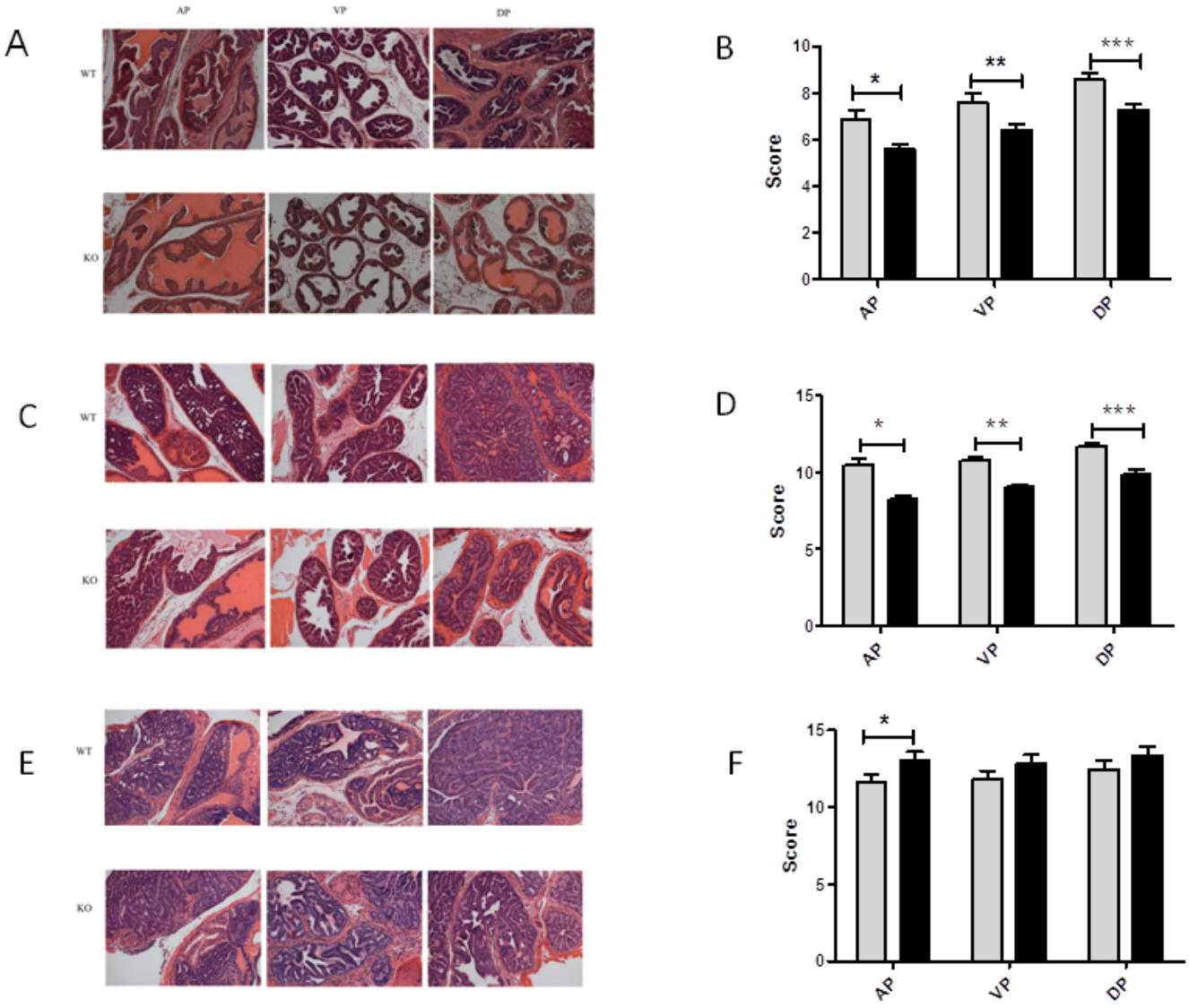

Figure 1-4. Assessment of prostate tumor grade/score in each lobe of the prostate in PSMA +/+ TRAMP +/+ and PSMA-/- TRAMP +/+ at 8, 18 and 30 weeks. **A.** Hematoxylin–eosin stained sections of AP, VP and DP prostate lobes of PSMA +/+ TRAMP +/+ (WT) and PSMA-/- TRAMP +/+ (KO) at 8 weeks with **B.** corresponding quantification. 8 weeks. **E-F**. 30 weeks. □ = WT ■ = KO. Each value is the mean ± SEM from 9-14 WT and 9-14KO, mice per group. *$P < 0.05$ versus control (Student's *t*-test). AP= anterior lobe, VP= ventral lobe, DP= dorsal lobe. 20x magnification.

3.5 PSMA null tumors have a reduced expression of markers of tumor progression. To confirm our tumor scoring data we assayed tumor lysates for alternate markers of tumor progression that have been previously shown to correlate with prostate tumor progression. Survivin is a member of the IAP protein family that acts as a tumor promoter by inhibiting cleavage and activation of the pro-apoptotic protein caspase 3. Consistent with our scoring results, PSMA null tumors expressed markedly reduced levels of survivin protein when compared to wild type counterparts at both the 8 and 18 week time points **(Fig 1-5).** Similarly, a corresponding increase in the levels of cleaved caspase 3 was evident in PSMA null tumors, suggesting proapoptotic phenotype that would promote tumor cell death.

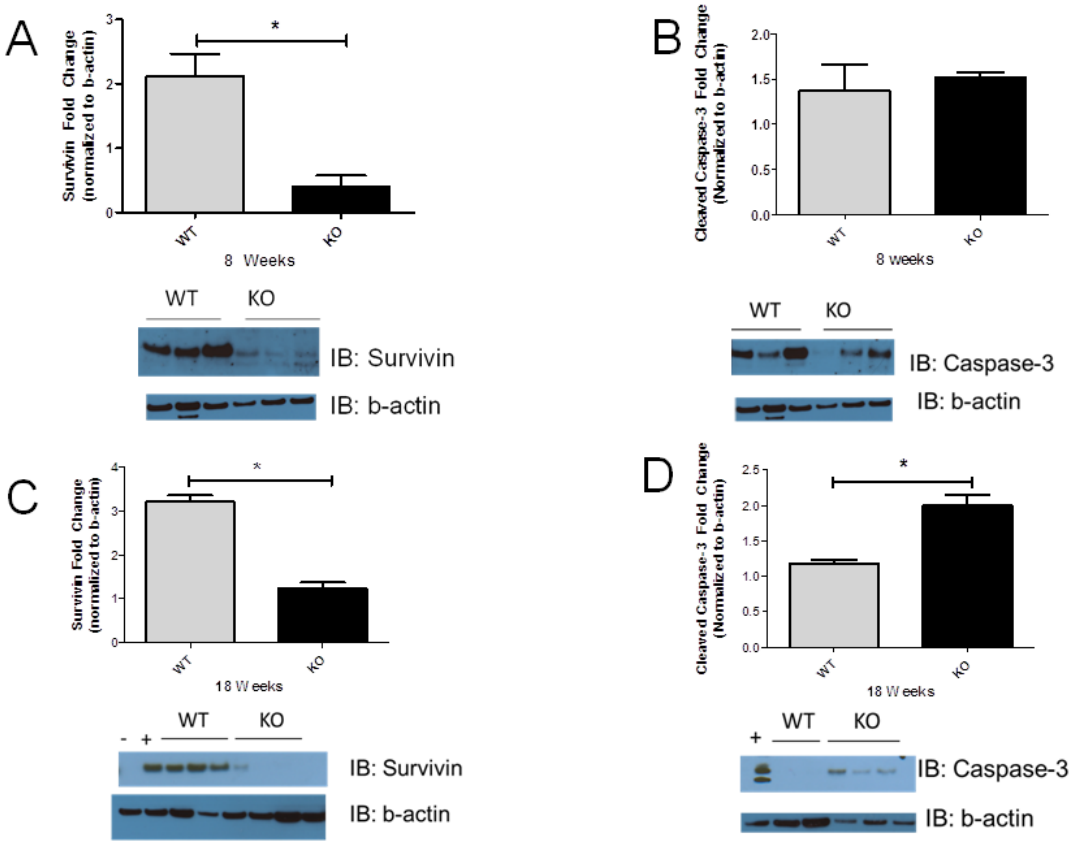

Fig 1-5. Survivin as a marker of tumor progression. Protein quantification by Western blotting of whole prostate lysates from PSMA +/+ TRAMP +/+ and PSMA-/- TRAMP +/+ for survivin and caspase-3 taken at 8 (**A**,**B**) and (**C**,**D**) 18 weeks. □= WT ■ = KO. Each value is the mean ± SEM from 3 WT and 3KO, mice per group compared to normal prostate control and normalized to b-actin. Positive control for cleaved caspase-3 = Jurkat cells treated with 25mM etoposide for 5h. **P* < 0.05 versus control (Student's *t*-test).

3.6 **Tumor survival pathways are dysregulated in the absence of PSMA.** Survivin expression is regulated by the Akt survival pathway that is often upregulated in tumors, primarily due to alterations or mutations in the tumor suppressor PTEN. PTEN catalyzes the dephosphorylation of PI(3,4,5)P3 to PI(4,5)P2, effectively blocking PI3K dependent Akt activation, thus inhibiting the cell cycle. To determine if this pathway is altered in PSMA null tumors we assessed the activation status of key members of this pathway. Protein quantification by Western blotting of whole prostate lysates at 18 weeks from PSMA +/+ TRAMP+/+ and PSMA-/- TRAMP +/+ show a decrease in P-PDK1 S241 and Akt T308 in PSMA-/- TRAMP +/+ as compared to PSMA +/+ TRAMP +/+ (Figure 1-6A) indicating a decrease in PI(3,4,5)P3 levels within the cell. This correlates with the decrease in tumor size, more "normal" vascularization and decreased survivin expression in the PSMA null tumors. Analysis of PTEN protein in whole prostate lysates at 18 weeks from PSMA +/+ TRAMP +/+ and PSMA-/- TRAMP +/+ show a considerable decrease in both nonphosphorylated- as well as S380 phosphorylated-PTEN in PSMA-/- TRAMP+/+ as compared to wild type (Figure 5B). However, total PTEN is not changed suggesting that other phosphorylated forms of PTEN, which were not assessed, may be increased.

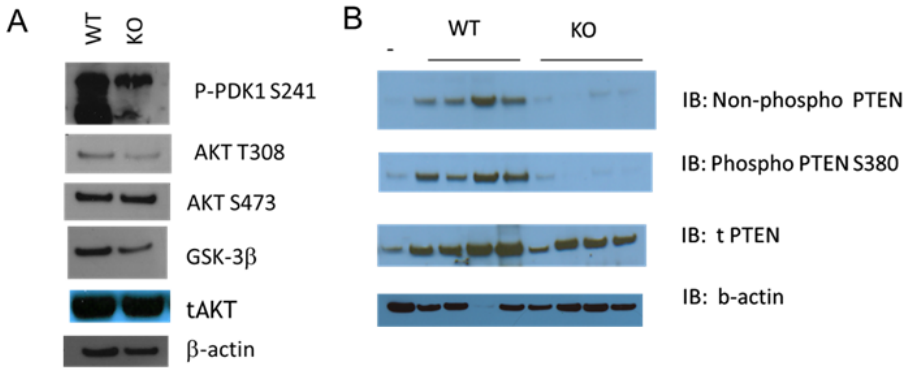

Fig 1-6. Analysis of AKT/PI3K and PTEN Pathways. Protein quantification by Western blotting of whole prostate lysates from PSMA +/+ TRAMP +/+ and PSMA-/- TRAMP +/+ for the A. Akt pathway(P-PDK1 S241, Akt T308, Akt S473, GSK-3b, total Akt, b-actin) and the B. PTEN pathway (Non-phospho PTEN, Phospho-PTEN S380, total PTEN, b-actin) taken at 18 weeks.

3.7 PSMA complexes with active PTEN. Numerous examples suggest a role for enzymatic peptidases in mediating cell migration by affecting signaling cascades. The interaction of the neutral endopeptidase (NEP) cytoplasmic tail with Lyn kinases blocks the activation of PI-3-kinase thus prevents FAK phosphorylation-mediated cell migration. NEP is also known to inhibit the proliferation of prostate epithelial cells by its direct association with PTEN. Mutational analysis of the cytoplasmic tail of NEP identified a basic amino acid-rich motif containing five lysine and arginine residues proximal to the transmembrane domain that mediates the interaction between NEP and PTEN. The cytoplasmic tail of PSMA contains basic residues that could also bind to PTEN. The cytoplasmic tail of hPSMA also has a stretch of three basic arginine residues proximal to the membrane-spanning domain. mPSMA also has a stretch of three basic residues proximal (R to H) to the membrane-spanning domain. To determine if PSMA also interacts with PTEN co-immunoprecipitates with PSMA in TRAMP-C1 cells and maintains its phosphatase activity against PI(3,4,5)P3. PTEN interacts with the cytoplasmic tail of PTEN at the plasma membrane.

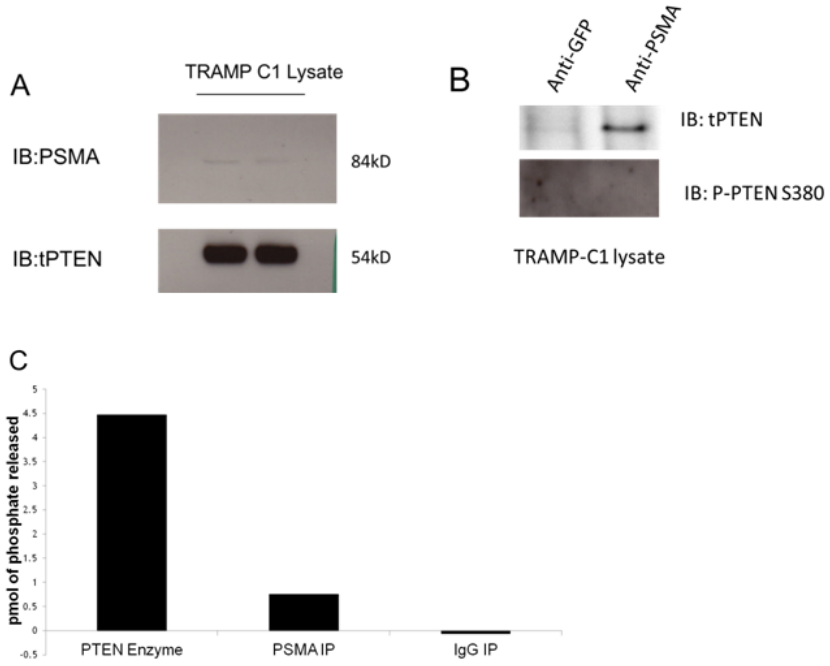

Fig 1-7. PTEN co-immunoprecipitates with PSMA in TRAMP-C1 cells and maintains its phosphatase activity. A. Protein quantification by Western blotting of TRAMP-C1 whole cell lysates for presence of PSMA and tPTEN. B. Total PTEN and Phospho-PTEN S380 immunoprecipitated with anti-PSMA mAb 3E2 from TRAMP-c1 lysates were analyzed by Western blotting. Anti-GFP mAb was used as a negative control. C. PSMA was immunoprecipitated with mAb 32 from TRAMP-C1 lysate and the associated phosphatase activity assessed using an *in vitro* malachite green phosphatase assay using PI(3,4,5)P3 as substrate. Activity is measured in pmol of phosphate released as compared to phosphate standards and normalized to background. Purified PTEN enzyme was used as a positive control for the assay. Anti-GFP mAb was used as a negative control for immunoprecipitation.

3.8 **PSMA null tumors signal through an alternate pathway.** Why do PSMA-/- TRAMP +/+ mice still develop tumors? Additional pathways that regulate proliferation may provide alternate routes. These tumors are smaller, less aggressive, more "normal" vasculature, downregulated AKT/PI3K expression & PTEN expression. Genes in the insulin and the insulin-like growth factor signaling pathways are plausible candidates for susceptibility genes for prostate cancer. We hypothesized that the IGFR1 may be associated with prostate cancer in our model of PSMA -/- Tramp +/+ prostate tumor progression. Analysis of IGF-1R Pathway shows that the IGFR1 is activated in prostate tumor progression in both PSMA +/+ TRAMP +/+ and PSMA-/- TRAMP +/+ mice **(Figure 1-8)**. However, there seems to be pathway switching taking place. Protein quantification by Western blotting of whole prostate lysates from PSMA +/+ TRAMP +/+ and PSMA-/- TRAMP +/+ show that phospho- IRS-1 S612, GRB-2, phosphor-ERK are upregulated in the PSMA-/- TRAMP +/+ but not in the PSMA +/+ TRAMP +/+.

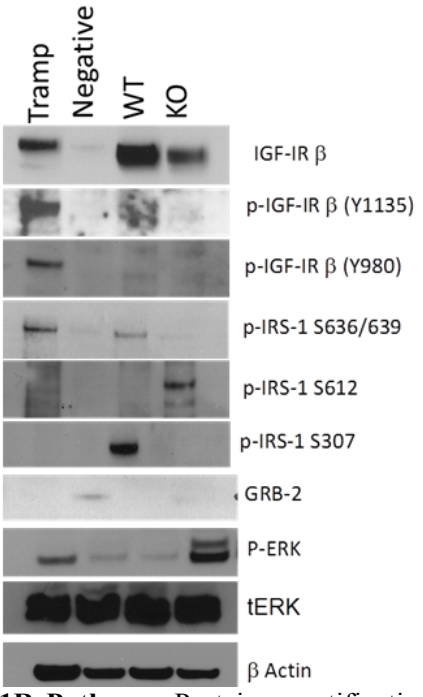

Fig 1-8. Analysis of IGF-1R Pathway. Protein quantification by Western blotting of whole prostate lysates from PSMA +/+ TRAMP +/+ and PSMA-/- TRAMP +/+ for the IGF-1R pathway (IGF-1Rb, phospho-IGF-1Rb Y1135, phospho-IGF-1Rb Y980, phospho- IRS-1 S636/639, phospho- IRS-1 S612, phospho-IRS-1 S307, GRB-2, phosphor-ERK, total-ERK and b-actin) taken at 18 weeks.

3.9 PSMA regulates prostate tumor metastasis.

PSMA is expressed at the highest level on metastatic prostate cancer in humans. Additionally, our in vitro data suggest that PSMA contributes to cellular processes necessary for metastasis, including cell adhesion to and migration through ECM and cell viability in an anchorage independent assay (Task 1-e). We therefore analyzed H&E stained sections of the liver from TRAMP mice for evidence of metastasis, in addition to any gross macro-metastasis observed during tissue harvest (such as the liver shown in **Figure 1-10,** arrows indicate metastatic foci). A section was considered positive for metastasis if it showed a cluster of "small blue cells", a feature not normally observed in the liver, consisting of at least 10 nuclei suggesting epithelial origin (**Figure 1-10**, yellow circles). We observed a high degree metastasis in both the wild-type and PSMA-null animals in the 18 and 30 week time points analyzed. Of the animals analyzed, wild type animals had evidence of more micrometastasis to the liver, kidney and lung than the PSMA null mice, suggesting that PSMA may contribute to metastasis as well (Table I).

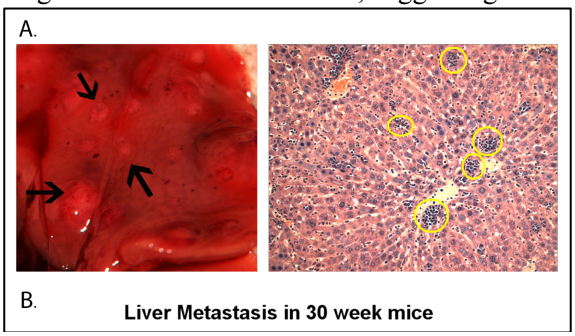

Figure 3-9- Deletion of PSMA leads to a change in prostate tumor cell metastasis to the liver: **a**. *left*-gross metastatic foci were observed in the liver of a 30 week old mouse (arrows); *right*-20x magnified image of an H&E stained liver section from a mouse exhibiting gross liver metastasis. Yellow circles indicate areas of micrometastasis.

Table I. Metastatic incidence and tissue distribution in PSMA+/+ TRAMP+/+ and PSMA-/- TRAMP +/+ mice at 18 and 30 weeks of age.

Cohort	n	Kidney	Liver	Lung	Lymph node	others
PSMA +/+ TRAMP +/+ 30W	21	4 (19.2%)	4 (19.2%)	4(19.2%)	7 (33.3%)	4 Adrenal Met 4 enlarged testicle
PSMA-/- TRAMP+/= 30W	24	2 (8%)			4 (16%)	1 Salivary gland 1 Bladder large 1 Necrotic mass
PSMA+/+ TRAMP +/+ 18W	23	3 (13.2%)		2 (8.7%)	3 (13.2%)	1 Salivary gland 1 Neck mass 1 Dermatitis 1 Head tilt
PSMA-/- TRAMP+/+ 18W	21	1 (4.8%)			2 (9.5%)	1 Spleen bump

3.10. **Proposed model**

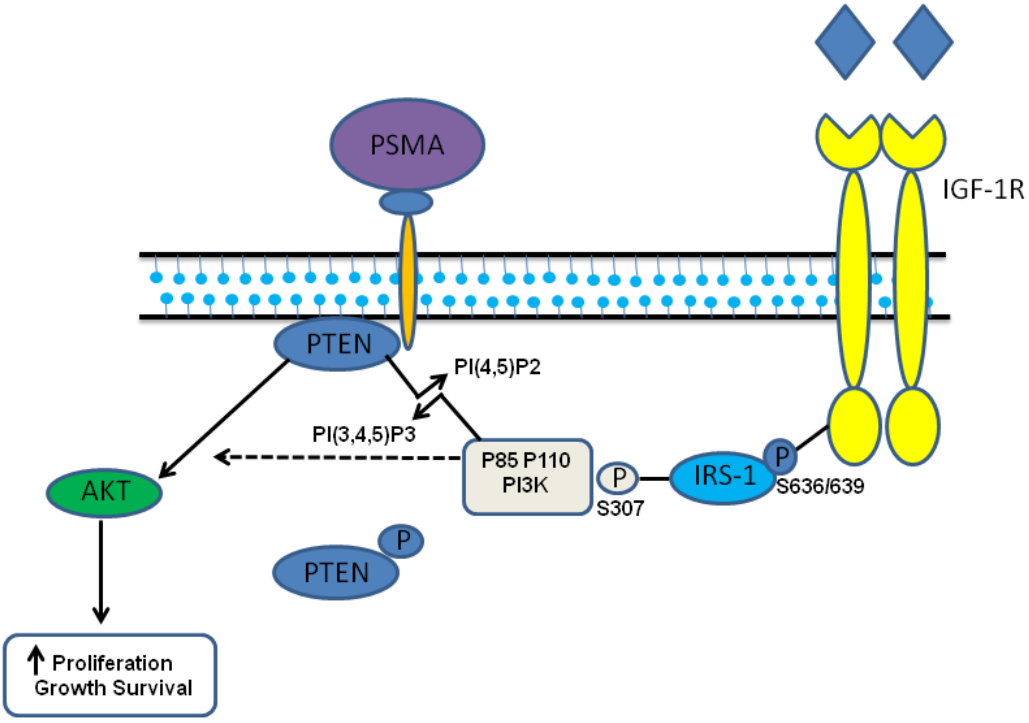

Figure 3-10 **Prostate tumors** When PSMA is present it binds to PTEN at the plasma membrane. PTEN at the membrane catalyzing the dephosphorylation of PI(3,4,5)P3 to PI(4,5)P2. This should shut down the AKT/PI3K activity by decreasing phosphorylation of PDK1 however it is actually more active than the control. Why? Explanation: In advanced prostate cancer the IGFR1 is known to be overactive due to increased amounts of circulating ligand. It is our thought that in our model, upregulation of the IGFR-1 leads to the increased phosphorylation of PI3K thus leading to increased levels of PI(3,4,5)P3 in the plasma membrane .PTEN gets overwhelmed and the AKT pathway gets activated. Leading to increased proliferation, growth and survival.

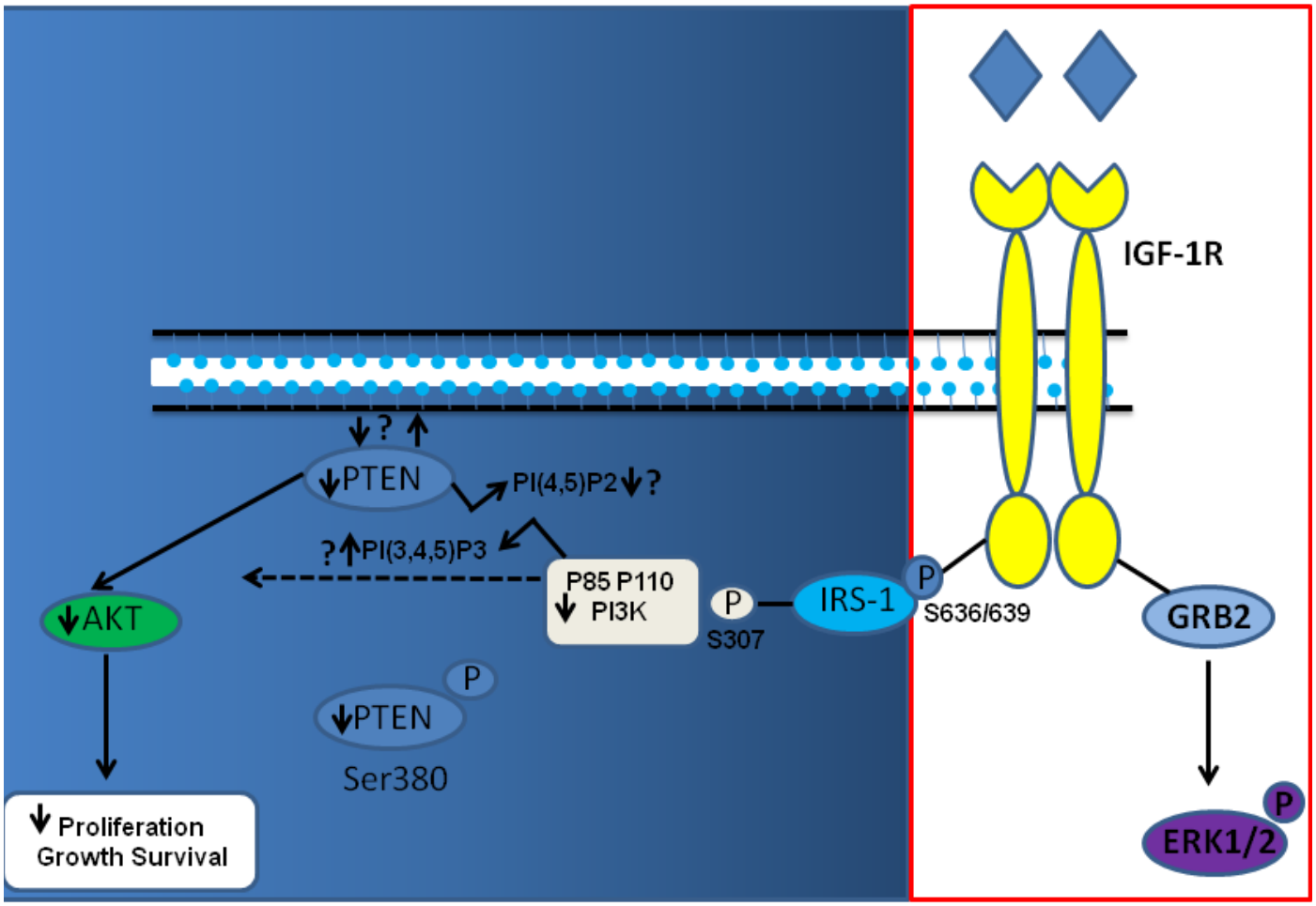

Figure 3.11 **PSMA null tumors**. If PSMA is absent, tumors will still grow albeit at a slower rate and they are less aggressive than that of the PSMA +/+ TRAMP +/+. We show that the in the PSMA-/- TRAMP +/+ mice the cell favors the activation and phosphorylation of ERK1/2 via GRB-2 via the IRSR-1 pathway. PTEN may or may not be at the plasma membrane and there is a slight increase in the AKT pathway compared to the control.

Future Studies:

The evidence that PSMA may contribute to prostate cancer metastasis is an exciting and very relevant to mortality from this disease. Future studies would include a thorough examination of this question using advanced imaging techniques and models specifically designed to assess metastasis.

Task 1.e. Assess tumor size, vascularity, necrosis, proliferation, apoptosis and relative hypoxia in PSMA expressing tumors from wild type vs. PSMA null animals.

PSMA is necessary for *in vitro* cell processes involved in metastasis

Task 1 e-1 Introduction

Angiogenesis is the process by which blood vessels grow into new areas. It involves endothelial cell invasion through the basal lamina, proliferation, adhesion to surrounding extracellular matrix (ECM), migration and invasion through ECM, and tube formation and stabilization[29]. Our lab has previously shown PSMA to be involved in endothelial cell adhesion to and invasion through ECM and tube formation. In order to metastasize, tumor cells go through similar functions: primary tumor growth and proliferation, local invasion through the basal lamina and into lymphatic or blood vessels, survival in the bloodstream and arrest and adhesion to the endothelial wall, invasion through the endothelial layer, adhesion to, migration and invasion through surrounding ECM, and survival and growth in the secondary site[30]. While our lab has been made progress in understanding the functions and mechanism of PSMA in endothelial cells, many questions remain. Among these are the functional significance of PSMA on tumor cells and tumors, and the mechanism of action in tumors. We hypothesized that PSMA on tumor cells works in a manner similar to endothelial cells. Therefore, we investigated the functional significance of PSMA in tumor cell functions *in vitro* which are necessary for successful tumor metastasis *in vivo*.

Task 1 e-2 Materials and Methods

2.1 *Expression Studies*- 15ug of cell lysates were analyzed by Western Blot using mouse-anti-mouse PSMA 3E2 antibody (gift from Dr Polly Gregor, Memorial Sloan Kettering) or anti-CD29 antibody. After imaging the blot was stripped and re-probed with mouse-anti-beta actin antibody (Abcam, ab6276) to ensure equal protein loading. Blots were imaged using Kodak Image System 2000MM and Kodak Molecular Imaging software.

2.2 *RT-PCR*- RNA was isolated using QIAGEN RNeasy kit according to manufacturer's instructions. cDNA was produced using 1ug of RNA and MMTV-reverse transcriptase from Invitrogen, according to manufacturer's instructions using Oligo-dT method. PCR was performed with Invitrogen Recombinant Taq Polymerase.

Primers:

mPSMA: F 5' GGG AAG ATT GTG ATT GCC AGA 3'
R 5' GCC TCC GTC CTT TCT TCT TCA 3'

RPL10: F 5' CAA CTA CAT GGT CTA CST GTT CCA GT 3'
R 5' TGA CCC GTT TGG CTC CA 3'

CD29: F 5' ATA CAA GCA GGG CCA AAT TG 3'
R 5' TAG CTA AAT GGG CTG GTG CA 3'

2.3 *Proliferation and Viability Assay*- $5x10^5$ cells in 100uL complete media was seeded in triplicate into wells of 10 96-well plates, and maintained in 5%CO_2, 37C. Media was changed every daily with fresh 2-PMPA. At indicated time points, 10uL 5mg/mL MTT ([3-(4,5-dimethylthiazol-2-yl)-2,5-diphenyltetrazolium bromide]) in H_20 (filtered) was added to each well and incubate 3hr 37C. Media was gently aspirated, and 100uL acidic isopropanol (0.1N HCL in isopropanol) was added to each well. Plate was read with a colorimetric plate reader, 540nm with a reference of 630nm[59]. Triplicate samples were averaged and converted to % time 1. Viability assay was performed in a similar manner, with increasing amounts of 2-PMPA added to wells in triplicate. After 24 hours, cells were analyzed using MTT as above.

2.4 *Adhesion Assay*-Wells of 96-well tissue culture treated plate were coated with 50uL 10ug/mL Laminin-1 (or indicated matrix) in PBS 4C overnight or 37C for 2 hours. Wells were blocked with boiled 1% BSA/PBS for 1 hour at RT, then washed 3 times with PBS. Cells were trypsinized, washed in

complete media, and re-suspended in a concentration of $1x10^6$ cells/mL in 5ug/mL Calcein AM in PBS for 45 min at 37C. Cells were then resuspended in complete media at $1x10^5$ cells/mL, with 100uM 2-PMPA where indicated, and 50uL of the cell suspension was added to each well, and incubated for 15 min at 37C. Wells were washed 3 times in PBS and imaged using a Zeiss Axiocam HRC camera on a fluorescent StemiSV11 dissecting microscope. Cell adhesion was quantified using Adobe Photoshop software calculating green pixels. Samples were run in triplicate. Adhesion is expressed ad % control adhesion to the same ECM.

2.5 *Invasion Assay*- Tramp-C1 or LnCaP cells (10^4) were suspended in serum-free, growth factor-free media and placed in the upper chamber of migration inserts (Corning Costar) coated with a 1:5 dilution of Matrigel:PBS. Complete HUVEC growth media containing 10% fetal bovine serum and numerous growth factors (EGM-2, Clonetics) was added to the lower chamber, and cells were allowed to invade for 18 hours at 37ºC. To quantify invasion, the invading cells were stained with Calcein AM and the bottom of the invasion inserts were imaged using a dissection microscope. Fluorescently labeled cells were counted by green pixel quantification in Adobe Photoshop.

2.6 *FAK Phosphorylation Studies*- Cells were plated in a 10cm dish coated with purified laminin or Matrigel in complete media and allowed to adhere overnight in the presence or absence of 100uM 2-PMPA. Media was aspirated and cells gently washed with PBS. Cells were lysed on the plate using NP-40 buffer containing protease inhibitor cocktail, NaF and NaVanadate. Protein concentration was quantified using a BCA assay, and equal amounts of were loaded onto a 4-15% gradient SDS PAGE. Primary antibodies are 1:1000 anti-FAK antibodies from Cell Signal (pFAK (Y397), pFAK (Y576/577), pFAK(Y925) and FAK(C-20). Anti-mouse Beta actin from AbCam, 1:5000). Blots were imaged on a Kodak Imager and band densitometry calculated. peak is expressed as peak/total FAK from the same blot.

2.7 *Soft Agar Assay*- Cells were grown in a 6 well plate. A lower layer of 0.6% agar with 50% *complete* media and 10% FBS was plated in each well to support the cells. $1x10^4$ cells/mL in 0.3% agar with 50% complete media, 10% FBS was gently mixed and layered onto the support layer. The cell layer was allowed to solidify for 10 minutes in a cell culture hood. Control media or media containing 100uM 2-PMPA was gently layered onto the cells. Cell plates were maintained in 5% CO2, 37C humidified incubator. Cells were re-fed with fresh media containing fresh 2-PMPA until evaluation.

2.8 *Statistics*- Statistical significance will be determined using a two-tailed paired student's t-test. Significance is $p \leq 0.05$.

2.9 Tumor Allografts- Tramp-C1 cells were obtained from ATCC and grown under normal conditions (DMEM, 5% FBS, 5% Nu-Serum IV, 0.005 mg/mL bovine insulin, 10 nM dehydroisoandrosterone). Four days before implantation, cells were subcultured to be 80% confluent two days before implantation. Cells were then subcultured 1:3 and grown under normal conditions overnight. On the day of implantation, cells were rinsed with PBS, trypsinized, and trypsin inactivated by addition of complete media. Cells were pelleted and rinsed 3 times in serum-free media, then resuspended in serum free media at a concentration of $5x10^7$ cells/ml and stored on ice. Animals were anesthetized using Tribromoethanol and the backs of animals were shaved. 100µL of cells was injected subcutaneously into the right dorsal flank of using a 21 gauge needle, and injection site was occluded for 1 minute to prevent cell leakage. Tumor dimensions was measured by caliper every 2 days, and tumors isolated after 10 weeks (for tumor size experiments) or when tumors reached 8mmx8mm (size-matched tumors), previously shown to correlate with a tumor weight of approximately 500mg.

2.10 Histology and Immunohistochemistry- Tissues were fixed in 10% formalin in PBS 8-16 hours at 4^oC then placed in 70% ethanol, paraffin embedded and sectioned by the histology core. Hematoxylin and eosin stained sections were scanned using a Microtek AtrixScan 4000tf slide scanner at 5000ppi. ImagePro Plus version 5.1 was used to quantify percent tissue necrosis. Live tumor area was defined by purple pixels and necrotic area was defined as pink or white pixels. The same pixel selection mask was used in each tumor.

2.11 For immunohistochemistry sections, slides were deparafinized and rehydrated. Antigen retrieval was conducted using 10mM Sodium Citrate (pH 6.0) in a pressure cooker. Endogenous peroxidase activity was quenched by incubating slides 15' in 3% H2O2. Stains requiring nuclear permeabilization (Ki67) were incubated in 0.1% Triton-X 100 in TBS. Slides were blocked in 5% normal goat serum (Ki67) 5% normal horse serum (CD31, cleaved Caspase 3) or 5% BSA (Carbonic Anhydrase IX), then incubated under primary antibody overnight in a humidified chamber (rabbit anti-Ki67 Abcam 15580 1:400, goat anti-Carbonic Anhydrase IX R&D AF2344 1:500, goat anti-CD31 Santa Cruz sc-1506 1:300, rabbit anti-Cleaved Caspase 3 Cell Signal 9661 1:200). Slides were washed 3 times in TBS/0.1%Tween-20 (Ki67, CA9) or PBS (CD31 or CC3). 1:500 biotinylated secondary antibody (VectorLabs horse anti-goat BA9500, goat anti-rabbit BA1000) was applied and slides incubated for 1 hr at room temperature in a humidified chamber. Slides were washed 3 times, then Vectastain Elite ABC Kit (Vector Labs SK-6100) was applied for 30 minutes. Slides were washed once in buffer, and once in H2O, then Novared (VectorLabs SK4800) was applied for 30 seconds to 4 minutes. Slides were washed in H2O, then counterstained using Methylgreen (Vector Labs H-3402) 2 minutes room temperature, rinsed, dehydrated and mounted under cytoseal 60.

2.12 Images were obtained using a Zeiss AxioCam HRc in an Axioplan2 microscope. Proliferation index was calculated as percent Ki67 positive nuclei in at least 3 40x fields.

2.13 Microvessel density was quantified by counting CD31 positively stained vessels with a lumen in 4 20x fields.

2.14 Carbonic Anhydrase IX stained slides were scanned using Microtek scanner and analyzed using ImagePro software. Brown and red pixels were considered positive; positive pixels and total tumor area was calculated. To obtain hypoxia index, %CAIX amount was divided by live tumor area to compensate for lack of CAIX staining in those areas of tumor already necrotic.

2.15

Task 1 e-3 Results and Discussion

3.1 TRAMP-C1 cells express PSMA and β1 integrin.

Cells must undergo similar processes in both endothelial cell angiogenesis and cancer cell metastasis, such as proliferation, invasion through the basement membrane, adhesion to the extracellular membrane, and remaining viable in their new environment. Due to previous results indicating that PSMA in human endothelial cells contributed to angiogenic processes through modulating β1 integrin activation and signaling, we examined prostate cancer cells in vitro to determine if PSMA was necessary for similar processes in this cell type. The TRAMP-C1 cell line is a mouse derived cell line and has been well described to express PSMA. To ensure the expression of PSMA and β1 integrin, we performed conventional RT-PCR and western blotting (Figure 3.1) for mouse PSMA and β1 integrin. Product corresponding to the expected size for PSMA was observed in the TRAMP-C1 reaction, but not in the EOMA negative control reaction (Figure 3.1A). RNA from both samples showed strong product in β-actin loading control bands, indicating that the lack of result in the negative control lane was due to lack of PSMA RNA expression, not lack of total RNA in the sample. We also observed product at the expected size for β1 integrin in both the TRAMP-C1 and positive control HUVEC samples (Figure 3.1B). Additionally, we observed bands at the expected size (approximately 120 kDa) for PSMA in TRAMP-C1 and HUVEC (positive control) but not EOMA (negative control) by immunoblot (Figure 3.1C). Bands corresponding to the approximate size of β1 integrin were observed by immunoblot in both TRAMP-C1 and HUVEC (positive control) lysate (Figure 3.1D). Therefore, we concluded that TRAMP-C1 would be an appropriate murine prostate cancer cell line in which to perform initial in vitro experiments to study the role of PSMA.

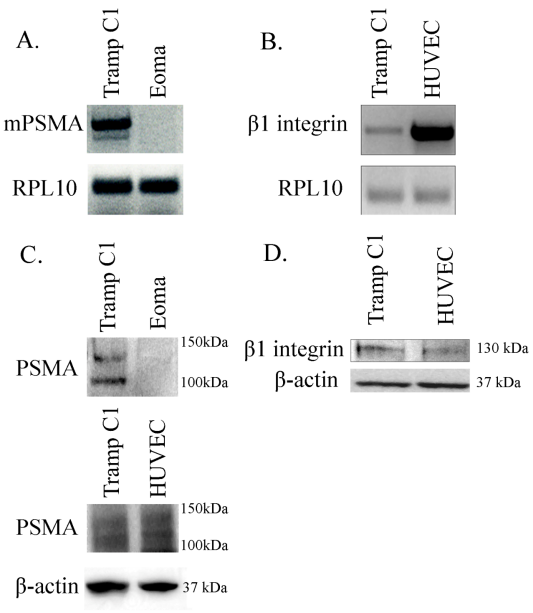

Figure 3.1- A. Tramp C1 cells express PSMA message, while Eoma (PSMA null) show no message. **B**. Tramp C1 cells express β1 integrin message, as do HUVEC (positive control). **C**. Tramp C1 cells express PSMA protein, as shown in western blot. Above, Tramp C1 but not Eoma cells show a band corresponding to the size of PSMA. Middle, both Tramp C1 and HUVEC cells show a band corresponding to the size of PSMA (100 kDa and 120 kDa doublet). **D**. Tramp C1 cells express β1 integrin protein (130kDa).

3.2 PSMA inhibition by 2-PMPA does not affect cell proliferation or viability in monolayer culture.

To investigate the role of PSMA in functional cell assays, we used the well described small molecule inhibitor 2-PMPA. To ensure that any observed effects were due to PSMA inhibition and not to a detrimental non-specific effect of 2-PMPA on the cells, we performed viability and cell proliferation assays (Figure 3.2). 2-PMPA does not significantly change TRAMP-C1 cell viability in monolayer culture over 24 hours in concentrations up to 100uM (Figure 3.2A). Additionally, since some of the assays used required cells to be exposed to 2-PMPA for periods longer than 24 hours, we performed cell proliferation assays. TRAMP-C1 cells grown in the presence of 100uM 2-PMPA under otherwise normal monolayer culture conditions showed no difference in cell proliferation compared to untreated cells (Figure 3.2B). Thus, any observed effect in functional assays can be assumed to be due to PSMA inhibition, not due to an increase in cell death or decrease in cell proliferation to do non-specific 2-PMPA effects.

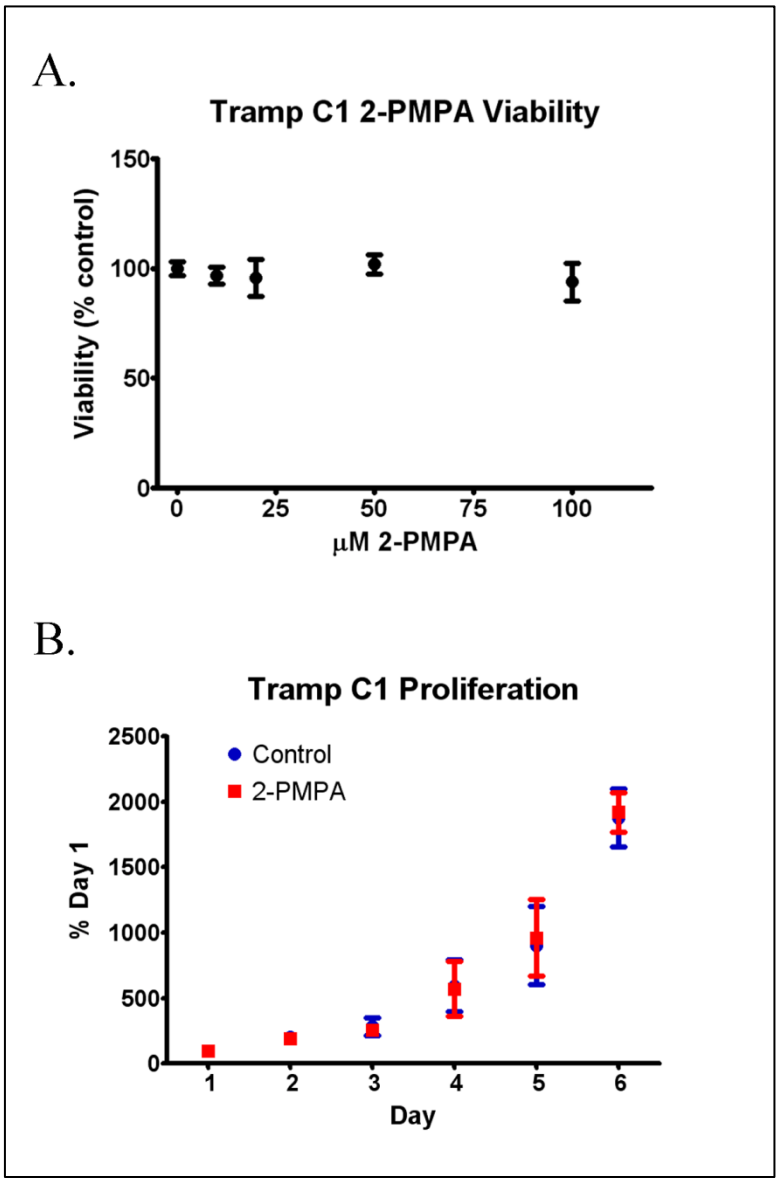

Figure 3.2- To ensure that any differences observed in functional assays would be due to PSMA activity rather than cell death from 2-PMPA exposure or a difference in proliferation, we performed MTT viability and proliferation assays. A. 2-PMPA at concentrations up to and including 100uM does not cause a significant change in cell viability over 24 hours. B. There is no significant difference between cells grown in the presence of vehicle or 100uM 2- PMPA in cell proliferation over 6 days.

3.3 PSMA inhibition decreases prostate tumor cell adhesion to Laminin but not other extracellular matrices.

Previous work has shown that in human endothelial cells, PSMA activity is required for cell adhesion to laminin but not to other ECM substrates such as Fibronectin, Collagen I or Collagen IV, consistent with PSMA contribution to β1 integrin activation and signaling. Cell adhesion to ECM is important for cancer cell metastasis during tumor cell extravasation from microvessels into a new site. To determine if PSMA activity in prostate cancer cells was similarly required for laminin specific cell adhesion, we performed cell adhesion assays (Figure 3.3). PSMA inhibition by 2-PMPA decreases TRAMP-C1 adhesion to both

laminin 1 and laminin 10 by approximately 40% (p= 0.015 and 0.019, respectively), but does not significantly change cell adhesion to collagen I or collagen IV (p= 0.97 and 0.66, respectively, Figure 3.3A). To determine if this result was true for both mouse and human prostate cancer cells, we also performed the assay using LnCaP cells, a highly PSMA expressing human prostate cancer cell line. As expected, PSMA inhibition significantly decreased LnCaP cell adhesion to Matrigel (a mixture of ECMs containing a high concentration of laminin) approximately 27% (p=0.037), and laminin 1 by approximately 60% (p=0.040), but did not decrease cell adhesion to collagen I, collagen IV, or to fibronectin (p= 0.11, 0.74, and 0.28, respectively, Figure 3.3B). To ensure that the observed decrease in cell adhesion to laminin is due to PSMA inhibition and not to non-specific effects of 2-PMPa, we assayed a PSMA non-expressing human prostate cancer cell line, DU145, adhesion to matrices in the presence or absence of PSMA inhibition. We observed no significant decreases in cell adhesion to Matrigel, laminin1, collagen I, collagen IV, or fibronectin in the presence of 2-PMPA compared to control (Figure 3.3C). Thus, PSMA is important in PSMA positive tumor cell adhesion to ECM, particularly laminin.

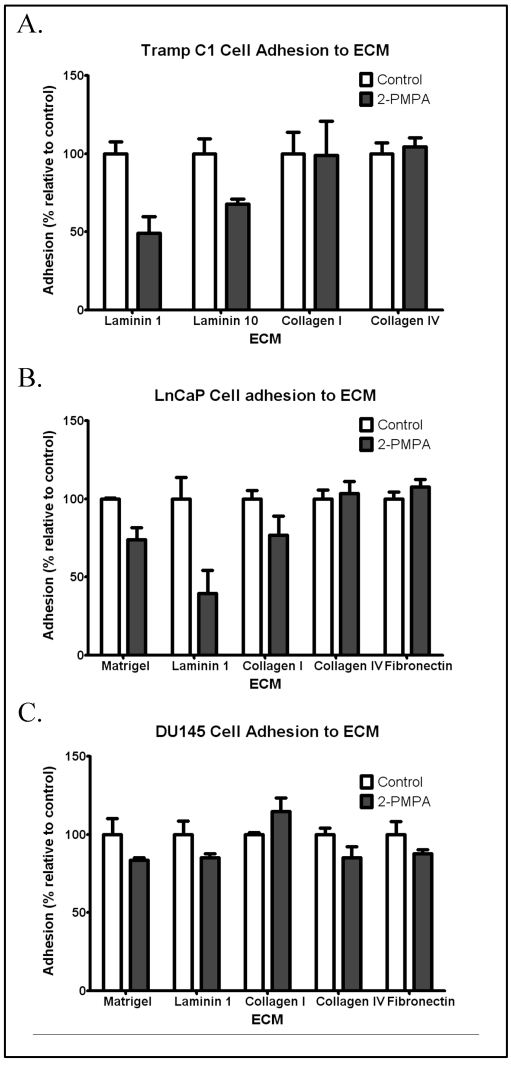

Figure 3.3 PSMA regulates cell adhesion to Laminin rich extracellular matrices but not other ECMs. A. A statistically significant decrease of approximately 50% was observed in Tramp-C1 cell adhesion to laminin, but not other ECM, when PSMA enzyme activity is inhibited. B. A similar decrease in cell

adhesion to Matrigel and laminin is observed in human PSMA expressing LnCaP cells, but not non-expressing DU145 cells (C).

3.4 PSMA inhibition decreases prostate cancer cell invasion through Matrigel

In addition to adhesion to ECM, tumor cells must invade through the basal lamina of microvessels in order to seed a new metastasis. Therefore, we examined whether PSMA inhibition contributed to prostate cancer cell invasion through a basement membrane preparation using a modified Boyden chamber assay. PSMA inhibition decreased Tramp-C1 cell invasion through Matrigel toward growth factor containing media. Figure 3.4A shows representative images of invaded Tramp-C1 cells under control (left) and PSMA inhibition (right) conditions. Quantifying the invaded cells shows that invasion is decreased by approximately 70% over 16 hours (p= 0.0001, Figure 3.4B). Human LnCaP cell invasion through Matrigel is also significantly decreased by approximately 50% with PSMA inhibition (p=0.031, Figure 3.4C).

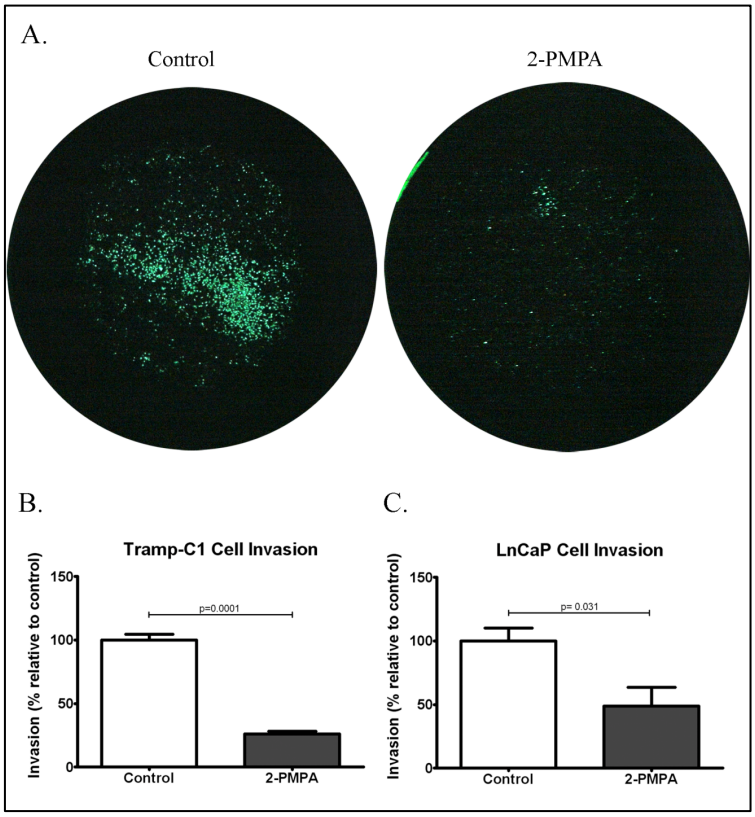

Figure 3.4- PSMA contributes to tumor cell invasion. A. Images of control (left) and 2-PMPA treated (right) invasion chambers. B. Quantified invasion assay- PSMA inhibition significantly decreases Tramp-C1 invasion through Matrigel toward a growth factor rich media compared to control non-treated cells. C. PSMA inhibition also significantly decreases LnCaP cell invasion through Matrigel.

3.5 PSMA inhibition decreases FAK phosphorylation in Tramp-C1 cells.

PSMA has previously been shown to contribute to β1 integrin activation and signaling through FAK in human primary endothelial cells. Our observation that PSMA contributes to Tramp-C1 cell adhesion to laminin is consistent with PSMA regulation of β1 integrin activation in prostate cancer cells as well. To validate this hypothesis, we treated cells with 2-PMPA, then used immunoblotting to detect the levels of phosphorylated FAK, a downstream signaling protein for β1 integrin, in the cell lysate using phospho-

specific antibodies (Figure 3.5). The amount of pFAK Y397 (Figure 3.5A, top left) and pFAK Y925 (Figure 3.5A, top right) were reduced in 2-PMPA treated cells compared to controls, while pFAK Y576/577 showed no change (Figure 3.5A top center). The amount of total FAK did not change. The amount of peak relative to total FAK was quantified and is expressed as percent relative to control. pFAK Y397 and pFAK Y925 were decreased by approximately 45% compared to controls (Figure 3.5B). These results, combined with laminin specific cell adhesion, support PSMA contribution to β1 integrin activation and signaling through FAK.

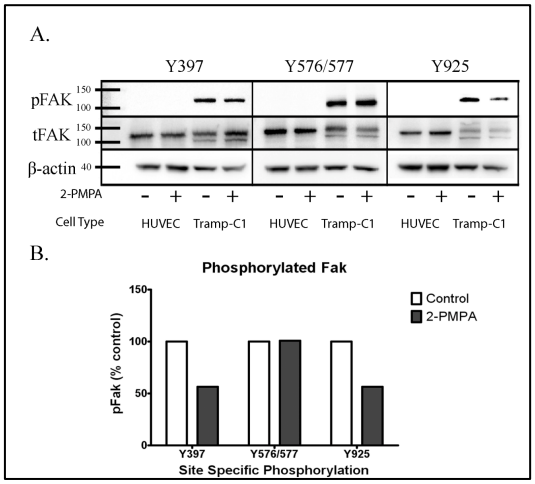

Figure 3.5- PSMA inhibition decreases FAK activation in Tramp-C1 cells. A. Representative blots showing a decrease in the amount of phosphorylated FAK in 2-PMPA treated cells compared to control at residues 397 (left) and 925 (right) but not 576/577 (center), with no change in total FAK. B. Band density was quantified and is expressed as pFAK per total FAK in the same blot. Phosphorylation at Y397 and Y925 but not Y576/577 is reduced.

3.6 PSMA inhibition decreases cell proliferation in 3-D culture.

One of the final steps in tumor metastasis relies on a cell's ability to survive and proliferate in a new site. A model to test this in vitro is by using soft agar and allowing tumor cells to grow in 3D culture. Tramp-C1 cells were grown in soft agar in the presence of 2-PMPA or under control conditions. After four weeks, the cell colonies were imaged (Figure 3.6A) and the number of colonies and average cell colony cell proliferation within a colony. However, we observed no change in the number of colonies per well (p=0.40), indicating equal cell viability in the presence or absence of PSMA inhibitor. Therefore, PSMA expression may contribute to cell proliferation in a 3-D system. PSMA inhibition significantly decreases average colony size by approximately 25% (p=0.003, Figure 3.6B), ind size were calculated. PSMA inhibition icating a decrease in

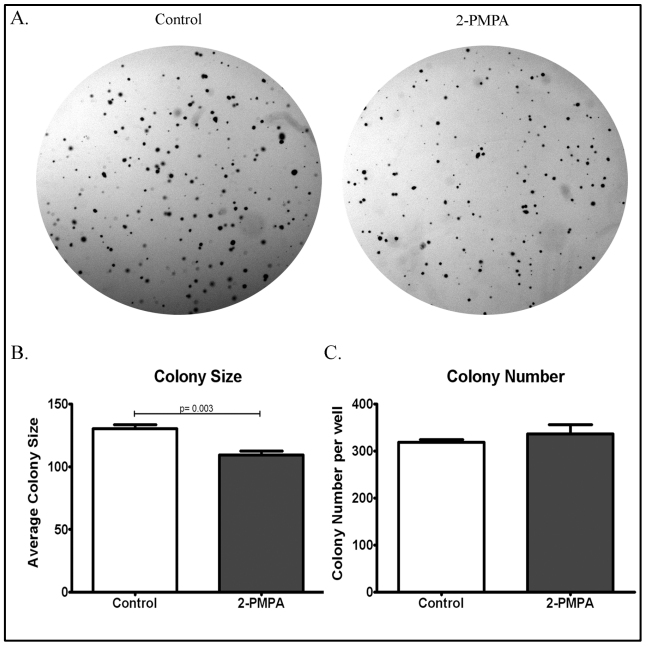

Figure 3.6- PSMA enzymatic inhibition decreases Tramp-C1 growth in 3D culture. A. Representative images of Tramp-C1 colony formation in soft agar under control (left) conditions or with 2-PMPA (right). B. Tramp-C1 cells in the control condition exhibited significantly larger colonies than the 2-PMPA treated condition, but C. no significant difference was observed in colony number.

3.7 Endothelial cell-expressed PSMA is necessary for tumor angiogenesis

PSMA expression has been described to be up-regulated on both advanced metastatic prostate cancer epithelial cells and on the neoangiogenic vessels of virtually all solid tumors. However, the relative contribution of PSMA expression on prostate cancer angiogenesis and metastasis is unclear. Therefore, we set out to mechanistically determine the relative contribution of tumor-derived vs. vascular endothelial cell-derived PSMA in tumor progression and angiogenesis. Inhibition of PSMA enzymatic activity on isolated endothelial cells leads to an integrin β1-dependent decrease in cell adhesion, migration, invasion, and capillary morphogenesis in vitro, suggesting that the extracellular enzymatic activity of PSMA is responsible for its function in angiogenesis. Additionally, lack of PSMA expression in vivo has been shown to significantly decrease pathologic angiogenesis in a well described mouse model. In a growing prostate tumor, it is conceivable that PSMA expression on neighboring tumor cells provides sufficient activity in *trans* to regulate endothelial angiogenesis. Conversely, if PSMA were required in *cis* to augment endothelial β1 integrin activation, we expect that angiogenesis would be impaired in mice lacking endothelial PSMA regardless of the amount of available extracellular PSMA. We therefore investigated whether PSMA expression in *trans* was sufficient to overcome lack of endothelial cell-expressed PSMA by using a murine prostate tumor allograft model. In this model, the tumor epithelial cells (Tramp-C1) with high levels of PSMA expression are implanted subcutaneously into wild-type or PSMA-null mice. In the wild-type mice, both tumor epithelial cells and the endothelial cells express PSMA. However, in the PSMA-null animals, the tumor epithelial cells will express PSMA but the mouse contributed endothelial cells do not. Since the enzymatic activity is in the extracellular domain of the PSMA molecule, it is conceivable that if only PSMA enzymatic function were responsible for its activity. We can use these tumors to determine if PSMA enzymatic function in the surrounding milieu (in *trans*) is sufficient to overcome the lack of PSMA expression on the endothelial cells (in *cis*) to allow tumor angiogenesis to occur.

Task 1 e-4 Tumor growth in vivo.

4.1 Lack of host PSMA expression does not decrease tumor growth, volume or mass.

To begin to examine the relative contribution of tumor cell-expressed vs. endothelial cell-expressed PSMA, Tramp-C1 cells were implanted into the dorsal flanks of 8-10 week old male mice and allowed to grow for 10 weeks. Tumors were measured over the skin and tumor volume was calculated from these measurements. Over the course of 10 weeks, there was no significant difference in the average rate of tumor growth between wild-type and PSMA-null animals (n=10-12, p=0.42 Figure 4.1A). Upon tumor harvest, final tumor dimensions were measured ex-vivo to ensure an accurate final tumor volume without variance due to underlying anatomical structure. While tumor volume was highly variable within genotype, the average tumor volume was not significantly different between tumors derived from wild type and PSMA null mice (average volume of 633.7mg ± 130.9 and 462.7mg ± 125.5 respectively; p=0.36, Figure 4.1B). Tumors were also weighed at harvest. Tumors isolated from wild type mice weighed 300-1230 mg with a mean of 589mg. Those isolated from PSMA null mice weighed 164-1615 mg with a mean of 645mg (p=0.81, Figure 4.1C).

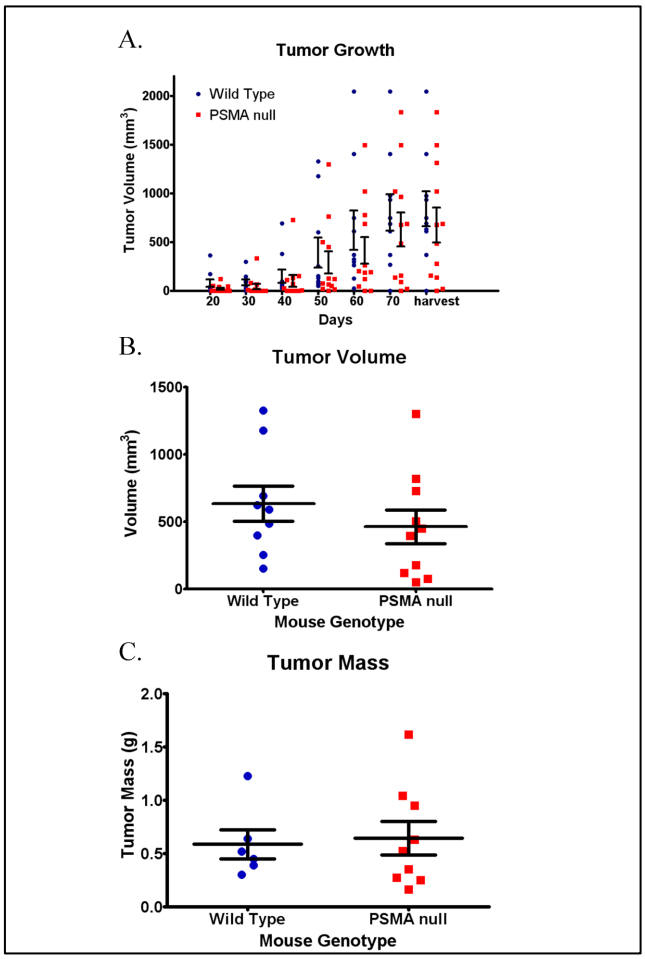

Figure 4.1- PSMA expression in the host animal does not alter tumor growth, size, or final volume. A. Tumor volume measurements over time; Tramp-C1 allografts in wild type (blue) and PSMA null (red) animals show no significant difference in growth over time. B. Final tumor volume at harvest; Wild-type (blue) and PSMA null (red) mice show similar sized allografts at 10 weeks after implantation. C. Tumor mass at harvest; Wild type and PSMA null mice show no significant difference in final tumor weight.

4.2 Lack of host PSMA expression leads to increased tumor necrosis in allografts isolated at 10 weeks.

Histological examination of Tramp C1 allograft tumors from wild type and PSMA null mice revealed a trend toward an increase in tumor necrosis in tumors isolated from PSMA null mice compared to wild type. Whole hematoxylin and Eosin (H&E) stained sections were scanned and analyzed for area of pink necrotic tissue (Figure 4.2A). Overall, there was a trend toward increased necrosis in tumors isolated from PSMA null mice compared to wild type ($p=0.11$). This trend was more apparent in tumors weighing under 500mg at harvest ($p=0.07$, Figure 4.2B). Area of necrosis was corrected for tumor size, since larger tumors had disproportionately increased necrosis.

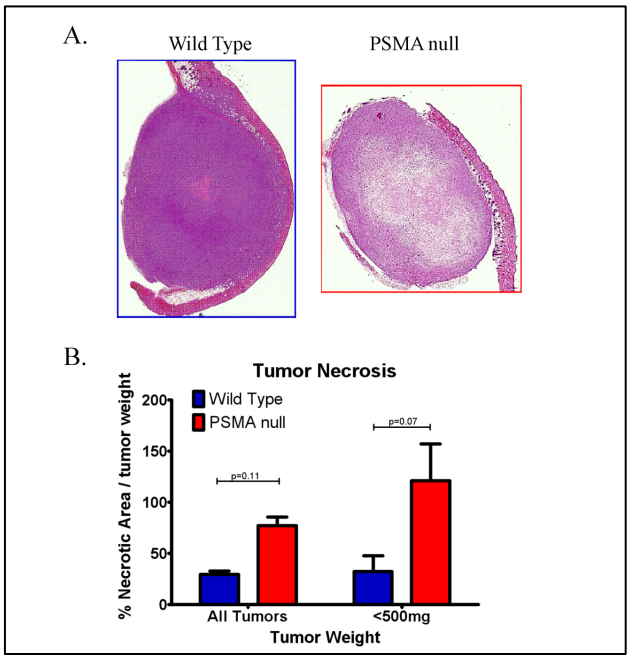

Figure 4.2- Tumors isolated from PSMA null mice show increased necrosis compared to tumors isolated from wild type mice. A. Wild type mice (blue border, left) show less tumor necrosis histologically than PSMA null mice (red border, right). B. Quantified tumor necrosis; tumors from PSMA null (red) mice show a trend of increased necrosis compared to wild type mice (blue); this trend approaches significance when analyzing smaller tumors, those weighing less than 500 mg.

4.3 Tramp-C1 allografts show similar growth rates when using tumor size as an endpoint.

Allograft studies can be performed using either time or tumor size as an endpoint. In the case of Tramp-C1 allografts, we obtained tumors which were highly variable in size and weight in using time as an endpoint. In order to analyze other tumor parameters without confounding results by highly variable tumor size, we also performed Tramp C1 allograft studies using tumor size as an endpoint for harvest. Given our above results showing more consistent results in tumors weighing under 500mg, we harvested allografts when tumors reached a volume shown to be correlated with this weight in the original study. There was no significant difference in allograft tumor formation incidence (Figure 4.3A), or time to harvest (Figure 4.3B). In addition, there was no significant difference in tumor weight at harvest (Figure 4.3C), so future analysis can be completed without the need to correct for tumor weight.

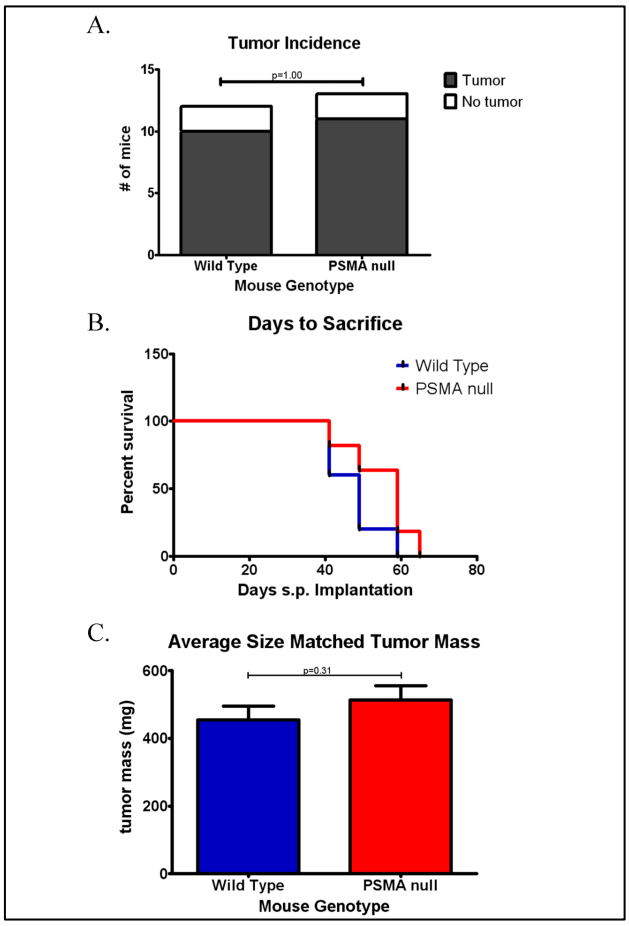

Figure 4.3- Tumors harvested using size as an endpoint show no difference in tumor growth. A. There was no difference in tumor incidence, the percent of mice where a Tramp-C1 allograft engrafted and grew within 10 weeks. B. There is no significant difference between wild type (blue) and PSMA null (red) survival, or time to tumor harvest. C. Since tumors were harvested at a volume expected to correlate with 500mg, we weighed tumors at harvest to ensure allografts were similar in weight. There is no significant difference between tumors from wild type (blue) and PSMA null (red) mice.

4.4 Lack of host PSMA expression leads to increased necrosis in tumors of similar size.

In our allograft tumors harvested at the same time point, we observed highly variable necrosis with increasing tumor size. Therefore, we examined tumors weighing 300-600mg at harvest to remove a confounding variable of tumor size. Allograft tumors isolated from PSMA null animals showed significantly more necrosis than those isolated from wild type mice ($p= 0.045$); PSMA null tumors showed a mean of 10% necrosis compared to approximately 6% in tumors isolated from wild type animals (Figure 4.3).

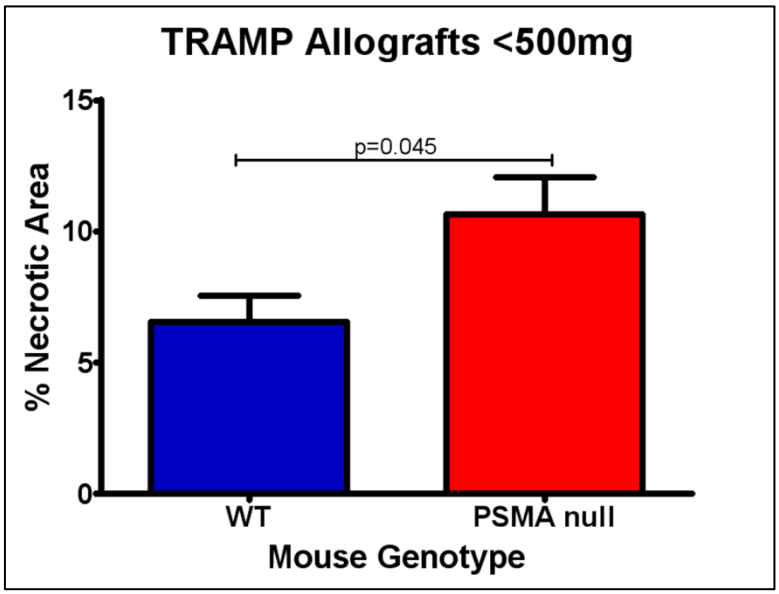

Figure 4.4- Lack of host animal derived PSMA leads to increased tumor allograft necrosis. Hematoxylin and eosin stained tumor sections were scanned using a Microtek slide scanner and analyzed for necrotic area using ImagePro software. Percent tumor necrosis is expressed as the necrotic area divided by total tumor area. Despite PSMA expression on the tumor cells of the allograft, PSMA null mice have significantly more tumor necrosis than wild type.

4.5 **Lack of host animal PSMA does not alter tumor cell proliferation.**

In order to investigate the mechanism behind the increase in tumor necrosis observed in the absence of host PSMA expression, we asked if there was a difference in tumor cell proliferation. We determined cell proliferation by quantifying the percent of Ki67 positive nuclei (a proliferation marker) in tumor sections. There was no significant difference in tumor cell proliferation between those tumors isolated from PSMA null and wild type mice (p=0.644, Figure 4.5). Thus, the increase in necrosis in PSMA null animals is not due to a difference in tumor cell proliferation.

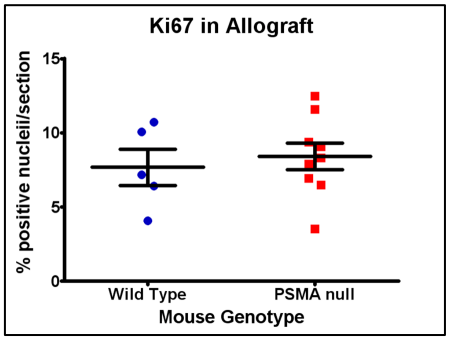

Figure 4.5- Tumor allograft proliferation is the same in wild type and PSMA null hosts. Tumor sections were stained for Ki67 expression and analyzed by two blinded observers. Positively stained nuclei in 3 fields of live tissue were counted and expressed as a percent of total nuclei observed. No difference in proliferation was observed between tumors isolated from wild type and PSMA null mice.

4.6 Allografts from PSMA null mice have significantly less angiogenesis than those from wild type mice.

Previous reports have shown PSMA to be necessary for angiogenesis into Matrigel (a basement membrane preparation) plugs in vivo. Our major question in performing allografts of PSMA positive cells into wild type and PSMA null mice was "Is PSMA expression on host endothelial cells necessary for tumor angiogenesis?" The answer to this question would help us to elucidate the relative contributions of tumor cell derived and host endothelial cell derived PSMA to tumor angiogenesis. Since PSMA expression has been shown to be necessary for angiogenic processes *in vitro* and in an in vivo model, the most logical explanation for the observed increase in tumor necrosis in tumors isolated from PSMA null mice is a lack of effective tumor angiogenesis.

To investigate this hypothesis, we stained tumor sections for CD31, (also known as PECAM, a marker for endothelial cells). Each tumor section was imaged by a blinded experimenter. Four 20x magnified images of each tumor section were analyzed for the number of CD31 positive lumens, quantified by 2 independent, blinded observers. Tumors isolated from wild type mice showed an average of 22.2 microvessels per field (Figure 4.6A, left), while tumors isolated from PSMA null mice showed an average of 17.1 microvessels per field (Figure 4.6A, right), a statistically significant difference (p=0.035, Figure 4.6B). Thus, lack of host PSMA expression leads to decreased tumor angiogenesis despite high levels of PSMA expression on the tumor cells.

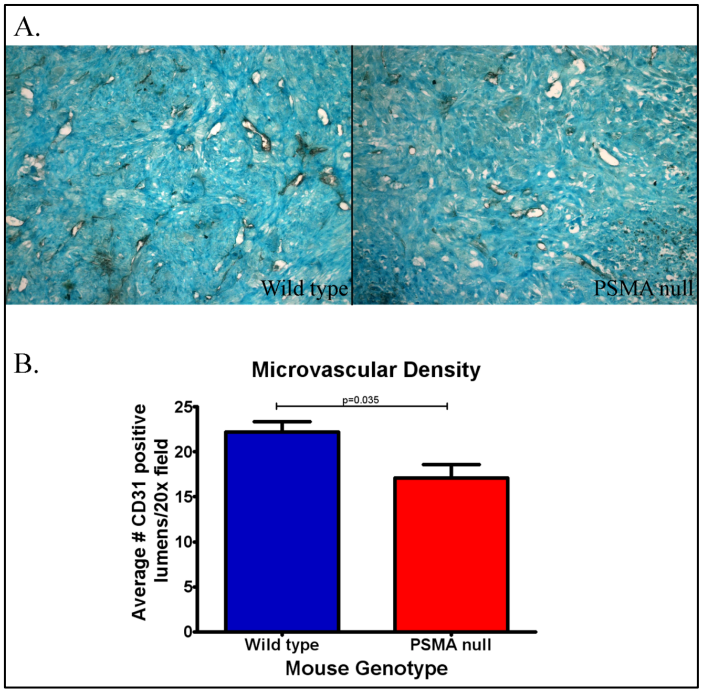

Figure 4.6- Lack of host animal expressed PSMA leads to decrease tumor angiogenesis. A. Representative images of CD31 stained histology sections of tumor allografts from wild type (left) and PSMA null (right) animals. B. There are significantly fewer microvessels in tumors from PSMA null (red) mice compared to wild type (blue).

4.7 Lack of host animal PSMA leads to a trend in increased sustained cell hypoxia.

To determine if the observed increase in tumor necrosis was attributable to decreased tumor perfusion with decreased microvascular density, we quantified the area of the tumor positive for Carbonic Anhydrase IX (CAIX), a marker of severe sustained hypoxia. We observed CAIX positive stain only in the live areas of tumor, typically surrounding areas of tumor necrosis. For example, Figure 4.7A shows a panel of serial sections of a representative Tramp C1 allograft stained with H&E with the pink areas indicating areas of necrosis, CA IX brown staining, and a merged image showing CA IX as green overlayed on H&E stained section. Therefore, the amount of CAIX stain was corrected for % live tumor in a serial section. While the increase in CAIX in tumors from PSMA null mice was not statistically significant (p=0.08, Figure 4.7B), more tumors from knockout mice CAIX staining in more than 2% of live tissue (66%) compared to wild type (17%) as shown in the frequency distribution curve (Figure 4.7C). Therefore, this trend indicates that the increase in tumor necrosis in PSMA null hosts is due to tissue hypoxia, consistent with decreased tumor angiogenesis.

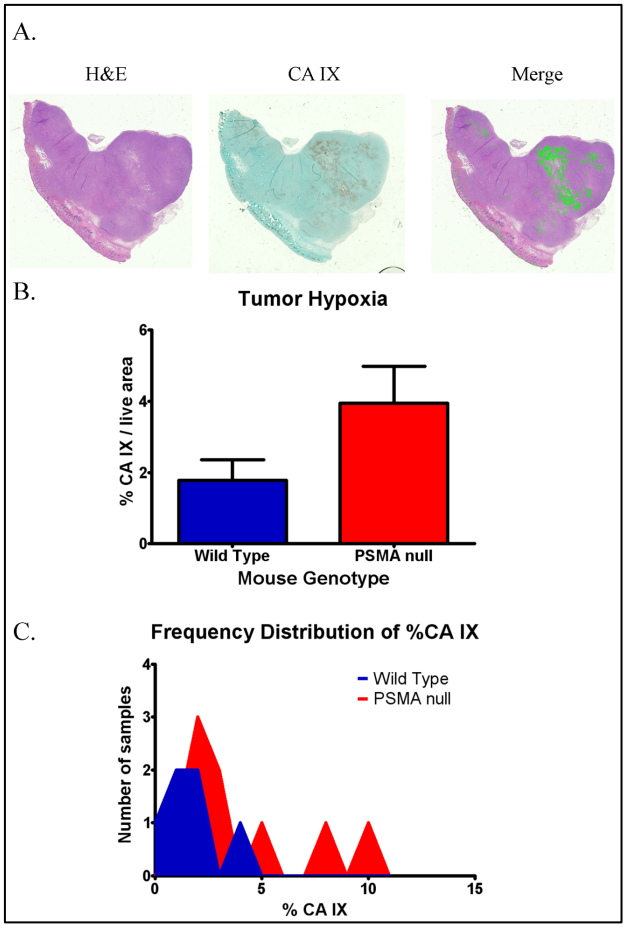

Figure 4.7- Lack of host PSMA expression leads to increased sustained tissue hypoxia. Tumor sections were stained for Carbonic Anhydrase IX (CA IX), a marker of sustained severe hypoxia. Slides were scanned using a Microtek scanner and CA IX and total tumor area were measured using Image Pro software. A. CAIX stain (center) is only expressed on live area (purple, left) as viewed in the merged image (right). B. Quantified CAIX stain; hypoxia is expressed as CA IX positive area divided by live tumor area. C. Frequency distribution shows that although the mean CAIX expression is not significantly different, allografts from PSMA null mice (red) have a higher frequency of greater than 2% CAIX stain compared to wild type (blue).

Task 1 f-1 PSMA Is Necessary For Pathologic Angiogenesis In Retinopathy Of Prematurity
Reference: Grant CL, Caromile, LA, Rahman MM, Durrani K, Claffey KP, Fong, GH and Shapiro LH. Prostate Specific Membrane Antigen (PSMA) Regulates Angiogenesis Independently of VEGF During Ocular Neovascularization. PLoS One in press 2012.

1.1 Introduction

To determine if the defects in tumor angiogenesis in PSMA null mice were tumor specific or if PSMA contributed to other forms of pathologic angiogenesis, we used the well described oxygen induced retinopathy, or retinopathy of prematurity (ROP) model.

In the Retinopathy of Prematurity (ROP) model, pups (with lactating dames) are placed in 75% oxygen from P7-P12, leading to attenuation of normal angiogenic signaling and regression of existing retinal vessels (vaso-obliterative phase). Pups are then returned to room air for P12-P17 (21% oxygen), and the lack of retinal vessels results in tissue hypoxia (vaso-proliferative phase, also call relative hypoxia). In response, hypoxia signals are up-regulated but lack the temporo-spacial organization of normal retinal angiogenesis signaling. This results in blood vessels that overgrow and are disorganized and tortuous. New capillaries vascularize the peripheral but not the central retina due to altered angiogenic signaling, and form glomerular structures in the vitreal space, beyond the inner limiting membrane of the retina, called vascular tufts. These vessels are typically immature and lack pericyte coverage found in normal retinal vessels, causing them to be leaky. Vessels have a higher potential for rupture into the vitreal space. This model is convenient for investigating *in vivo* pathologic angiogenesis because vascular networks of the retina are easily visualized in 3D space. This is in contrast to other pathologic angiogenesis models, which typically result in samples that must be examined histologically for angiogenesis. In contrast, the retina is thin enough that the vessel network does not need to be disrupted to be examined. In addition, this model is completed more quickly than the typical tumor angiogenesis model and uses physiologic (or pathophysiologic) vascular growth factors, compared to exogenous growth factors in the Matrigel plug model. In addition, the vascular tissue can be targeted systemically or topically via intravitreal injection.

Task 1 f-2 Materials and Methods

2.1 Oxygen Induced Retinopathy Model- Seven day old mouse pups and their lactating mothers were maintained in 75% oxygen for five days. After 2.5 days in 75% oxygen, the lactating females were replaced with surrogate dames. Mice were then returned to room air (relative hypoxia) for up to 5 days. Mice were euthanized humanely by CO_2 narcosis followed by decapitation. As indicated, mice were anesthetized with Tribromoethanol and perfused with fluorescently labeled RCA1 to label perfused capillaries, before enucleation. Eyes used for retinal whole mounts were pre-fixed in PFA on ice 30 minutes, retinas isolated, then post-fixed 45 minutes in PFA. After rinsing with PBS, retinas were blocked with 10% normal goat serum in PBS for 1 hour, then stained overnight 4^{o}C with the required marker or antibody. Retinas used for RNA isolation were stored in PBS or RNAlater on ice and RNA isolated using Qiagen RNA isolation kit.

2.2 Quantitative analysis of ROP- Eyes used for histology sectioning were fixed overnight in 4% paraformaldehyde (PFA) at 4^{o}C, then stored in 70% ethanol, paraffin embedded, and 6μM sections cut. To analyze the number of extra-retinal vascular tufts, paraffin embedded eyes in a sagital orientation were sectioned 6μM apart. Each eye was analyzed using 5 H&E stained sections on either side of the optic nerve; vascular tufts, defined as endothelial cells on the vitreal side of the inner limiting membrane, were quantified under 40x by a blinded observer. To quantify avascular area, retinal whole mounts were blocked using 5% normal goat serum (Zymed), then stained overnight at 4C with 0.001mg/mL Alexa594 conjugated isolectin B4 (Invitrogen I21413). After mounting whole mounts on slides, retinas were imaged using a 5x objective on a Zeiss LSM Confocal microscope and an image of the entire retina obtained using the tile-scan feature. Central avascular area was outlined in ImageJ using polygonal select tool by a blinded observer. Avascular area and total retina area were calculated using Area measure tool

and Avascular area/total retinal area was calculated. Branch points were quantified in a 40x image of the outer edge of a retinal leaflet.

2.3 Immunohistochemistry- Slides were deparafinized and rehydrated. Antigen retrieval was conducted using 10mM Sodium Citrate (pH 6.0) in a pressure cooker. Endogenous peroxidase activity was quenched by incubating slides 15' in 0.3% H2O2. Slides were blocked in 1% BSA for 30 minutes at room temperature in a humidified chamber then incubated under 1:50 3E2 antibody overnight in a humidified chamber. Slides were washed 3 times in PBS. 1:500 biotinylated secondary antibody (VectorLabs goat anti-mouse BA9200) in 1% BSA was applied and slides incubated for 1 hr at room temperature in a humidified chamber. Slides were washed 3 times, Vectastain Elite ABC Kit (Vector Labs SK-6100) was applied for 30 minutes. Slides were washed once in buffer, once in H2O, then Novared (Sigma D-4293) was applied for 5 minutes. Slides were washed in H2O, then counterstained using Hematoxylin (Vector Labs H-3404) 45 seconds room temperature, rinsed, dehydrated and mounted under Cytoseal 60.

2.4 Quantitative RT-PCR- RNA was isolated from retinas using Qiagen RNA isolation kit according to manufacturer's instructions. cDNA was produced using BioRad iScript reagent, including a reaction with no reverse transcriptase to control for DNA contamination. qPCR reaction was performed in triplicate using BioRad iQSupermix as indicated in manufacturer's directions and an Eppendorf thermocycler. Data was collected and cT were analyzed. All experimental gene levels were normalized to Cyclophillin A levels. Fold change calculations were performed using the appropriate control, the wild-type 750 retina sample in each plate. Primers used in qPCR as follows:

Cyclophillin A forward: 5'- ATGGCAAATGCTGGACCAAA-3';
reverse: 5'- TGCCATCCAGCCATTCAGT-3'
VEGF forward, 5'- CACGACAGAAGGAGAGCAGAAGT-3'
reverse, 5'- TTCGCTGGTAGACATCCATGAA -3'
PSMA forward: 5"- GATGTAGTGCCACCATACAGTG-3',
reverse: 5'- GCCAGTTGAGCATTTTTAACCAT 3'
Ang-2. forward, 5'- TCAACAGCTTGCTGACCATGAT-3'
reverse, 5'- GGTTTGCTCTTCTTTACGGATAGC-3'

2.5 PSMA Inhibition Studies

On P15 mice were anesthetized using 12.5 mg/mL Avertin (250 mg/Kg). Using a dissecting microscope, the eyelids are opened using a sterile scalpel or by gently teasing eyelid apart using jewelers forcepts. The tip of a 33 gauge needle attached to a Hamilton syringe was positioned adjacent to the pars plana, 2.5 mm posterior to the limbus, and 1uL or 10ug/uL or 1ug/uL 2-PMPA dissolved in PBS was injected into the vitreous cavity. The needle was kept in place for at least 20 seconds before being removed to prevent leakage. The eyelids were approximated over the eye and antibiotic ointment was applied. The opposite eye was injected with sterile PBS as a control. Mice were monitored until regaining consciousness then returned to the home cage.

For systemic inhibition studies, 100mg/kg or 50 mg/kg 2-PMPA (10mg/mL) in sterile PBS was injected intraperitoneally using a 30 gauge needle on the days indicated. Sterile PBS was injected into control mice.

Task 1 f-3 Results and Discussion

3.1 Wild Type mice in the ROP model express PSMA

To determine if the ROP model of pathologic angiogenesis was appropriate to examine the role of PSMA, we first determined if PSMA was expressed in the retinal neovasculature during angioproliferation. Retinas isolated from wild type mice undergoing ROP on P17 were analyzed for PSMA expression by conventional RT-PCR and immunohistochemistry. Product consistent with the expected size for PSMA

was observed in 3 independent wild type retinas and 2 positive controls, but not in the negative control (Figure 5.1A). To ensure that PSMA expression was on the neovasculature and not solely due to background from the neural tissue, immunohistochemistry was performed. PSMA staining was observed on both retinal neural tissue and on a retinal neovascular tuft (arrow, Figure 5.1B) in an ROP retina isolated from a wild type mouse, but no staining was observed on the extra-retinal vascular tufts in a PSMA null ROP retina (arrows, Figure 5.1C). Therefore, PSMA is expressed on the neovasculature in wild-type mice undergoing ROP.

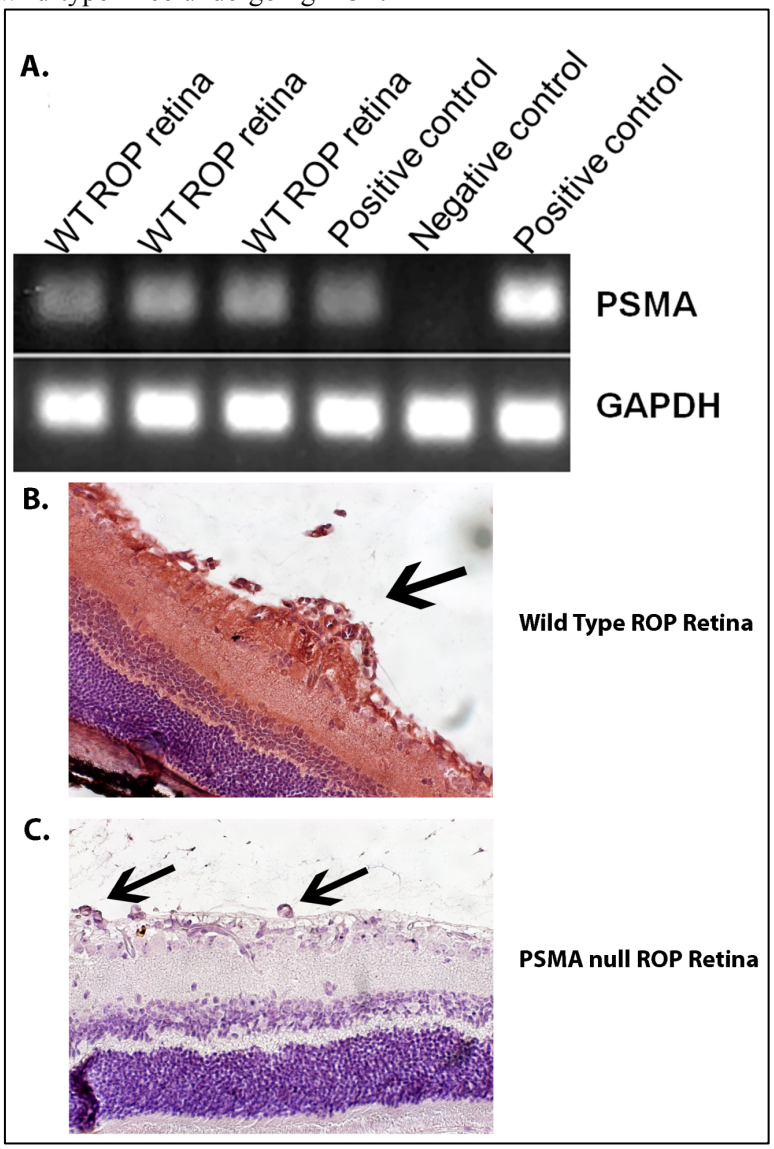

Figure f-3.1- A: Conventional RT-PCR of RNA isolated from wild-type ROP retinas shows a product of the expected length for PSMA; known PSMA positive samples also show product, while known PSMA negative samples do not.
B-C: Paraffin embedded ROP retinas were immunostained for PSMA. Staining (red-brown) was observed on vascular tufts (arrows) of wild-type (B) but not PSMA-null (C) retinas.

3.2 PSMA null mice have normal developmental retinal angiogenesis.
To ensure that PSMA null mice have normal developmental retinal angiogenesis, retinas were isolated from postnatal-day 19 mice (P19) and vessels stained with fluorescently labeled GS Isolectin β4, a sugar

binding protein that labels endothelial cells. Whole mounts of both wild type and PSMA null mice show normal radial vessel patterning, with vessels perfusing the entire area of the retina (Figure 5.1). Upon closer inspection, inset 40x magnified images of the mid periphery show a branched pattern of vessels with space between them, which allows light to pass through to the neural layers.

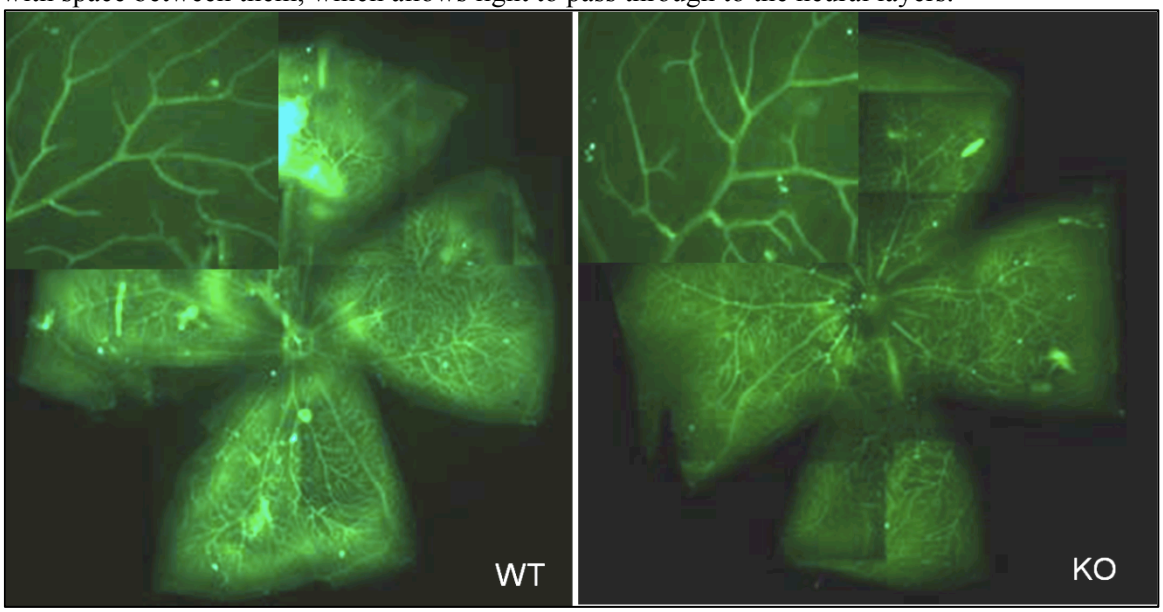

Figure f-3.2- Loss of PSMA does not affect development of normal retinal vasculature. Normal P19 retinas from wild-type (left) and PSMA-null (right) animals. Insets are higher (40X) magnification of the same retina and show normal radial branching pattern in both wild type and PSMA null animals.

3.3 PSMA null mice showed a less pathologic angiogenic phenotype than wild-type animals in the ROP model.

Retinas isolated from P17 pups (the most severe degree of vasculoproliferative disease) were examined to determine the degree of pathologic angiogenesis. Wild type mice show the expected hypo-perfused avascular central area and an overgrowth of vessels in the periphery (Figure 5.3A). The capillary structure in the mid periphery is a honey-combed pattern with vessels spaced closely together, instead of a radial branched pattern expected in mice raised in room air (Figure 5.3B). In contrast, retinas isolated from PSMA null animals show a more normal pattern, with less avascular central retina and a more branched (yet still with a degree of honeycombed, disorganization) capillary bed in the periphery (Figures 5.3C and 5.3D).

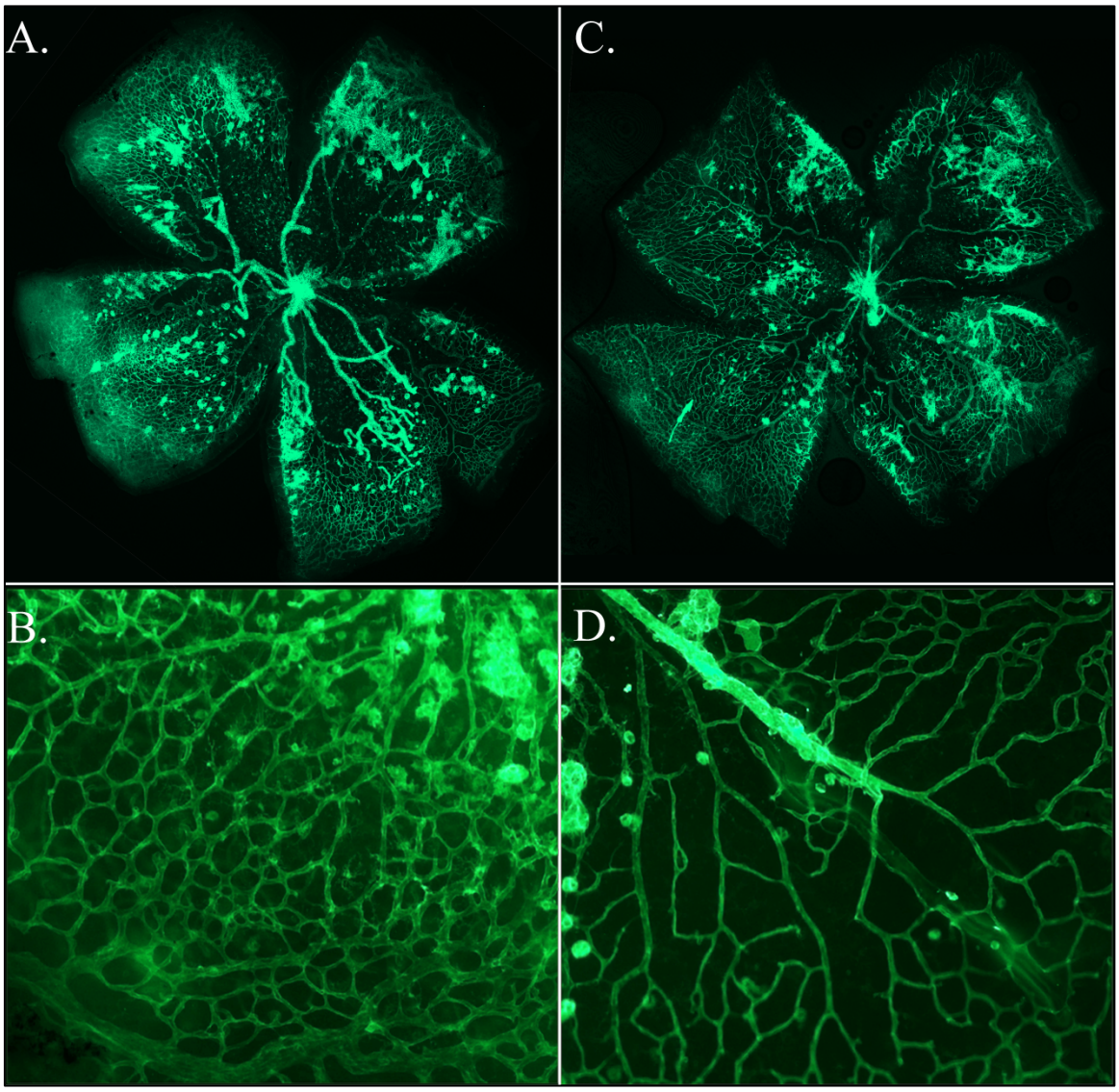

Figure 3.3- **A, C**. Whole mount retinas stain with fluorescent conjugated lectin to stain endothelial cells. Wild type retinas in the ROP model (A) show more central avascular area than retinas from PSMA null mice (C). **B, D.** Higher magnification views of wild-type and PSMA-null capillary networks at the outer edge of the retina: Retinas isolated from wild-type mice (B) show disorganized, tortuous vessels and vascular tufts. In contrast, the vessels in PSMA-null retinas (D) are less tortuous and more closely resemble normal organization.

3.4 PSMA null mice show significantly less central avascular area and significantly fewer extra-retinal vascular tufts.

When quantified, PSMA null animals showed significantly less central avascular area than wild type animals. Wild type mice showed an average of 28.7% avascular area at P17, compared to 18.4% avascular area in the retinas isolated from PSMA null mice, approximately 40% decrease (n=4 per group, p=0.004, Figure 5.4A).

In addition to a decrease in retinal avascular area, the number of extra-retinal vascular tufts (glomerular-like capillary structures growing beyond the inner limiting membrane into the vitreous of the eye) is significantly decreased in PSMA null animals compared to wild type controls. Wild type animals had an

average of 8.8 vascular tufts per histologic section, compared to an average of 5.2 tufts per section in PSMA null eyes (n=8 per group, p=0.017, Figure 5.4B).

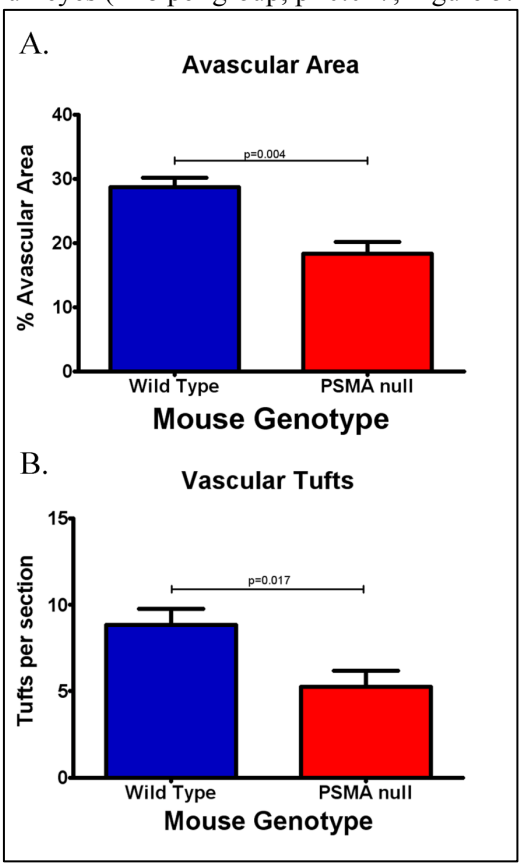

Figure 3.4- A. The area of each retinal whole mount free of capillaries was determined using Image J Software, and is represented as capillary-free area divided by total area. The PSMA-null animals have less capillary-free retinal area than the wild-type animals. **B**. Vascular tufts (defined as cells on the vitreal side of the inner limiting membrane) in sections of paraffin embedded retinas were counted under 40x magnification. PSMA-null mice had less vascular tufts per section than wild-type mice.

3.5 Wild type and PSMA null mice show no difference in microvessel perfusion in ROP.

To ensure that the differences observed in vessel density and pattern between wild type and PSMA null animals was due to perfused vessels (and not to an overgrowth of non-perfused endothelial cells in wild type mice) we perfused animals undergoing ROP with FITC labeled Ricin communis A (RCA-FITC, binds to endothelial cells it comes into contact with) immediately prior to sacrifice and retinal harvest. Both wild type and PSMA null animals show RCA-FITC signal co-localizing with of virtually all lectin stained vessels, indicating that the observed difference in avascular area and microvessel patterning is due to patent, perfused vessels, and not to an overgrowth of single non-perfused endothelial cells (Figure 5.5A). Whole mount retinas imaged for both RCA FITC and lectin-594 were merged using Adobe Photoshop to show red (lectin) only where it was not co-localized with green (perfused RCA) stain. Retinas isolated from both genotypes show lectin staining large glomerular like structures which lack FITC staining (extra retinal vascular tufts) indicating a large mass of non-perfused endothelial cells. While there appears to be a greater amount of non-co-localized lectin staining in the wild-type retinas compared to PSMA null (Figure 5.5B), this correlates with the decrease in extra-retinal vascular tufts in the PSMA null mice described above.

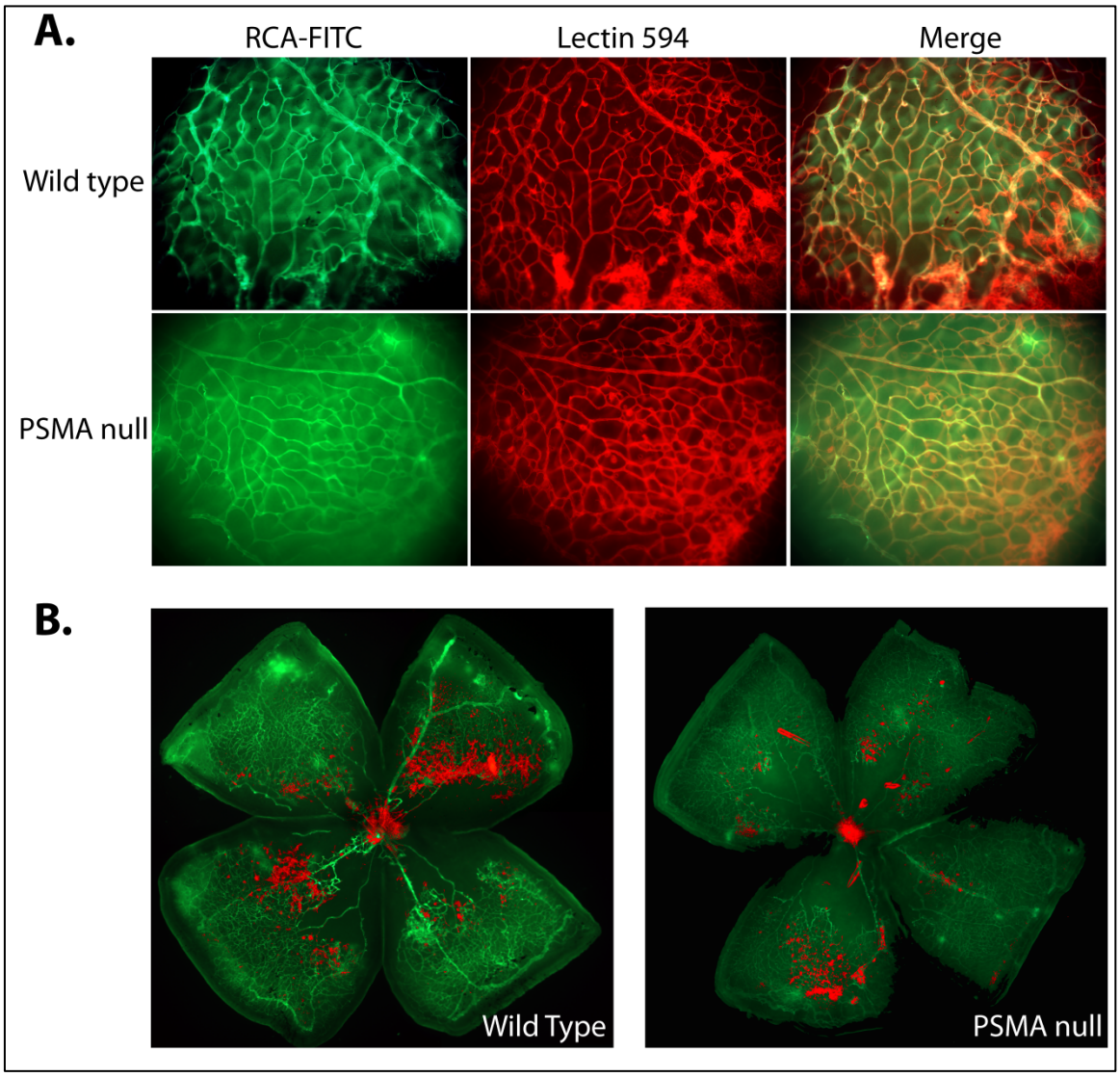

Figure 3.5- Wild type and PSMA null animals show similar perfusion of lectin stained vessels. ROP mice were given RCA-FITC via cardiac puncture, to labeled perfused endothelial cells, prior to sacrifice and then stained with lectin 594 to stain all endothelial cells. **A**. Panel showing RCA staining (right), lectin staining (center), and a merged image (left) of representative wild type (top) and PSMA null (bottom) retinas. **B**. Perfusion stain of whole flat mount retinas show similar vascular bed pattern to lectin stained retinas. Images were merged to show red (lectin) only in areas not co-localized with green (RCA perfusion), and non-perfused endothelial cells are observed only in the glomerular structures of the retinas correlating with vascular tufts.

3.6 PSMA abrogates pathology in the ROP model during the vasculoproliferative phase but not the angio-obliterative phase.

To determine which stage in the ROP model is PSMA dependent, we harvested retinas from pups undergoing the ROP protocol at different stages: P12 immediately after hyperoxia, corresponding with the highest degree of vascular regression, P15 corresponding with the beginning of retinal revascularization, and P17 exhibiting the most severe angiogenic pathology observed in the model (n=3/group Figure 5.6A). Avascular area was quantified (Figure 5.6B); we found that PSMA null animals have the same amount of central avascular area as wild-type on P12 (35.7% and 32.8%

respectively, p=0.58). At P15, there is a trend toward decreased central avascular area in the PSMA-null animals compared to the wild-type (24.6% PSMA null, 31.4% wild type, p=0.14), and on P17 PSMA-null animals show a significant decrease in central avascular area (7.4%) compared to wild-type (17.1%, p=0.01). This indicates that the observed decrease in retinal angiogenic pathology in the PSMA-null mice is due to a decrease in angiogenesis during the angio-proliferative phase of relative hypoxia, not due to a persistence of retinal vessels during the angio-obliteration phase of hyperoxia.

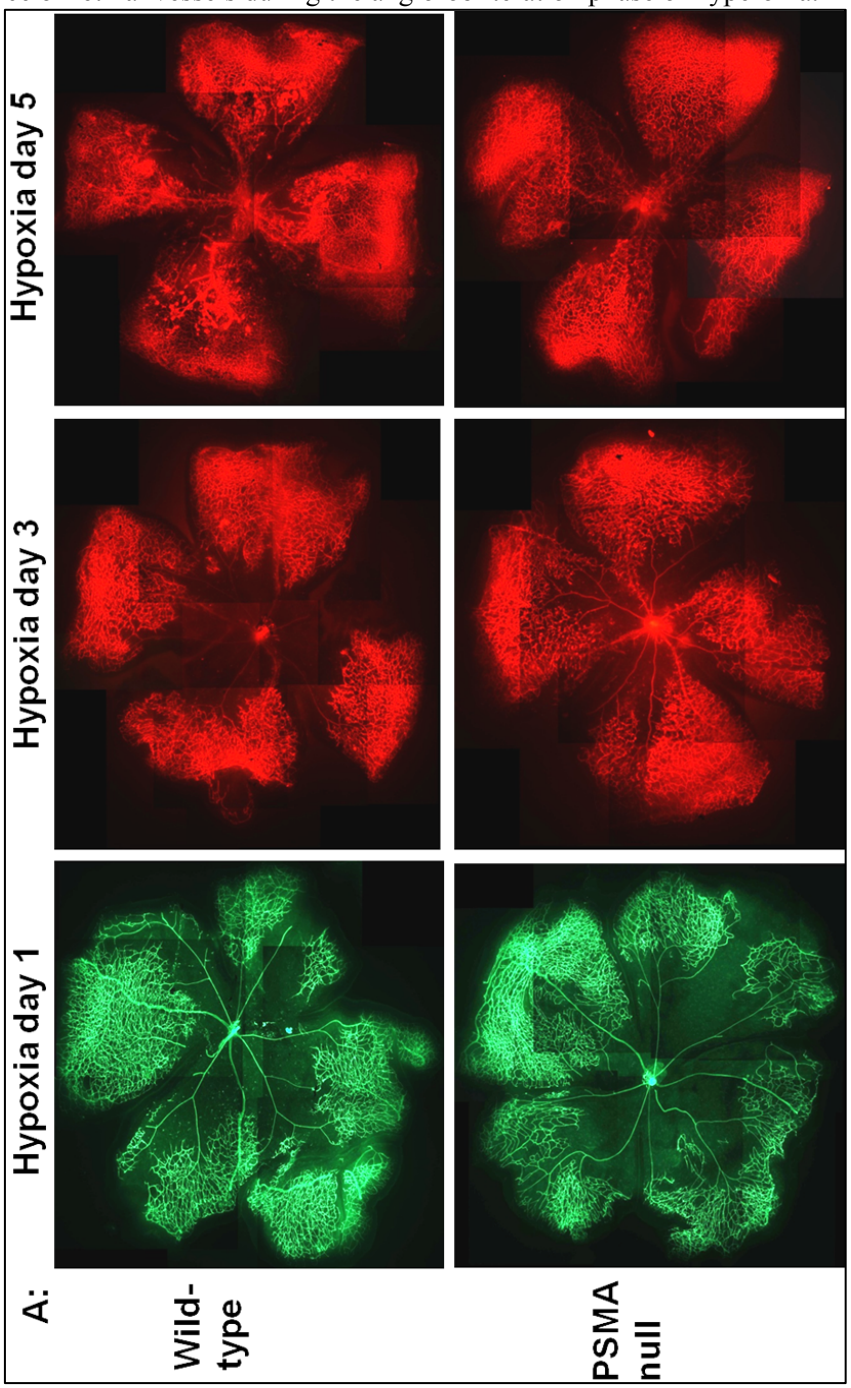

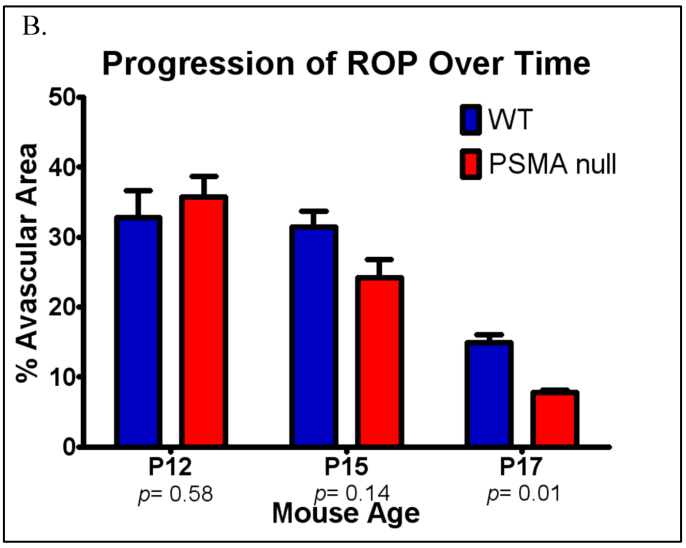

Figure 3.6- Lack of PSMA leads to a decrease in vascular pathology in the Retinopathy of prematurity model. **A**. Retinas were harvested from mouse pups exposed to hyperoxia in the ROP model immediately after hyperoxia (P12, left), and during the relative hypoxia vasoproliferative stage (P15, center and P17, right). **B**. Vasculature was stained using GS Isolectin β4 and the central avascular area of each retina was measured using ImageJ software. Retinas isolated from wild type and PSMA null animals show no difference in avascular area on P12, indicating that the existing vessels regress to the same degree during the hyperoxia treatment. There is a trend toward decreased avascular area in retinas isolated from PSMA null animals compared wild type on P15, and a statistically significant decrease in central avascular area in retinas of PSMA null mice compared to wild type on P17, indicating that the PSMA null mice have less pathologic angiogenesis than wild type mice.

3.7 PSMA expression is significantly increased on P16 and P17

We used quantitative RT-PCR to determine the relative expression levels of PSMA over time during the relative hypoxia phase of the ROP model. We expected PSMA to increase by at least P15 until P17, since these times are when we observed a decrease in pathology in the PSMA null mice. We calculated the fold difference in PSMA expression using P12 as reference. P13 has significantly less PSMA expression ($p=0.0006$). P14 and P15 are not significantly different from P12 ($p=0.586$ and 0.548) but are significantly increased compared to P13 ($p=0.0045$ and 0.083). P16 has a statistically significant approximately 4 fold increase in PSMA expression over P12 and P14-15 ($p<0.0001$ in both cases) and P17 PSMA remains significantly elevated, approximately 2-fold over P12 ($p=0.034$ Figure 5.7).Therefore, PSMA expression decreases after 1 day of tissue hypoxia, after which it significantly increases reaching a peak increase at P17.

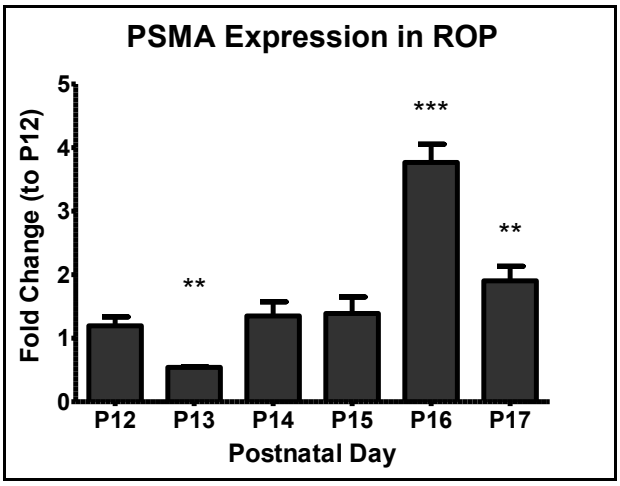

Figure 3.7- PSMA expression in the ROP model of time. When measured by qRT-PCR, PSMA expression decreases after 1 day of tissue hypoxia, after which it increases over time to peak at P16 before slightly decreasing at P17. This expression data correlates well with our observations of when PSMA null mice show decreased angiogenesis in the model. **p,0.05, ***p,0.001.

3.8 VEGF and Ang-2 mRNA levels are not different between wild type and PSMA null mice in the ROP model.

To determine if the decrease in angiogenic pathology in PSMA null mice was due to a decrease in hypoxia signaling, we examined the levels of VEGF (a significant regulator of angiogenesis) and Angiopoietin-2 (Ang-2, which also drives angiogenesis in the presence of VEGF) in ROP retinas over time using quantitative RT-PCR. Normally, VEGF increases about 2-3- fold on P13, and remains elevated until P17. We performed qRT-PCR on retinas isolated on each day of relative hypoxia (n=2 per time point) for VEGF levels. Fold change is relative to average of P12, immediately following hyperoxia. In wild type mice, VEGF levels increased by about 2.5-fold on P13 and remain elevated through P17. There is no statistically significant difference between VEGF levels in wild type and PSMA null retinas (Figure 3.8A). Ang-2 levels typically remain low until P16-17, when they increase by approximately 10-15 fold. We observed a 5-fold increase in wild type retinas on P17, and an approximately 10-fold increase in PSMA null animals on the same day. However, these results were highly variable and were not statistically different (Figure 3.8B).

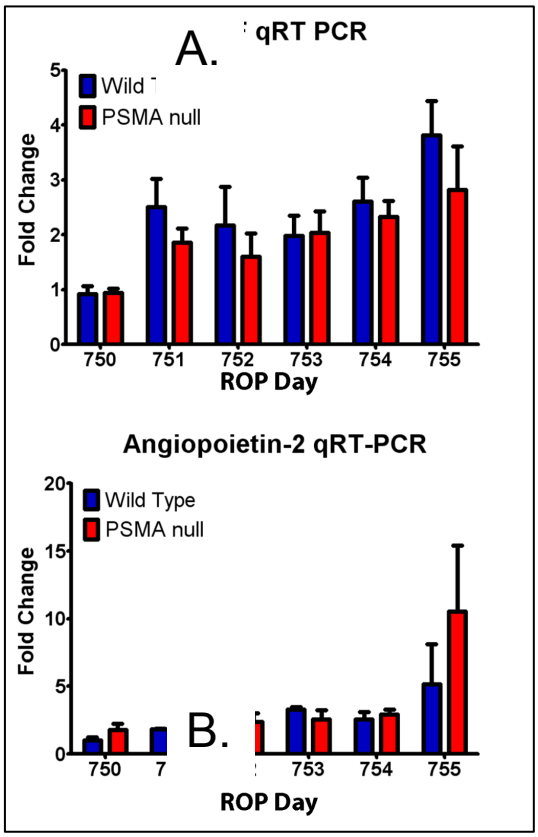

Figure 3.8- Wild type (blue) and PSMA-null (red) mice show similar levels of VEGF and Ang-2 over time. **A**. PSMA expression does not alter VEGF expression in ROP, with a 2 fold increase on P13 sustained until P17. **B**. PSMA null mice show similar Ang-2 levels to wild type mice over time.

3.9 Wild type and PSMA null mice show equal retinal neuronal survival.

PSMA inhibition has shown to be protective in retinopathy models of acute ischemia. To evaluate whether PSMA null mice show decreased pathology due to a decrease in excitotoxic effects from lack of PSMA in the neural layers of the retinal, we measured the width of the inner and outer nuclear layers, which would show a decrease with neural tissue death. After five days of tissue hypoxia, we observed no significant difference between wild type (Figure 3.9A, left) and PSMA null (Figure3.9, right) mice in either neuronal nuclear layer thickness ($p=0.367$ in the ONL and $p=0.266$ in the INL, Figure 3.9B)

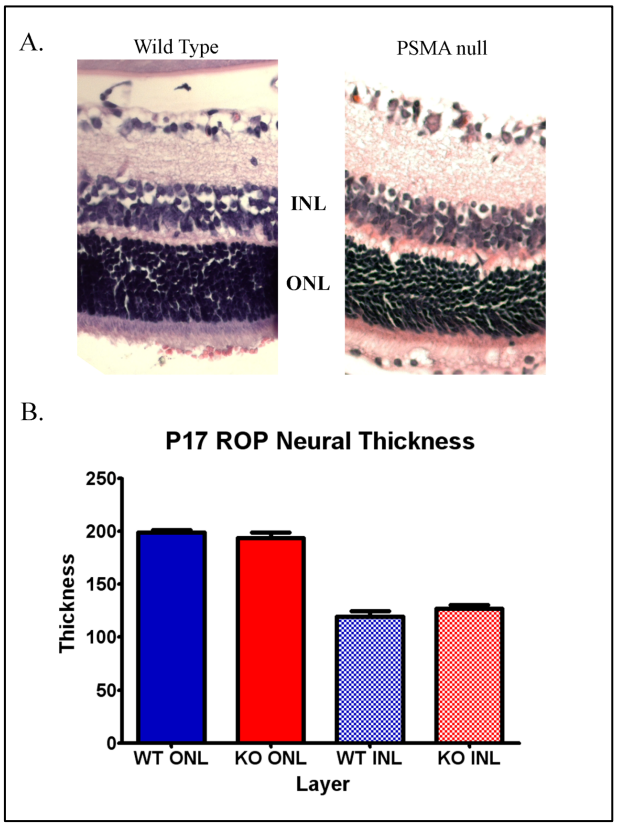

Figure 3.9- There is no difference in neural nuclear layer thickness between wild type and PSMA null mice in the ROP model. **A**. Representative images of wild type (left) and PSMA null (right) retinal cross sections showing equal layer thickness. **B**. Nuclear layer thickness was quantified. We observed no statistically significant difference in nuclear layer thickness between wild type and PSMA null mice.

3.10 Exogenous PSMA inhibition with 2-PMPA in wild type mice recapitulates the phenotype observed in PSMA null mice.

To determine if exogenous inhibition of PSMA recapitulates the decrease in retinal pathology observed in PSMA null mice in the ROP model, we used the small molecule inhibitor 2-PMPA. In Figure 5.10, wild-type mice in the ROP protocol were treated systemically with 100mg/kg 2-PMPA on either P14 (day 3 of relative hypoxia) or from P14-P16 (days 3-5 relative hypoxia) (Figure 3.10 A-B). Due to inherent variability in avascular area between groups of pups in the ROP model, data are expressed relative to the control from within the same ROP replicate. Wild-type mice treated only on P14 showed a slight but not statistically significant decrease (16%) in avascular area compared to vehicle control (n=4 p=0.099). Wild-type mice treated on P14-P16 showed a statistically significant 23 percent decrease in avascular area compared to control (n=7, p=0.005). PSMA-null animals treated on P14 (18% increase, n=4, p=0.67) and from P14-P16 (12% decrease, n=4, p=0.25) showed no significant change in avascular area compared to vehicle treated control (Figure 3.10C).

We treated wild-type and PSMA null mice in the ROP model with intravitreal 2-PMPA to determine if local PSMA inhibition would also pheno-copy the results observed in PSMA null mice. 10ug of 2-PMPA (10mg/ml) was injected into the vitreous of the eye on P15. 1uL vehicle (PBS) was injected into the contralateral eye as control. A high degree of variability between mice was observed, most likely due to effects of anesthesia on individual mice. Therefore, data is expressed relative to control eye in each mouse. In wild-type mice, the retina treated with 2-PMPA showed statistically less avascular area (16.66%) than the retina from the vehicle injected eye (Figure 5.10D, n=3, p=0.04). PSMA-null mice showed no significant difference between treated and vehicle control eyes (Figure

5.10E, n=3, p=0.767). While the degree of the decrease in pathology was not as striking as in the systemic treatment, we expect that repeated 2-PMPA injections would increase the differences. However, due to the size of the mouse eye, we are able to perform only 1 injection without inflicting confounding trauma to the eye.

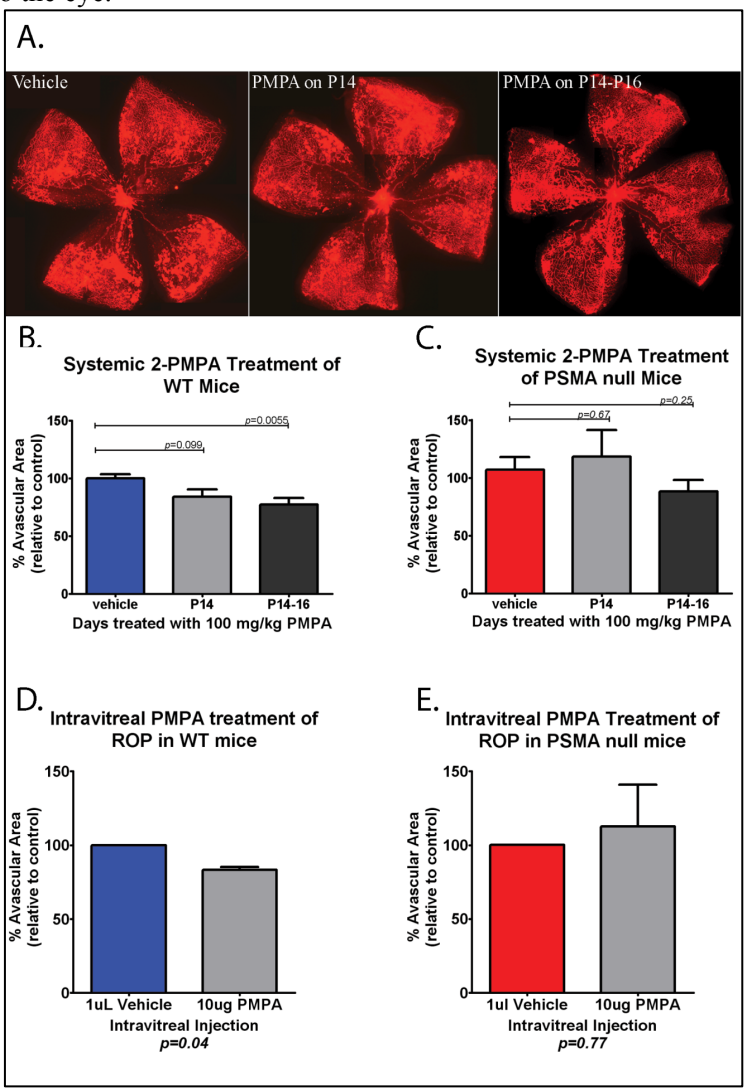

Figure 3.10- PSMA inhibition leads to a decrease in pathologic angiogenesis in a mouse model of retinopathy of prematurity. **A**. Wild type mouse pups treated with hyperoxia in the ROP protocol were treated systemically with 100mg/kg 2-PMPA on either P14 (day 3 of relative hypoxia, n=3, center) or from P14 through P16 (days 3-5 relative hypoxia, n=6, left), controls received vehicle (PBS, right). **B**. Retinas were isolated on P17 and avascular area calculated using Image J software. Mice treated on P14 showed a slight but not statistically significant decrease in avascular area, and mice treated from P14-16 showed a significant decrease in avascular area compared to vehicle treated controls (p=0.0055). **C**. PSMA null mice in the ROP model treated systemically with 100mg/kg 2-PMPA in the same manner as wild type mice in A showed no difference in avascular area compared to control. **D**. Wild type mice treated with hyperoxia in the ROP protocol were treated on P14 with 10ug intravitreal 2-PMPA (10mg/ml, 1uL) in one eye and 1uL Vehicle (PBS) in the contralateral eye. Retinas treated with intravitreal 2-PMPA showed a significant decrease in avascular area compared to control retinas. **E**.

PSMA null mice treated in the same manner as in **D** do not show a difference in avascular area with intravitreal 2-PMPA, indicating that the effect observed in wild type mice is specific to PSMA inhibition.

3.11 **Constitutively active FAK increases ROP vascular pathology in PSMA null mice.**

Previous results indicate that PSMA modulates β1 integrin signaling through FAK phosphorylation. Therefore, we set out to determine if expressing constitutively active FAK in PSMA null retinas undergoing angio-proliferation in the ROP model could "rescue" the pathology observed in wild type mice. Plasmids for IL2R FAK driven by a CMV promoter were injected intravitreally on P12. The contralateral eye was injected with a plasmid encoding GFP (PSMA null eyes) or with PBS (wild-type eyes). Retinas were harvested on P17 and retinas stained for vessels, and whole mounts of the retinas were analyzed. Retinas from PSMA null mice injected with constitutively active FAK show a trend in increased central avascular area, consistent with the phenotype observed in wild type mice. Two out of 3 mice showed an approximately 2-fold increase in avascular area compared to control (Figure 3.11A). In the wild type mice, one mouse (out of 2 injected) showed a similar increase in avascular area (Figure 3.11B). While these results are not conclusive, it supports our hypothesis that PSMA modulating β1 integrin signaling through FAK to contribute to disorganized vessel overgrowth in the ROP model.

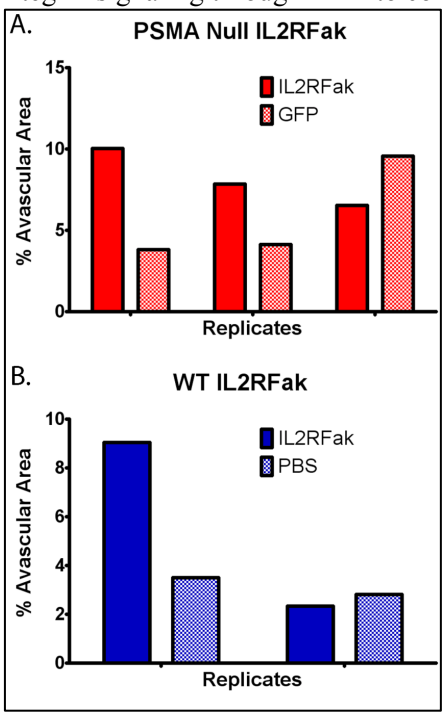

Figure 3.11- Expressing constitutively active IL2RFAK in the retinas of PSMA null mice rescues the pathologic phenotype in ROP. **A**. Two of 3 mice showed a rescue of the pathologic phenotype with reconstitution of active FAK. **B**. One of the wild type mice treated with IL2RFAK showed an increase in avascular area compared to the control eye. Therefore, the over-expression of constitutively active FAK leading to increased retinal pathology is not PSMA specific. However, it supports our hypothesis that lack of PSMA and decreased FAK signaling lead to the abrogated pathologic angiogenic response observed in PSMA null mice.

Task 1- RELATIONSHIP OF FINDINGS WITH PREVIOUSLY REPORTED FINDINGS:

Prostate Specific Membrane Antigen (PSMA) was originally described as a marker of prostate cancer (PCa) progression where its expression was upregulated on advanced and metastatic PCa but not on low grade carcinoma or benign prostatic disease. Although PSMA expression is used as a target for clinical therapeutics, its functional role in PCa disease progression and metastasis remains unknown. Therefore, we set out to determine if a lack of PSMA expression could decrease prostate cancer disease parameters in a murine model of prostate cancer, the Transgenic Adenocarcinoma of the Mouse Prostate (TRAMP) model. To date, we have harvested and analyzed prostate tumors from 30 week old wild type and PSMA null TRAMP mice, a time point well described to correlate with both late stage PCa and to exhibit 80-100% metastasis to liver, lung, and lymph nodes in wild type animals. We predicted that if PSMA was necessary for disease initiation, progression, or metastasis that we would observe a difference in tumor incidence, grade, or metastasis. However, we observed no difference between wild type and PSMA null mice at the 30 week time point. All TRAMP positive animals (by genotype) exhibited tumor grades corresponding with well differentiated carcinoma or more advanced disease in at least one prostate lobe. Thus, in this model, PSMA is not necessary for prostate cancer initiation. Additionally, there was no significant difference in mean tumor weight or tumor score between wild type and PSMA null mice at 30 weeks. Both wild type and PSMA null cohorts showed a wide range of tumor grade scores, from well differentiated carcinoma to poorly differentiated gross tumors. However, analysis of earlier timepoints show significantly smaller tumors that are less aggressive and progress more slowly.

These results indicate that PSMA expression influences PCa progression but not initiation or incidence. However, there are drawbacks to the TRAMP model in evaluating functional contribution of molecules to PCa progression. PCa formation in the TRAMP model is induced by SV40 Large T Antigen driven by an androgen sensitive probaicin promoter. Since the TRAMP model uses SV40 Large T Antigen to drive tumor development, it is possible that the loss of p53 and Rb is significant enough to overcome any effect the loss of PSMA may have on tumor parameters. However, any transgenic model may be too robust to determine the effect of PSMA loss on prostate cancer progression, and other available models have not been shown to recapitulate the progression of prostate cancer seen in humans as well as the TRAMP model.

We found that tumor grade and metastasis in the 18 week old TRAMP mice were less in the PSMA null mice, although tumors were evident in all of the mice. 18 week old TRAMP mice have been described to exhibit some metastasis to lymph nodes and liver, albeit at a reduced rate compared to the 30 week mice. We found that at 18 weeks, the PTEN and Akt pathways are active in wild type but less so in the null tumors, and that PSMA is in a precipitable complex with PTEN strongly suggesting that PSMA regulates its activity to slow tumor progression.

Another consideration for these unexpected results is the effect of mouse background; however, the background of both WT and PSMA mice is C57BL6; therefore any differences seen in tumor parameters will be attributable to the presence of PSMA without extraneous genetic background effects. PSMA is not highly expressed in early stages of prostate cancer, and early neoplastic changes are typically not large enough to necessitate angiogenesis, therefore we do not expect a difference in tumor incidence between wild-type and PSMA-null mice at the earlier 8 week time point. Since PSMA chemical inhibition had no effect on cancer cell viability or proliferation except in anchorage independent growth *in vitro*, lack of PSMA on tumor cells alone is not expected to cause a decrease in tumor size and in fact did not on the tumors already analyzed.

Another exciting future study would be to treat wild type TRAMP mice with PSMA inhibitors. Given that PSMA expression is not unique to tumors and its expression is more highly upregulated on advanced tumors than less advanced, it is not clear at which point inhibition could hinder cancer progression, and could in fact cause side effects if inhibition acts in other areas, such as nervous system or gastrointestinal

tissue. The fact that we see less aggressive tumors even at 8 weeks may may indicate that early intervention with external PSMA inhibition may be beneficial.

Our in vivo studies have identified a significant difference in tumor phenotype, our in vitro results indicate an important role for PSMA in cell processes necessary for tumor cell metastasis. Using the Tramp-C1 cell line, isolated from the above described TRAMP model by Greenberg's lab[3], we investigated the influence of PSMA enzymatic activity on cell processes imperative to metastasis. In order for a tumor cell to metastasize, it is required to escape from the tumor environment including migration through the basement membrane. The cell must then survive in the circulation and adhere to the vessel wall. Once adhered to a vessel in a new environment, the cell then invades through the endothelial cell layer and surrounding basement membrane into the new environment. In order for a single tumor cell to evolve into a metastatic focus, it must remain adherent to the ECM in the new environment and not only survive but proliferate.

To determine if the Tramp-C1 line is an appropriate model for *in vitro* analysis, we evaluated whether it expresses both PSMA and β1 integrin (which has been shown to be involved in PSMA contribution to endothelial cell angiogenic functions[4]). We used the small molecule PSMA inhibitor 2-PMPA to evaluate the contribution of PSMA to metastatic functions. 2-PMPA is suitable because it does not affect cell viability or proliferation in monolayer culture, which had the potential to affect the outcome of quantitative assays.

PSMA activity has previously been shown to regulate endothelial cell adhesion via β1 integrin. Integrins regulate cell adhesion and motility by interacting with extracellular components, such as ECM, and undergoing outside-in signaling leading to a cascade of signal transduction. Since β1 integrin expression has been shown to increase with tumor cell metastasis, and to be involved in prostate cancer cell adhesion [5-8], we examined whether PSMA positive prostate cancer cells exhibited PSMA dependent adhesion in a manner consistent with mediating β1 integrin mediated ECM adhesion. In both Tramp-C1 murine prostate cancer cells and LnCaP human prostate cancer cells, PSMA inhibition significantly decreases cell adhesion to laminin and laminin-containing ECM, but not to other ECM such as collagen or fibronectin, consistent with β1 integrin activity. In addition, 2-PMPA did not show non-specific effects in ECM adhesion in a PSMA non-expressing prostate cancer cell line, DU145.

We also showed the PSMA contributes to cancer cell invasion through the laminin-rich ECM Matrigel in both murine and human prostate cancer cell lines. This functional contribution of PSMA to the cellular process of cell invasion through ECM is an important key to cancer metastasis, the tumor cells' ability to invade into a new environment to form a new metastatic focus.

Both cell adhesion to and invasion through ECM require well-regulated signaling pathways. An important signaling molecule involved in both processes is Focal Adhesion Kinase (FAK)[9,10] previously shown to be inhibited by PSMA inhibition in adhering endothelial cells[4]. Consistent with PSMA contributing to β1 integrin activation, we observed a decrease in FAK phosphorylation with PSMA inhibition in Tramp-C1 cells.

Interestingly, when we investigated specific tyrosine phosphorylation sites, Y397 and Y925 showed decrease in phosphorylation with PSMA inhibition, while Y567/577 showed no change. In the inactive form of FAK, the Y397 auto-phosphorylation site is concealed by the FERM domain in the FAK molecule. Upon integrin activation and binding to the FERM domain, the Y397 site is exposed and auto-phosphorylation occurs[10]. Therefore, the increased pFAK Y397 with PSMA activity substantiates a role for PSMA contribution to β1 integrin activation.

FAK phosphorylation at Y397 leads to Src activation, which in turn phosphorylates the Y567/577 tyrosine phosphorylation site[9,11]. We did not observe a difference in the level of phospho-FAK Y567/577

with PSMA inhibition. However, other adhesion molecules including β3 integrin can activate Src and therefore Fak independently of FAK Y397 phosphorylation. Since PSMA inhibition decreases, but does not completely obliterate cell adhesion or invasion, other adhesion molecules and signaling mechanisms must be at play. Therefore, the lack of decrease in Y576/577 FAK phosphorylation is likely due to PSMA independent signaling mechanisms[12].
Intriguingly, the decrease in FAK phosphorylation at Y925, as we observed with PSMA inhibition, has been shown to reduce angiogenesis-promoting VEGF expression via altering Grb2/SOS and Erk2 signaling in murine breast carcinoma 4T1 cells. When implanted into mice, these cells resulted in less vascular tumors, which could be rescued by expressing constitutively active downstream signaling molecule MEK[11]. Indeed, Tsui et al descried a significant correlation between VEGF and PSMA expression in LnCaP tumors across various treatment modalities including androgen deprivation and chemotherapy[13]. Therefore, it is conceivable that PSMA expression on tumor cells can influence angiogenesis. One of the aims of the allograft experiments in Chapter 4 was to determine if the tumor cell-expressed PSMA or endothelial expressed PSMA was responsible for contributing to prostate tumor angiogenesis.

Although PSMA expression on the vasculature of virtually all solid tumors was described in 1997,[14,15] indicating that it may be functionally relevant in angiogenesis, further investigation has not been pursued until recently. In addition to the contribution of PSMA in tumorigenic events explored in Chapter 2, it is important to mechanistically determine the relative contribution of tumor-derived vs. vascular endothelial cell-derived PSMA in tumor progression and angiogenesis. Therefore, we investigated whether PSMA function is dependant on only its presence in the extracellular space, in which case tumor cell-derived PSMA could offset the lack of endothelial expression, or if the cellular source of PSMA determines its function and PSMA expression on endothelial cells is necessary for tumor angiogenesis. By implanting tumor cells highly expressing PSMA into wild type and PSMA null mice, we were able to determine that PSMA expression on endothelial cells was necessary for efficient tumor angiogenesis. Using both time and tumor size as tumor harvest endpoints, we determined that there was no statistically significant difference in the rate of tumor growth between wild type or PSMA null mice, or in final tumor size in the case of tumors grown for the same amount of time. Based on the wide variability in tumors grown using time as an endpoint, we repeated the allograft study using 500mg size as an endpoint to tumor harvest.

Tumors grown in PSMA null hosts showed significantly more necrosis than those grown in wild type mice. Tumors did not exhibit any change in cell proliferation depending on host. This result is expected since the allografts are of the same cell line. Based on previous studies showing PSMA function to be necessary for angiogenic cell processes, the increase in tumor necrosis in the absence of host PSMA expression is likely due to deficient angiogenesis. Indeed, tumors with PSMA null vasculature show significantly fewer microvessels, indicating a decrease in angiogenesis. In addition, tumors isolated from PSMA null hosts show a trend in increased carbonic anhydrase IX staining, indicating severe sustained hypoxia which is consistent with decreased perfusion. Therefore, we conclude that despite highly expressed PSMA by tumor cells, including the extracellular enzymatic activity, that PSMA must be expressed on host endothelial cells for pathologic tumor angiogenesis to occur. These allograft experiments indicate that PSMA must be expressed in *cis* on endothelial cells, and that tumor expressed PSMA is insufficient to overcome the angiogenic defect.

The influence of FAK phosphorylated at Y925 on VEGF production as discussed above, and the contribution of PSMA to phospho-FAK Y925 may indicate a role for tumor expressed PSMA in angiogenesis by normal vessels with the capacity to express PSMA. Future directions include performing similar allograft experiments using a PSMA non-expressing tumor cell line. Our Tramp-C1 allograft experiments indicate that PSMA expression on endothelial cells is necessary for efficient tumor angiogenesis despite tumor PSMA expression, but does not address whether tumor expressed PSMA may

contribute to angiogenesis in the presence of a "normal" endothelial environment, including a capacity for PSMA expression.

To determine if PSMA contribution to pathologic angiogenesis was restricted to tumor angiogenesis (the tumor allograft studies directly examine angiogenesis within a tumor environment, and the previously described Matrigel plug assay tests angiogenesis into tumor derived ECM which contains pro-angiogenic growth factors) or if PSMA contributed to other modes of pathologic angiogenesis, we used a second angiogenic mouse model. The retinopathy of prematurity (ROP) model measures angiogenesis in response to tissue hypoxia and an overabundance of disorganized hypoxic signaling. Mice are born with immature retinal vasculature which develops over time until about 3 weeks of age. Exposure to hyperoxia in infancy leads to arrest of normal retinal angiogenesis and regression of any existing retinal vessels. When mice are returned to room air, the retina is relatively hypoxic due to the loss of vessels during hyperoxia. The normally well-regulated temporo-spacial hypoxia signals which drive retinal angiogenesis in an organized fashion are disrupted due to the severe degree of hypoxia. The vessels in the periphery respond to the overabundance of hypoxia signaling markers and overgrow in a disorganized fashion. The endothelial cells are overwhelmed and unable to grow normally into the central retina, and leave an avascular area. The resulting capillary network that results is tortuous and disorganized.

We have shown that retinas isolated from wild type mice undergoing ROP express PSMA at the RNA and protein level by RT-PCR and immunohistochemistry, respectively, and that PSMA is expressed on the vascular tufts. Additionally, PSMA null mice have decreased vascular pathology in the ROP model compared to wild type, evidenced by decreased central avascular area (less hypoperfusion) and fewer extraretinal vascular tufts, despite having normal developmental retinal angiogenesis.

To further investigate PSMA contribution to pathologic retinal angiogenesis, we investigated the progression of ROP over time in wild type and PSMA null mice. Wild type and PSMA null mice show similar vessel regression after hyperoxia, indicating that PSMA does not protect vasculature from degeneration in the absence of pro-survival signals. PSMA null mice showed less pathology starting at three days of relative hypoxia, and statistically less non-perfused area and a more normal vascular pattern after five days of relative hypoxia. We also examined ROP retinas by perfusing mice with RCA-FITC to determine if the endothelial cells stained by the GS lectin were patent vessels or a network of disorganized endothelial cells. We found that retinal perfusion in wild type and PSMA null mice showed nearly complete colocalization to lectin stained endothelium, with the exception of glomerular like structures likely to be vascular tufts. Therefore, the observed networks in the ROP retinas are perfused and the observed differences are not due to the growth of non-perfused endothelial networks.

We observed no significant difference in the mRNA expression levels of vascular endothelial growth factor (VEGF) or Angiopoietin-2 levels over time between wild type and PSMA null retinas. The lack of difference in VEGF expression levels from P12-P15 indicates that the decrease in pathologic angiogenesis in PSMA null mice is not due to deficient hypoxia signaling. We expected to observe a possible decrease in VEGF in the PSMA null retinas at P17 given the more normal vascular network compared to wild type, but this was not observed. Ang-2 is implicated in promoting angiogenesis in the presence of VEGF, and in vessel regression in the absence of VEGF[16]. We observed the expected Ang-2 expression in both wild type and PSMA null mice, with no statistical difference between the genotypes. Therefore, PSMA null mice show decreased vascular pathology despite similar hypoxia and pro-angiogenic signal molecules.

Previous results have shown PSMA inhibition to be neuroprotective in a glaucoma model of retinopathy by decreasing excitotoxic neuronal death. A possible effect of tissue hypoxia in ROP is neuronal excitotoxicity. To ensure that the observed decrease in ROP pathology was due to endothelial effects and not to differences in neural tissue, we measured the thickness of neural layers in wild type and PSMA null

mice in the ROP model. There is no significant difference in neural layer thickness in the absence of PSMA, indicating that the observed effects were not due to differences in neuronal excitotxocity.

To determine if PSMA is a potential therapeutic target, we exogenously inhibited PSMA using 2-PMPA. Systemic PSMA inhibition starting on P14 through P16 significantly decreased retinal vascular pathology compared to vehicle treated controls in wild type but not PSMA null mice, indicating that the 2-PMPA treatment is specific to PSMA. However, systemic PSMA inhibition has potential side effects based on PSMA expression in other tissues, such as folate insufficiency due to small intestine effects, or possible neurologic effects due to decreased glutamate neurotransmitter in the brain. Therefore, we treated ROP mice with intravitreal 2-PMPA to avoid systemic PSMA inhibition effects. Mice were injected on hypoxia day 3, the time point at which PSMA contribution begins to become evident. Intravitreal PSMA inhibition significantly reduces avascular area compared to vehicle treated contralateral eye in wild type but not PSMA null animals. The observed effect is less than that observed in P14-P16 2-PMPA treated mice, but more than the single day treated mice. We expect that repeated injections would increase the degree of the observed effect, however the mouse eye is too small to withstand repeated injections without significant scarring, confounding the results. The decrease in retinal vascular pathology with exogenous PSMA inhibition indicates that PSMA inhibition may be an attractive target for therapy development for human ROP.

Given the decreased angiogenesis in tumors described above, at first glance the more normal angiogenesis in PSMA null mice is counterintuitive. However, in spite of highly expressed proangiogenic molecules, the PSMA null mice show a more normal phenotype. We attribute this to a lack of ability to respond to the disorganized pathologic angiogenic signals. Without PSMA modulation of β1 integrin signaling and its concomitant FAK signaling in the endothelial cells (as previously described), the vasoproliferative effect in ROP may be decreased. Endothelial cells responding less strongly to hypoxic signals may adhere, migrate, and form new vascular networks more slowly; thus the perfusion from vessels that do form would decrease hypoxia signaling in that particular area of the retina, leading to attenuation of disorganized over expression of vascular growth factors.

To test whether restoring FAK activation in PSMA null retinas could recapitulate the retinal pathology observed in wild type mice the ROP model, we expressed constitutively active FAK (IL2R FAK) in ROP retinas. Compared to the control contralateral eye, 2 of 3 mice showed an increase in the non-perfused central avascular area. While not statistically significant, this exciting result indicated that restoration of decreased FAK signaling could restore the ability of PSMA null endothelium to undergo pathologic angiogenesis in the ROP model. Wild-type mice showed a similar result with constitutively active FAK in 1 of 2 treated mice. This is expected, as an increase in FAK would lead to disorganized signaling within the endothelial cell, causing an inability to respond in a structured manner. Thus, the retina is not reperfused and disorganized hypoxia signaling continues.

Tasks 2 and 3 Analyze candidate PSMA substrates:

Prostate Specific Membrane Antigen Produces Laminin Peptides downstream of MMPs in Endothelial Cell Activation and Angiogenesis.

2/3.1 Introduction

The extracellular matrix is a dynamic and integral component of the tumor microenvironment. Numerous studies have demonstrated changes in the extracellular matrix composition throughout tumor progression (Sprenger CC 2010, Schedin P 2011, Bremnes RM 2011, Schulz 2010), and specific extracellular matrix proteins and peptides have been shown to modulate tumor activity and angiogenesis (Humphries MJ 1986, Ponce ML 2003, Yamada 2011, Maeshima 2000, O'Reilly 1997, O'Reilly 1004, Maeshima 2002, Kamphaus GD 2000). The discovery of multiple cryptic extracellular matrix fragments that potently inhibit angiogenesis further illustrates the complex relationship between tumors cells, the extracellular matrix, and nearby endothelial cells in determining tumor progression and metastasis. For example, tumstatin, a 28 kDa type IV collagen fragment (Maeshima 2002), endostatin, a 20 kDa type XVIII collagen fragment, (O'Reilly 1997) and angiostatin, a 38 kDa plasmin fragment (O'Reilly 1994) are well-studied naturally occurring anti-angiogenic extracellular matrix-derived fragments. While angiostatin is generated by plasmin autolysis, endostatin and tumstatin are cleaved by secreted proteases (Felbor 1999). Additionally, cryptic peptides of collagen IV and laminin 5 have been found that promote tumor cell motility (Xu J 2001; Koshikawa N 2000). Thus, extracellular matrix peptides are important regulators of tumor and endothelial cell function.

Altered protease expression or activity is a common observation in tumor progression; most notable is the increased expression and activity of the matrix metalloproteinases during tumorigenesis **(**Zhang B 2008; Wu ZS 2008; La Rocca G 2004; Poola I 2005; Ory R 2004; Koc M 2006; Morgia 2005**)**. Classically, this MMP up-regulation has been thought to provide clearance of the extracellular matrix during tumor invasion of the basal lamina, but extracellular matrix degradation is also an integral step to angiogenesis (Montesano 1985, Pepper MS 1009, Ingber and Folkman 1988). Additionally, protease degradation of the extracellular matrix is known to produce smaller fragments with anti-angiogenic activity that affect integrin function (Maeshima 2000; O'Reilly 1997; O'Reilly 1994). Thus, the concept has emerged that proteases may not only be physically clearing the ECM barrier during tumor progression but also generating bioactive ECM fragments that signal specific tumor or endothelial cell functions (Lane 1994, Wang B 2006, McDaniel SM 2006, Roy M 2009). In support of this idea, numerous cell-surface and secreted proteases other than the MMPs have been implicated in angiogenesis and tumor progression including aminopeptidase N/CD13, Aminopeptidase A, and glutamate carboxypeptidase II/prostate specific membrane antigen (Bhagwat 2001, Chen 2003, Marchio 2004, Conway 2006). These peptidases are transmembrane proteases increased in the vasculature associated with many solid tumors, but their expression is low or absent in quiescent vasculature. Inhibition of these enzymes reduces angiogenesis in *in vivo* animal models, suggesting that these proteases are pro-angiogenic. The exact mechanism of how these peptidases regulate angiogenesis is largely unknown.

We have previously shown that glutamate carboxypeptidase II/prostate specific membrane antigen (hereby referred to as PSMA) regulates endothelial cell adhesion and invasion in a laminin-specific manner. Additionally, PSMA contributes to initial ligand binding by integrin β_1, the major laminin-binding integrin, leading to full activation of the integrin and propagation of pro-angiogenic signaling pathways in endothelial cells (Conway 2006). These data implicate PSMA as a novel modulator of laminin in angiogenesis, acting to process integrin β_1-activating peptide fragments. While it is tempting to speculate that PSMA could directly digest laminin to produce an integrin-activating fragment, the known active site structure (Mesters 2006) and previously identified substrates of this enzyme in the brain and intestines (NAAG and folate, respectively) (Pinto JT 1996, Carter 1996, Tiffany 1996) suggest that PSMA prefers small, terminally glutamated peptide substrates. Thus, we propose that PSMA processes laminin downstream of matrix metalloproteinases to activate endothelial cells and angiogenesis. Here, we provide evidence in support of this idea.

Figure 1: Huvec-digested laminin

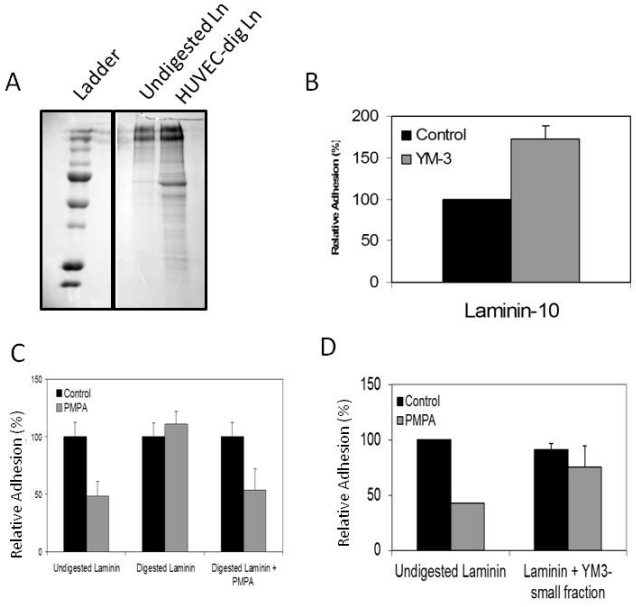

2/3.2 Results

2.1 Endothelial cells process laminin to generate endothelial cell activating small peptide fragments.

It is well-established that physiologically-derived proteolytic fragments of the extracellular matrix can regulate angiogenesis, and these inhibitory fragments range from 20-40 kDa (O'Reilly 1994, O'Reilly 1997, Maeshima 2000, Maeshima 2002). Additionally, many studies have implicated smaller, synthetic extracellular matrix-derived peptide fragments, ranging from approximately 1-2 kDa, as potent regulators of endothelial cell activation and angiogenesis (Nomizu 1995; Malinda 1999; Once 1999). In a physiological context however, cells may not be exposed to these active ECM fragments. Therefore, we wished to assess whether small peptides generated naturally by endothelial cell proteases and peptidases can activate endothelial cells. To test this concept, we digested laminin with primary human umbilical vein endothelial cells (HUVECs). After incubation of laminin with HUVECs in suspension, numerous smaller molecular weight fragments were visible by Coomassie Staining of SDS-PAGE gels (Figure 1A). To specifically determine if small laminin peptides (3 kDa or less) could be bioactive, the digested laminin was separated by column chromatography, and the small fraction (YM3-S) was tested for activity. Importantly, inclusion of these small digestion fragments with intact laminin resulted in a significant increase in endothelial cell adhesion (Figure 1B). This result suggests that endothelial cells process laminin to generate endothelial cell activating small peptide fragments.

2.2 PSMA produces small laminin peptides that are important in endothelial cell activation. Previous studies in our lab have shown that PSMA functions specifically through laminin to activate angiogenesis. To test the hypothesis that PSMA contributes to endothelial cell activation by processing laminin, we incubated laminin with HUVEC cells in the presence or absence of a specific PSMA inhibitor, 2-PMPA. Adhesion of HUVEC cells to laminin was then tested in the presence or absence of the specific PSMA inhibitor, 2-PMPA. Adhesion of HUVEC cells to intact laminin is partially inhibited in the presence of 2-PMPA, confirming that PSMA is required for adhesion to laminin. However, this inhibition is rescued when laminin is digested by HUVEC cells expressing PSMA and other proteases (Figure 1C). Importantly, including 2-PMPA during HUVEC digestion of laminin restores the requirement for PSMA during endothelial cell adhesion. Further, isolation of the small peptide fraction of digested laminin (YM-3 small) is sufficient to rescue adhesion in the presence of the PSMA inhibitor (Figure 1D). Together, these results support our hypothesis that PSMA produces small laminin peptides that are important in endothelial cell activation.

2.3 PSMA functions downstream of MMPs in proteolytically processing laminin. To more thoroughly characterize the pathway by which PSMA processes laminin, we asked whether PSMA digests laminin downstream of matrix metalloproteases (MMPs). MMPs are the major family of proteases implicated in extracellular matrix degradation, releasing bioactive fragments that regulate angiogenesis

Figure 2: MMPs process laminin upstream of PSMA

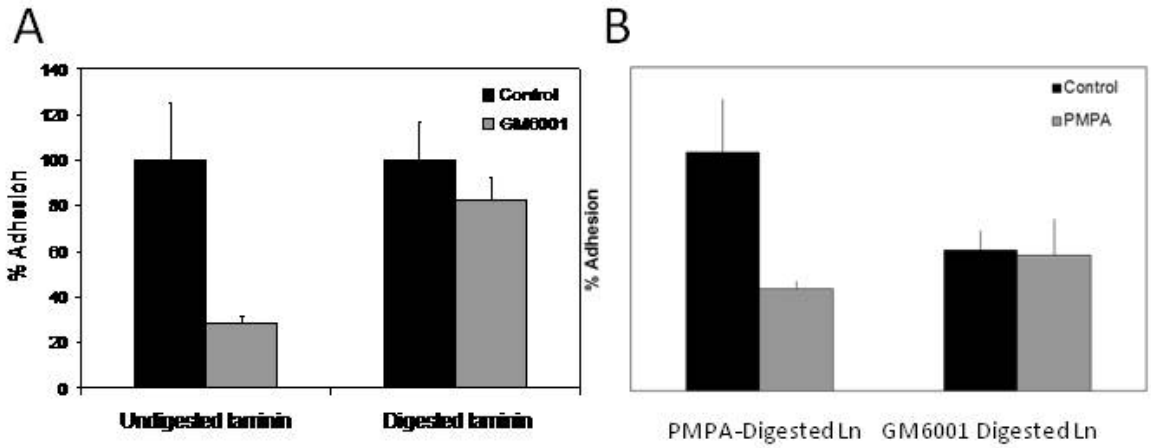

(reviewed in Kessenbrock 2010), and a number of MMPs have been shown to efficiently process laminin (Mydel 2008; Udayakumar 2003; Ohuchi 1997). To initially address whether PSMA degrades laminin downstream of MMPs, we reasoned that if PSMA functions downstream of MMPs in laminin digestion, then pre-digestion of laminin in the presence of an MMP inhibitor would fail to generate PSMA substrates. The failure to generate PSMA substrates would likely decrease overall endothelial cell adhesion but should remove the sensitivity to PSMA inhibition. Therefore, we incubated laminin with HUVECs in the presence or absence of the broad MMP inhibitor, GM-6001. As expected, inhibiting multiple MMPs during laminin digestion resulted in decreased endothelial cell adhesion. Digesting laminin with HUVECs prior to MMP inhibition rescued the loss of adhesion in response to the MMP inhibitor (Figure 2A). Notably, endothelial cell adhesion to laminin peptides generated in the presence of GM-6001 was not further decreased when PSMA was inhibited (Figure 2B). These results support our hypothesis that PSMA functions downstream of MMPs in proteolytically processing laminin.

Figure 3: PSMA degradation of laminin after MMP-2 and MMP-14 increases EC activation

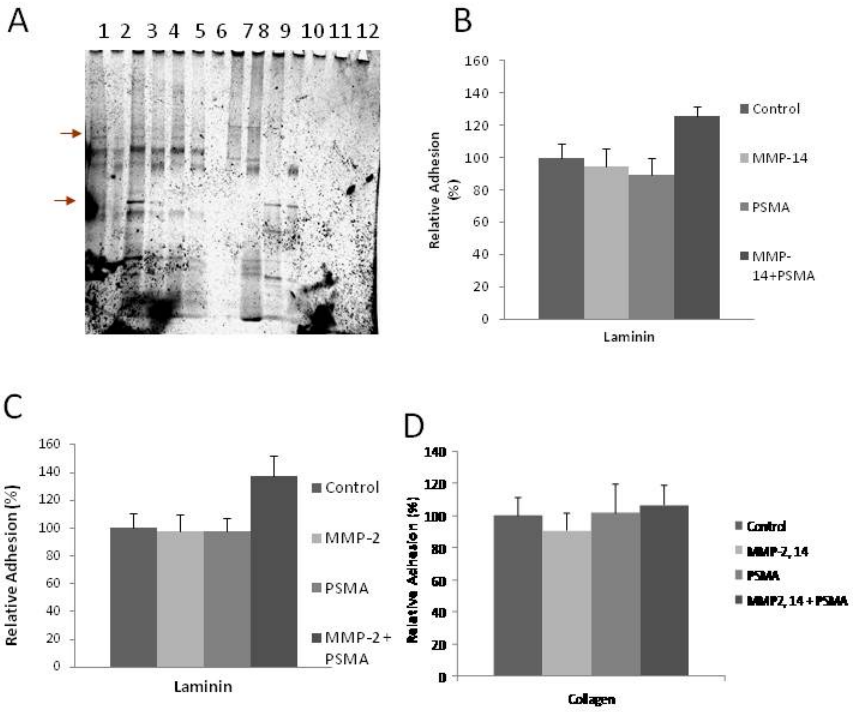

2.3 PSMA processes laminin downstream of MMP-2 and MMP-14 to generate endothelial-cell activating peptides. With the initial evidence obtained in our early experiments suggesting that PSMA participates with MMPs in a proteolytic pathway to generate endothelial cell-activating laminin peptides, we wished to determine which MMPs might be involved in this novel proteolytic pathway. MMP-2 and MMP-14 (MT1-MMP) are two known laminases which have been implicated in regulating integrin β_1 activation (Bair 2005, Gu 2002, Gianelli 2000, Siu 2004). Therefore, we tested whether MMP-2 and MMP-14 might work upstream of PSMA in laminin digestion. Recombinant MMP-2 and MMP-14 were incubated with intact laminin, and the resulting fragments were tested for endothelial cell activity. Sequential digestion of MMP-generated laminin fragments with recombinant PSMA was performed, and these peptides were also tested for endothelial cell adhesion. Separation of these laminin fragments by SDS-PAGE followed by silver staining revealed a few bands that changed in intensity or were no longer detected after further processing by PSMA (Figure 3A; arrows). Addition of laminin digested with MMP-2, MMP-14, or PSMA alone to intact laminin had no impact on endothelial cell adhesion. However, when laminin was digested sequentially with MMP-2 then PSMA, these fragments significantly increased endothelial cell activation. Similar results were found with laminin digested sequentially with MMP-14 and PSMA (Figure 3B). Therefore, PSMA processes laminin downstream of MMP-2 and MMP-14 to generate endothelial-cell activating peptides.

2.5 PSMA specifically degrades laminin downstream of MMP-2 and MMP-14. To determine if the proteolytic cascade involving MMP-2, MMP-14, and PSMA was specific to laminin, we incubated collagen first in the presence of both MMP-2 and MMP-14, then in the presence of recombinant PSMA. Adhesion to intact collagen was not altered by the presence of collagen fragments generated by either the

MMPs or PSMA alone or the MMPs and PSMA combined (Figure 4C). Thus, PSMA specifically degrades laminin downstream of MMP-2 and MMP-14.

Figure 4: peptides in angiogenesis (in vivo)

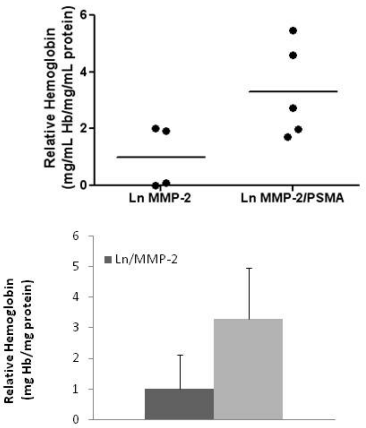

2.6 PSMA activates angiogenesis *in vivo* by degrading MMP-derived laminin fragments While endothelial cell adhesion is a simple assay commonly used to test initial endothelial cell activation, angiogenesis is a complex process that is best modeled *in vivo*. We therefore used the Matrigel implant model in C57/Bl6 mice to test if the presence of laminin peptides sequentially generated by MMP and PSMA increased angiogenesis *in vivo*. Hemoglobin content from the Matrigel implants that contained laminin fragments generated by both MMP-2 and PSMA showed an average 3-fold increase compared to implants containing laminin fragments derived from digestion with MMP-2 alone (Figure 4). Thus, laminin fragments generated by sequential digestion with MMP-2 and PSMA increase angiogenesis *in vivo*. This data supports our hypothesis that PSMA activates angiogenesis *in vivo* by degrading MMP-derived laminin fragments.

2.7 The candidate peptide did not increase HUVEC adhesion in our experiments. While we ultimately plan to identify the specific physiological laminin peptide(s) generating by PSMA that activate endothelial cells, this is beyond the scope of our current experiments. However, numerous synthetic laminin peptides have been reported to increase endothelial or tumor cell adhesion (Malinda 1999; Ponce 1999; Noizu 1995; Makino 2002; Sasaki 2001). Because PSMA is a glutamate carboxypeptidase, we searched the list of published synthetic laminin peptides shown to activate endothelial cells to find ones with a terminal glutamate at the carboxy terminus. Additionally, our previous research demonstrated that PSMA activates endothelial cells through integrin β_1 – dependent pathways. Integrin β_1 is the major laminin-binding integrin, and previous studies have repeated demonstrated that it commonly binds to the globular (G)-domain in the laminin α chain (Hozumi 2006; Yokoyama 2005; Rissanen 2003). Therefore, we narrowed the published list of synthetic laminin peptides that are derived from the G- domain of the laminin α chain and have a terminal glutamate at or near the C-terminus. From this list, we selected a single candidate peptide, AG-56 (Malinda 1999) to test for endothelial cell activation. This peptide sequence was modified to include the next 3 amino acids in the laminin α_1 chain, VDE, to incorporate a carboxy-terminal glutamate. We further reasoned that if PSMA cleavage of a laminin peptide activates endothelial cell adhesion, then a peptide lacking the terminal glutamate (and thus mimicking PSMA cleavage) would further increase endothelial cell activation. Thus, we tested endothelial cell adhesion to laminin in the presence of the candidate peptide and the peptide lacking the terminal glutamate (ΔE). Surprisingly, addition of the candidate peptide resulted in a statistically significant decrease in endothelial cell adhesion, and the ΔE peptide further reduced adhesion (Figure 5). Thus, the selected candidate peptide did not increase HUVEC adhesion in our experiments.

Figure 5: Synthetic peptides

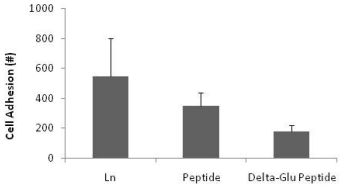

2.8 **Other angiogenesis-regulating peptidases produce small, bioactive peptides in vitro.** The previously described results implicate PSMA as a key participant in a novel proteolytic cascade of laminin in endothelial cell activation and angiogenesis. However, as PSMA is only one of several peptidases that regulates angiogenesis, it is possible that other angiogenesis-regulating peptidases may be participating in similar digestion schemes that produce small, bioactive peptides. To more generally test the concept that small ECM peptides can regulate endothelial cell activation, we used trypsin to generate small (3 kDa or less) peptides from Matrigel, which contains a mixture of multiple extracellular matrix proteins including collagen, laminin, and fibronectin. Coomassie staining of SDS-PAGE fragments confirmed successful digestion of the matrix by trypsin, and separation of the large and small fragments (Figure 6A). Including these fragments in adhesion assays showed a statistically significant increase in adhesion to Matrigel (Figure 6B). Similar results were observed when Matrigel was digested with intact HUVEC cells (Figure 6C).

Figure 6: small Collagen peptides regulate angiogenesis

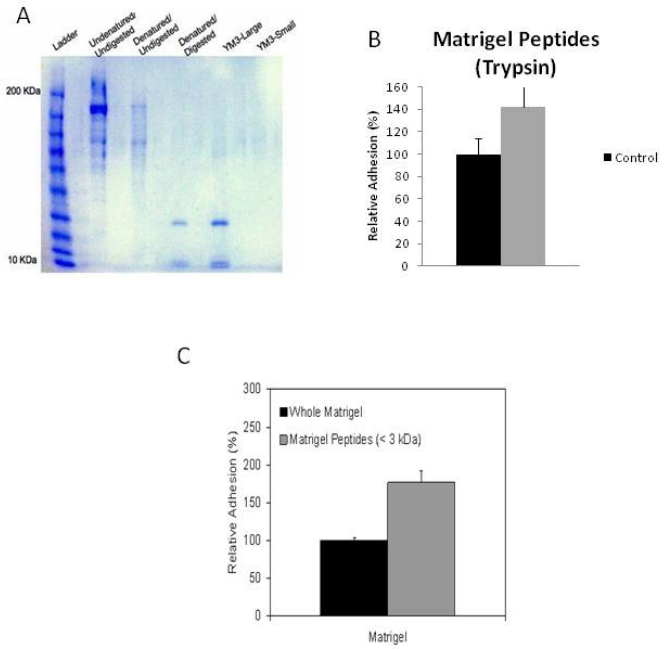

Figure 7

2.9 small, bioactive peptides support angiogenesis in vivo. Matrigel is primarily composed of laminin and collagen IV. To test if small collagen peptides were capable of activating angiogenesis *in vivo*, we injected Matrigel plugs containing trypsin-derived collagen fragments 3 kDa or less in size (YM3-small). We observed a statistically significant increase in angiogenesis *in vivo* using the mouse Matrigel implant model (Figure 7). Undigested collagen did not alter angiogenesis, and inclusion of the large collagen fragments (larger than 3 kDa) showed a trend of increased angiogenesis, though this was not statistically significant. Together, these results suggest that small ECM fragment activation of endothelial cells and angiogenesis could be a common theme repeated with multiple peptidases and extracellular matrix substrates.

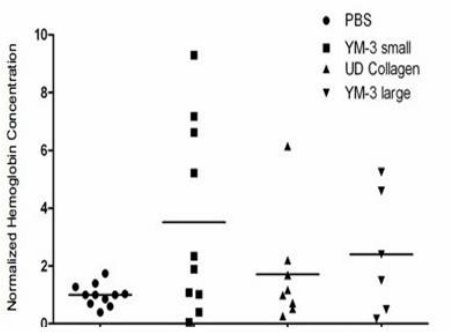

2/3.4 RELATIONSHIP OF FINDINGS WITH PREVIOUSLY REPORTED FINDINGS:

The dynamic relationship between the extracellular matrix and endothelial cells throughout angiogenesis has been studied extensively, but these studies have primarily focused on relatively large proteolytic fragments of the ECM and synthetically generated small ECM peptides. Thus, whether physiologically relevant small ECM peptides could actively

regulate angiogenesis has been largely untested. In this study, we demonstrated that small, bioactive peptide fragments physiologically generated from naturally-occurring endothelial cell proteases and peptidases increase endothelial cell activation (Figure 1). That these small peptides increase endothelial cell adhesion contrasts with the well-characterized ECM fragments such as tumstatin, angiostatin, and endostatin, which serve to potently inhibit angiogenesis. This suggests that the interaction between endothelial cells and the extracellular matrix is complex, and that further processing of extracellular matrix proteins by peptidases up-regulated in angiogenesis may help activate the angiogenic switch.

We are specifically interested in characterizing the precise role that the angiogenic peptidase PSMA plays in activating endothelial cells. Our previous studies revealed important clues of the mechanism of PSMA in angiogenesis, including the laminin-specific requirement for PSMA, and the function of PSMA in inducing ligand-dependent binding and activation of integrin β_1. In this study, we found that PSMA works downstream of MMP-2 and MMP-14 to generate laminin peptide fragments that activate endothelial cell adhesion (Figures 2 and 3). Furthermore, *in vivo* tests confirmed that these peptides are capable of inducing angiogenesis (Figure 4). Not only does this reveal that PSMA activates endothelial cells through its proteolytic activity of laminin, but it also describes a novel proteolytic cascade in angiogenesis that may apply to other angiogenic peptidases whose mechanism in inducing endothelial cell activation remains largely unknown. Further study of the laminin fragments derived from MMP and PSMA digestion will enable us to isolate, sequence, and assay the specific resulting peptide(s) for angiogenic activity.

Though the current study did not include specific experiments involving integrin β_1, it is known to be the major integrin laminin receptor expressed on endothelial cells (Belkin AM 2000; Carter W 1990; Kramer RH 1994). Degradation of the extracellular matrix is known to produce smaller fragments that modulate integrin function (Maeshima 2000, O'Reilly 1994, O'Reilly 1997), and many integrin binding sites are cryptic and must be first exposed by proteolysis (Yamada 1991). Furthermore, short extracellular matrix-derived peptide sequences such as RGD mediate integrin activation (reviewed in Calderwood 2004). Therefore, it is reasonable to hypothesize that PSMA degradation of MMP-generated laminin fragments may release a cryptic, integrin β_1-activating peptide fragment, leading to integrin-substrate interactions that activate downstream signaling cascades leading to endothelial cell motility and invasion. This hypothesis is consistent with our previous findings that PSMA is involved in activation of focal adhesion kinase and p21-activated kinase, both signaling proteins downstream of integrin β_1.

While isolating and characterizing the physiologically-generated peptide(s) resulting from sequential digestion by MMP and PSMA is our ultimate goal, we realize that this process may be technically challenging. Meanwhile, we hypothesized that a carefully-chosen synthetic peptide previously described in the literature to activate endothelial cells may reveal important clues regarding the nature of the natural PSMA substrate. We therefore selected the AG-56 peptide as a rationale candidate, based on its location in the globular domain of the laminin α chain (Malinda 1999), and the presence of a glutamate three residues past the end of the sequence. We tested the modified AG-56 peptide, which included the nearby glutamate, as well its counterpart peptide which was identical except for the removal of the terminal glutamate for their ability to induce endothelial cell adhesion in the presence of intact laminin. Unexpectedly, we observed that inclusion of this modified AG-56 laminin α chain peptide instead resulted in significant inhibition of endothelial cell adhesion. More strikingly, removal of the terminal glutamate of this peptide proved to inhibit adhesion more efficiently. Though these results were not anticipated, they may indicate that the synthetic, AG-56 derived peptide is similar in sequence to the naturally-occurring activating laminin peptides, and could be inhibiting endothelial cell adhesion by competing with the uncharacterized activating peptide(s) for binding to integrin β_1. Further testing of this hypothesis is required in the future.

Finally, we tested whether small extracellular matrix peptide activation of endothelial cells and angiogenesis might represent a broader concept that could apply to other angiogenic peptidases, whose mechanism of promoting angiogenesis is largely uncharacterized. Here, we demonstrated that small peptides (3 kDa or less) derived from Matrigel and collagen retained bioactive function in endothelial cell

adhesion (Figure 6) and angiogenesis *in vivo* (Figure 7). These findings suggest that proteolytic cascades involving large-substrate proteases such as the MMPs and angiogenic peptidases preferring small substrates such as PSMA may be a primary mechanism of modulating the balance between pro- and anti-angiogenic factors in the tumor microenvironment.

Collectively, our data outlines a specific laminin digestion scheme involving MMPs and PSMA, and suggests that other peptidases and extracellular matrix proteins could be involved in similar pro-angiogenic pathways.

KEY RESEARCH ACCOMPLISHMENTS:

1) **PSMA on tumor cells significantly contributes to tumor progression and metastasis by interacting with and regulating PTEN which affects the Akt survival pathways.**
   -Characterization of tumor cell-derived PSMA in tumor incidence, progression and metastasis in the TRAMP model:
   a) Lack of PSMA in prostate cancer does not alter tumor incidence, but tumors are significantly smaller, more necrotic and the vasculature is more 'normalized'.
   b) Lack of PSMA significantly alters tumor grade at early time points but in advanced tumors.
   c) PSMA null tumors have reduced expression of markers of tumor progression.
   d) Tumor PTEN and Akt survival pathways are dysregulated in the absence of PSMA.
   e) PSMA complexes with active PTEN.
   f) PSMA null tumors signal through an alternate, less aggressive pathway.
   g) Wild type animals had evidence of more micrometastasis to the liver, kidney and lung than the PSMA null mice, suggesting that PSMA may contribute to metastasis.

2) **PSMA is necessary for *in vitro* cell processes involved in metastasis**
   -Characterization of PSMA in Prostate tumor cells *in vitro*
   a) TRAMP-C1 cells express PSMA and β1 integrin.
   b) PSMA does not contribute to cell proliferation or viability in monolayer culture.
   c) PSMA regulates prostate tumor cell adhesion to laminin but not other extracellular matrices.
   d) PSMA regulates prostate cancer cell invasion
   e) PSMA regulates FAK phosphorylation in Tramp-C1 cells
   f) PSMA regulates cell proliferation in 3-D culture

3) **PSMA expression on endothelial cells is required for tumor angiogenesis.**
   -Characterization of prostate tumor allografts *in vivo*.
   a) Lack of host PSMA expression does not decrease tumor growth, volume or mass
   b) Lack of host PSMA expression leads to increased tumor necrosis.
   c) Tramp-C1 allografts show similar growth rates in wild type and PSMA null hosts.
   d) Lack of host PSMA expression leads to increased necrosis in tumors.
   e) Lack of host PSMA does not alter tumor cell proliferation.
   f) Allografts from PSMA null mice have significantly less angiogenesis than those from wild type mice.
   g) Lack of host PSMA trends toward in increase in sustained tumor hypoxia

4) **PSMA Regulates Pathologic Angiogenesis in Oxygen Induced Retinopathy Independently of VEGF**
   a) PSMA is induced in response to hypoxia in the OIR model.
   b) PSMA null mice have normal developmental retinal angiogenesis.
   c) PSMA null mice showed a less pathologic angiogenic phenotype than wild-type animals in the OIR model.

d) PSMA null mice show significantly less central avascular area and significantly fewer extra-retinal vascular tufts.
e) Wild type and PSMA null mice show no difference in microvessel perfusion in OIR
f) PSMA abrogates pathology in the OIR model during the vasculoproliferative phase but not the angio-obliterative phase.
g) VEGF and Ang-2 mRNA levels are not different between wild type and PSMA null mice in the OIR model.
h) Wild type and PSMA null mice show equal retinal neuronal survival.
i) Exogenous PSMA inhibition with 2-PMPA in wild type mice recapitulates the phenotype observed in PSMA null mice.
j) Constitutively active FAK increases ROP vascular pathology in PSMA null mice.

5) **PSMA Produces Laminin Peptides downstream of MMPs in Endothelial Cell Activation and Angiogenesis**.
a) Endothelial cells process laminin to generate endothelial cell activating small peptide fragments.
b) PSMA produces small laminin peptides that are important in endothelial cell activation
c) PSMA functions downstream of MMPs in proteolytically processing laminin
d) PSMA processes laminin downstream of MMP-2 and MMP-14 to generate endothelial-cell activating peptides.
e) PSMA specifically degrades laminin downstream of MMP-2 and MMP-14
f) PSMA activates angiogenesis *in vivo* by degrading MMP-derived laminin fragments
g) the selected candidate peptide did not increase HUVEC adhesion in our experiments.
h) other angiogenesis-regulating peptidases produce small, bioactive peptides

-REPORTABLE OUTCOMES:

1. **Manuscripts**
   - We have published our findings on PSMA in oxygen-induced retinopathy in PLoS One: Grant CL, Caromile, LA, Rahman MM, Durrani K, Claffey KP, Fong, GH and Shapiro LH. Prostate Specific Membrane Antigen (PSMA) Regulates Angiogenesis Independently of VEGF During Ocular Neovascularization. PLoS One in press 2012. (Appendix 1)
   - We have completed both the allograft and TRAMP transgenic projects and plan to submit these as individual publications within the year.
2. **Abstracts and presentations**
   - Grant, CL, RE Conway and LH Shapiro (2007). *Prostate Specific Membrane Antigen Regulates Cell Adhesion and Invasion of Prostate Tumor Cell Lines*. Abstract for poster presented at Prostate Cancer Foundation Retreat, Lake Tahoe, CA.
   - Grant, CL, RE Conway and LH Shapiro (2008). Prostate Specific Membrane Antigen Regulates Cell Adhesion and Invasion of Prostate Tumor Cell Lines. Abstract for poster presented at UCONN Health Center Cardiovascular Retreat, Farmington CT.
   - Grant, CL, RE Conway and LH Shapiro (2009). Prostate Specific Membrane Antigen Reg*ulates Angiogenesis in Tumor Allografts and a Mouse Model of Retinopathy of Prematurity.* Abstract for poster presentation at ASCI/AAP 2009 Joint Meeting, Chicago, IL.
3. **Degrees obtained that are supported by this award:**
   - Ph.D. awarded to Christina L. Grant, June 2012 (thesis completed August 2009).
4. **Animal models:**
   - We have created a PSMAnull X TRAMP+ murine strain that spontaneously develops prostate tumors that do not express PSMA.

5. **Employment received based on experience/training supported by this award:**
   - Christina Grant, MD/PhD is currently a pediatrics intern at Northwestern University Hospital, Chicago, IL.

CONCLUSION:

In conclusion, we have established that PSMA expression on endothelial cells is necessary for tumor angiogenesis and that PSMA expression in the extracellular milieu is insufficient to compensate for this deficiency. We have also shown that PSMA in tumor cells operates by similar mechanisms as in endothelial cells, specifically consistent with modulating β1 integrin activation and subsequent FAK signaling. In addition to being a marker of advanced prostate cancer to be exploited for targeted prostate cancer therapeutics, PSMA appears to functionally contribute to prostate cancer progression and metastasis by physically interacting with and regulating the tumor suppressor PTEN and downstream survival pathways. Interestingly, without PSMA, the tumors switch to an alternate tumorigenic pathway, which results in tumors that are less aggressive than those where PSMA is present. In combination with the evidence of the necessity for PSMA in pathologic angiogenesis, both in tumor neovascularization and oxygen induced retinopathy, PSMA's contribution to tumor progression and metastatic cell processes make it an attractive target in itself for drug development beyond its use for targeting advanced prostate cancer. Future directions include careful dissection of PSMA in metastasis, determining how PSMA regulates PTEN, identifying the molecular basis of pathway switch in PSMA null prostate tumors and drug studies to assess the efficacy of PSMA inhibition as treatment for prostate cancer growth, metastasis and pathologic angiogenesis *in vivo*.

REFERENCES:

1. United States Cancer Statistics: 1999–2006 Incidence and Mortality Web-based Report, in Cancer Among Men. 2010, Department of Health and Human Services, Centers for Disease Control and Prevention, and National Cancer Institute. p. Prostate Cancer Statistics.
2. Foster, B.A., et al., Characterization of prostatic epithelial cell lines derived from transgenic adenocarcinoma of the mouse prostate (TRAMP) model. Cancer Res, 1997. 57(16): p. 3325-30.
3. Gingrich, J.R., et al., Metastatic prostate cancer in a transgenic mouse. Cancer Res, 1996. 56(18): p. 4096-102.
4. Greenberg, N.M., et al., Prostate cancer in a transgenic mouse. Proc Natl Acad Sci U S A, 1995. 92(8): p. 3439-43.
5. Kaplan-Lefko, P.J., et al., Pathobiology of autochthonous prostate cancer in a pre-clinical transgenic mouse model. Prostate, 2003. 55(3): p. 219-37.
6. Williams, T.M., et al., Caveolin-1 promotes tumor progression in an autochthonous mouse model of prostate cancer: genetic ablation of Cav-1 delays advanced prostate tumor development in tramp mice. J Biol Chem, 2005. 280(26): p. 25134-45.
7. Gingrich, J.R., et al., Pathologic progression of autochthonous prostate cancer in the TRAMP model. Prostate Cancer Prostatic Dis, 1999. 2(2): p. 70-75.
8. Winter, S.F., A.B. Cooper, and N.M. Greenberg, Models of metastatic prostate cancer: a transgenic perspective. Prostate Cancer Prostatic Dis, 2003. 6(3): p. 204-11.
9. Moore, M.L., et al., Deletion of PSCA increases metastasis of TRAMP-induced prostate tumors without altering primary tumor formation. Prostate, 2008. 68(2): p. 139-51.
10. Yang, D., et al., Murine six-transmembrane epithelial antigen of the prostate, prostate stem cell antigen, and prostate-specific membrane antigen: prostate-specific cell-surface antigens highly expressed in prostate cancer of transgenic adenocarcinoma mouse prostate mice. Cancer Res, 2001. 61(15): p. 5857-60.

11. Oh, Y.T., et al., Adenoviral interleukin-3 gene-radiation therapy for prostate cancer in mouse model. Int J Radiat Oncol Biol Phys, 2004. 59(2): p. 579-83.
12. Tsai, C.H., et al., Tetracycline-regulated intratumoral expression of interleukin-3 enhances the efficacy of radiation therapy for murine prostate cancer. Cancer Gene Ther, 2006. 13(12): p. 1082-92.
13. Rayburn, E.R., et al., Experimental therapy of prostate cancer with an immunomodulatory oligonucleotide: effects on tumor growth, apoptosis, proliferation, and potentiation of chemotherapy. Prostate, 2006. 66(15): p. 1653-63.
14. Torry, R.J. and B.J. Rongish, Angiogenesis in the uterus: potential regulation and relation to tumor angiogenesis. Am J Reprod Immunol, 1992. 27(3-4): p. 171-9.
15. Takeda, Y., et al., Deletion of tetraspanin Cd151 results in decreased pathologic angiogenesis in vivo and in vitro. Blood, 2007. 109(4): p. 1524-32.
16. Guaiquil, V., et al., ADAM9 is involved in pathological retinal neovascularization. Mol Cell Biol, 2009.
17. Folkman, J., Tumor angiogenesis: therapeutic implications. N Engl J Med, 1971. 285(21): p. 1182-6.
18. Folkman, J., et al., Isolation of a tumor factor responsible for angiogenesis. J Exp Med, 1971. 133(2): p. 275-88.
19. Dayan, F., et al., A dialogue between the hypoxia-inducible factor and the tumor microenvironment. Cancer Microenviron, 2008. 1(1): p. 53-68.
20. Lyons, J.M., 3rd, et al., The role of VEGF pathways in human physiologic and pathologic angiogenesis. J Surg Res. 159(1): p. 517-27.
21. Folkman, J., Angiogenesis. Annu Rev Med, 2006. 57: p. 1-18.
22. Chung, A.S., J. Lee, and N. Ferrara, Targeting the tumour vasculature: insights from physiological angiogenesis. Nat Rev Cancer. 10(7): p. 505-14.
23. Sridhar, S.S. and F.A. Shepherd, Targeting angiogenesis: a review of angiogenesis inhibitors in the treatment of lung cancer. Lung Cancer, 2003. 42 Suppl 1: p. S81-91.
24. Hosoi, F., et al., N-myc downstream regulated gene 1/Cap43 suppresses tumor growth and angiogenesis of pancreatic cancer through attenuation of inhibitor of kappaB kinase beta expression. Cancer Res, 2009. 69(12): p. 4983-91.
25. Sleijfer, S., et al., Pazopanib, a multikinase angiogenesis inhibitor, in patients with relapsed or refractory advanced soft tissue sarcoma: a phase II study from the European organisation for research and treatment of cancer-soft tissue and bone sarcoma group (EORTC study 62043). J Clin Oncol, 2009. 27(19): p. 3126-32.
26. Parsons, M.F., et al., The in vivo properties of STX243: a potent angiogenesis inhibitor in breast cancer. Br J Cancer, 2008. 99(9): p. 1433-41.
27. Lau, D.H., et al., Paclitaxel (Taxol): an inhibitor of angiogenesis in a highly vascularized transgenic breast cancer. Cancer Biother Radiopharm, 1999. 14(1): p. 31-6.
28. Hwang, C. and E.I. Heath, Angiogenesis inhibitors in the treatment of prostate cancer. J Hematol Oncol. 3(1): p. 26.
29. Gariano, R.F. and T.W. Gardner, Retinal angiogenesis in development and disease. Nature, 2005. 438(7070): p. 960-6.
30. Gebarowska, D., et al., Synthetic peptides interacting with the 67-kd laminin receptor can reduce retinal ischemia and inhibit hypoxia-induced retinal neovascularization. Am J Pathol, 2002. 160(1): p. 307-13.
31. Kornberg, L.J., et al., Focal adhesion kinase overexpression induces enhanced pathological retinal angiogenesis. Invest Ophthalmol Vis Sci, 2004. 45(12): p. 4463-9.
32. Skoura, A., et al., Essential role of sphingosine 1-phosphate receptor 2 in pathological angiogenesis of the mouse retina. J Clin Invest, 2007. 117(9): p. 2506-16.
33. Chen, J., et al., Suppression of retinal neovascularization by erythropoietin siRNA in a mouse model of proliferative retinopathy. Invest Ophthalmol Vis Sci, 2009. 50(3): p. 1329-35.

34. Chen, J. and L.E. Smith, Retinopathy of prematurity. Angiogenesis, 2007. 10(2): p. 133-40.
35. Aguilar, E., et al., Chapter 6. Ocular models of angiogenesis. Methods Enzymol, 2008. 444: p. 115-58.
36. Weidemann, A., et al., Astrocyte hypoxic response is essential for pathological but not developmental angiogenesis of the retina. Glia. 58(10): p. 1177-85.
37. Zayed, M.A., et al., CIB1 regulates endothelial cells and ischemia-induced pathological and adaptive angiogenesis. Circ Res, 2007. 101(11): p. 1185-93.
38. Shaw, L.C., et al., Proliferating endothelial cell-specific expression of IGF-I receptor ribozyme inhibits retinal neovascularization. Gene Ther, 2006. 13(9): p. 752-60.
39. Drixler, T.A., et al., Angiostatin inhibits pathological but not physiological retinal angiogenesis. Invest Ophthalmol Vis Sci, 2001. 42(13): p. 3325-30.
40. Horoszewicz, J.S., E. Kawinski, and G.P. Murphy, Monoclonal antibodies to a new antigenic marker in epithelial prostatic cells and serum of prostatic cancer patients. Anticancer Res, 1987. 7(5B): p. 927-35.
41. Israeli, R.S., et al., Molecular cloning of a complementary DNA encoding a prostate-specific membrane antigen. Cancer Res, 1993. 53(2): p. 227-30.
42. Tiffany, C.W., et al., Characterization of the enzymatic activity of PSM: comparison with brain NAALADase. Prostate, 1999. 39(1): p. 28-35.
43. Pinto, J.T., et al., Alterations of prostate biomarker expression and testosterone utilization in human LNCaP prostatic carcinoma cells by garlic-derived S-allylmercaptocysteine. Prostate, 2000. 45(4): p. 304-14.
44. Rajasekaran, A.K., G. Anilkumar, and J.J. Christiansen, Is prostate-specific membrane antigen a multifunctional protein? Am J Physiol Cell Physiol, 2005. 288(5): p. C975-81.
45. Castelletti, D., et al., Apical transport and folding of prostate-specific membrane antigen occurs independent of glycan processing. J Biol Chem, 2006. 281(6): p. 3505-12.
46. Christiansen, J.J., et al., N-glycosylation and microtubule integrity are involved in apical targeting of prostate-specific membrane antigen: implications for immunotherapy. Mol Cancer Ther, 2005. 4(5): p. 704-14.
47. Schulke, N., et al., The homodimer of prostate-specific membrane antigen is a functional target for cancer therapy. Proc Natl Acad Sci U S A, 2003. 100(22): p. 12590-5.
48. Christiansen, J.J., et al., Polarity of prostate specific membrane antigen, prostate stem cell antigen, and prostate specific antigen in prostate tissue and in a cultured epithelial cell line. Prostate, 2003. 55(1): p. 9-19.
49. Anilkumar, G., et al., Prostate-specific membrane antigen association with filamin A modulates its internalization and NAALADase activity. Cancer Res, 2003. 63(10): p. 2645-8.
50. Williams, T. and R. Kole, Analysis of prostate-specific membrane antigen splice variants in LNCap cells. Oligonucleotides, 2006. 16(2): p. 186-95.
51. Mlcochova, P., et al., Prostate-specific membrane antigen and its truncated form PSM'. Prostate, 2009. 69(5): p. 471-9.
52. Rojas, C., et al., Kinetics and inhibition of glutamate carboxypeptidase II using a microplate assay. Anal Biochem, 2002. 310(1): p. 50-4.
53. Mesters, J.R., K. Henning, and R. Hilgenfeld, Human glutamate carboxypeptidase II inhibition: structures of GCPII in complex with two potent inhibitors, quisqualate and 2-PMPA. Acta Crystallogr D Biol Crystallogr, 2007. 63(Pt 4): p. 508-13.
54. Su, S.L., et al., Alternatively spliced variants of prostate-specific membrane antigen RNA: ratio of expression as a potential measurement of progression. Cancer Res, 1995. 55(7): p. 1441-3.
55. Drachenberg, D.E., et al., Circulating levels of interleukin-6 in patients with hormone refractory prostate cancer. Prostate, 1999. 41(2): p. 127-33.
56. Israeli, R.S., et al., Expression of the prostate-specific membrane antigen. Cancer Res, 1994. 54(7): p. 1807-11.

57. Denmeade, S.R., et al., Dissociation between androgen responsiveness for malignant growth vs. expression of prostate specific differentiation markers PSA, hK2, and PSMA in human prostate cancer models. Prostate, 2003. 54(4): p. 249-57.
58. Yao, V. and D.J. Bacich, Prostate specific membrane antigen (PSMA) expression gives prostate cancer cells a growth advantage in a physiologically relevant folate environment in vitro. Prostate, 2006. 66(8): p. 867-75.
59. Colombatti, M., et al., The prostate specific membrane antigen regulates the expression of IL-6 and CCL5 in prostate tumour cells by activating the MAPK pathways. PLoS One, 2009. 4(2): p. e4608.
60. Wright, G.L., Jr., et al., Upregulation of prostate-specific membrane antigen after androgen-deprivation therapy. Urology, 1996. 48(2): p. 326-34.
61. Kinoshita, Y., et al., Targeting epitopes in prostate-specific membrane antigen for antibody therapy of prostate cancer. Prostate Cancer Prostatic Dis, 2005. 8(4): p. 359-63.
62. Huang, X., M. Bennett, and P.E. Thorpe, Anti-tumor effects and lack of side effects in mice of an immunotoxin directed against human and mouse prostate-specific membrane antigen. Prostate, 2004. 61(1): p. 1-11.
63. Bander, N.H., Technology insight: monoclonal antibody imaging of prostate cancer. Nat Clin Pract Urol, 2006. 3(4): p. 216-25.
64. Bander, N.H., et al., Phase I trial of 177lutetium-labeled J591, a monoclonal antibody to prostate-specific membrane antigen, in patients with androgen-independent prostate cancer. J Clin Oncol, 2005. 23(21): p. 4591-601.
65. Bander, N.H., et al., Targeted systemic therapy of prostate cancer with a monoclonal antibody to prostate-specific membrane antigen. Semin Oncol, 2003. 30(5): p. 667-76.
66. Bander, N.H., et al., Targeting metastatic prostate cancer with radiolabeled monoclonal antibody J591 to the extracellular domain of prostate specific membrane antigen. J Urol, 2003. 170(5): p. 1717-21.
67. Galsky, M.D., et al., Phase I trial of the prostate-specific membrane antigen-directed immunoconjugate MLN2704 in patients with progressive metastatic castration-resistant prostate cancer. J Clin Oncol, 2008. 26(13): p. 2147-54.
68. Henry, M.D., et al., A prostate-specific membrane antigen-targeted monoclonal antibody-chemotherapeutic conjugate designed for the treatment of prostate cancer. Cancer Res, 2004. 64(21): p. 7995-8001.
69. Buhler, P., et al., A bispecific diabody directed against prostate-specific membrane antigen and CD3 induces T-cell mediated lysis of prostate cancer cells. Cancer Immunol Immunother, 2008. 57(1): p. 43-52.
70. Wolf, P., et al., Anti-PSMA immunotoxin as novel treatment for prostate cancer? High and specific antitumor activity on human prostate xenograft tumors in SCID mice. Prostate, 2008. 68(2): p. 129-38.
71. Chang, S.S., et al., Prostate-specific membrane antigen is produced in tumor-associated neovasculature. Clin Cancer Res, 1999. 5(10): p. 2674-81.
72. Chang, S.S., et al., Five different anti-prostate-specific membrane antigen (PSMA) antibodies confirm PSMA expression in tumor-associated neovasculature. Cancer Res, 1999. 59(13): p. 3192-8.
73. Chang, S.S., et al., Comparison of anti-prostate-specific membrane antigen antibodies and other immunomarkers in metastatic prostate carcinoma. Urology, 2001. 57(6): p. 1179-83.
74. Baccala, A., et al., Expression of prostate-specific membrane antigen in tumor-associated neovasculature of renal neoplasms. Urology, 2007. 70(2): p. 385-90.
75. Conway, R.E., et al., Prostate-specific membrane antigen regulates angiogenesis by modulating integrin signal transduction. Mol Cell Biol, 2006. 26(14): p. 5310-24.
76. Mitra, S.K., et al., Intrinsic FAK activity and Y925 phosphorylation facilitate an angiogenic switch in tumors. Oncogene, 2006. 25(44): p. 5969-84.
77. Mitra, S.K. and D.D. Schlaepfer, Integrin-regulated FAK-Src signaling in normal and cancer cells. Curr Opin Cell Biol, 2006. 18(5): p. 516-23.

78. Calderwood, D.A., et al., Increased filamin binding to beta-integrin cytoplasmic domains inhibits cell migration. Nat Cell Biol, 2001. 3(12): p. 1060-8.
79. Shappell, S.B., et al., Prostate pathology of genetically engineered mice: definitions and classification. The consensus report from the Bar Harbor meeting of the Mouse Models of Human Cancer Consortium Prostate Pathology Committee. Cancer Res, 2004. 64(6): p. 2270-305.
80. Okazaki, K., et al., Enhancement of metastatic activity of colon cancer as influenced by expression of cell surface antigens. J Surg Res, 1998. 78(1): p. 78-84.
81. Basson, M.D., An intracellular signal pathway that regulates cancer cell adhesion in response to extracellular forces. Cancer Res, 2008. 68(1): p. 2-4.
82. Craig, D.H., et al., Increased extracellular pressure enhances cancer cell integrin-binding affinity through phosphorylation of beta1-integrin at threonine 788/789. Am J Physiol Cell Physiol, 2009. 296(1): p. C193-204.
83. Hu, S., et al., Prosaposin down-modulation decreases metastatic prostate cancer cell adhesion, migration, and invasion. Mol Cancer. 9: p. 30.
84. Zhao, J. and J.L. Guan, Signal transduction by focal adhesion kinase in cancer. Cancer Metastasis Rev, 2009. 28(1-2): p. 35-49.
85. Kuphal, S., R. Bauer, and A.K. Bosserhoff, Integrin signaling in malignant melanoma. Cancer Metastasis Rev, 2005. 24(2): p. 195-222.
86. Tsui, P., M. Rubenstein, and P. Guinan, Correlation Between PSMA and VEGF Expression as Markers for LNCaP Tumor Angiogenesis. J Biomed Biotechnol, 2005. 2005(3): p. 287-90.
87. Silver, D.A., et al., Prostate-specific membrane antigen expression in normal and malignant human tissues. Clin Cancer Res, 1997. 3(1): p. 81-5.
88. Liu, H., et al., Monoclonal antibodies to the extracellular domain of prostate-specific membrane antigen also react with tumor vascular endothelium. Cancer Res, 1997. 57(17): p. 3629-34.
89. Lobov, I.B., P.C. Brooks, and R.A. Lang, Angiopoietin-2 displays VEGF-dependent modulation of capillary structure and endothelial cell survival in vivo. Proc Natl Acad Sci U S A, 2002. 99(17): p. 11205-10.

OPEN ACCESS Freely available online

PLoS one

Prostate Specific Membrane Antigen (PSMA) Regulates Angiogenesis Independently of VEGF during Ocular Neovascularization

Christina L. Grant, Leslie A. Caromile, Khayyam Durrani, M. Mamunur Rahman, Kevin P. Claffey, Guo-Hua Fong, Linda H. Shapiro*

Center for Vascular Biology, University of Connecticut Health Center, Farmington, Connecticut, United States of America

Abstract

Background: Aberrant growth of blood vessels in the eye forms the basis of many incapacitating diseases and currently the majority of patients respond to anti-angiogenic therapies based on blocking the principal angiogenic growth factor, vascular endothelial growth factor (VEGF). While highly successful, new therapeutic targets are critical for the increasing number of individuals susceptible to retina-related pathologies in our increasingly aging population. Prostate specific membrane antigen (PSMA) is a cell surface peptidase that is absent on normal tissue vasculature but is highly expressed on the neovasculature of most solid tumors, where we have previously shown to regulate angiogenic endothelial cell invasion. Because pathologic angiogenic responses are often triggered by distinct signals, we sought to determine if PSMA also contributes to the pathologic angiogenesis provoked by hypoxia of the retina, which underlies many debilitating retinopathies.

Methodology/Principal Findings: Using a mouse model of oxygen-induced retinopathy, we found that while developmental angiogenesis is normal in PSMA null mice, hypoxic challenge resulted in decreased retinal vascular pathology when compared to wild type mice as assessed by avascular area and numbers of vascular tufts/glomeruli. The vessels formed in the PSMA null mice were more organized and highly perfused, suggesting a more 'normal' phenotype. Importantly, the decrease in angiogenesis was not due to an impaired hypoxic response as levels of pro-angiogenic factors are comparable; indicating that PSMA regulation of angiogenesis is independent of VEGF. Furthermore, both systemic and intravitreal administration of a PSMA inhibitor in wild type mice undergoing OIR mimicked the PSMA null phenotype resulting in improved retinal vasculature.

Conclusions/Significance: Our data indicate that PSMA plays a VEGF-independent role in retinal angiogenesis and that the lack of or inhibition of PSMA may represent a novel therapeutic strategy for treatment of angiogenesis-based ocular diseases.

Citation: Grant CL, Caromile LA, Durrani K, Rahman MM, Claffey KP, et al. (2012) Prostate Specific Membrane Antigen (PSMA) Regulates Angiogenesis Independently of VEGF during Ocular Neovascularization. PLoS ONE 7(7): e41285. doi:10.1371/journal.pone.0041285

Editor: Michael E. Boulton, University of Florida, United States of America

Received March 21, 2012; **Accepted** June 19, 2012; **Published** July 18, 2012

Copyright: © 2012 Grant et al. This is an open-access article distributed under the terms of the Creative Commons Attribution License, which permits unrestricted use, distribution, and reproduction in any medium, provided the original author and source are credited.

Funding: This work was supported by the Prostate Cancer Foundation and the Department of Defense Prostate Cancer Program #PC073976 to LHS. The funders had no role in study design, data collection and analysis, decision to publish, or preparation of the manuscript.

Competing Interests: The authors have declared that no competing interests exist.

* E-mail: lshapiro@neuron.uchc.edu

Introduction

It is estimated that by 2050 nearly 15% of the global population will be 65 years of age or older [1]. When coupled with the escalating prevalence of diabetes worldwide, this increase in lifespan has prompted predictions of a striking rise in the incidence of retinal neovascular diseases such as diabetic retinopathy and age-related macular degeneration by 2020 [2]. Paradoxically, improvements in neonatal care have increased the survival of very premature infants who are at highest risk for a third neovascular disease, retinopathy of prematurity, contributing to increasing incidence in this condition that had previously been declining [3,4]. This cumulative increase in vision loss due to various forms of retinal angiogenesis is becoming a significant public health problem [2]. While the initiating events in these diseases are unique, they each give rise to tissue hypoxia and high levels of angiogenic growth factors that trigger the pathologic overgrowth of new vascular networks that eventually obscure vision [5]. Treatments largely focuses on halting this process and include surgical resection of the neovasculature and laser photocoagulation of affected areas [6]. Recently, a regimen of frequent intravitreal injections of angiogenesis-inhibiting anti-VEGF reagents has proven to be a very successful treatment for age-related macular degeneration [7,8] and shows promise for diabetic retinopathy [9]. However, complications associated with repeated injections and potential long-term secondary effects could potentially limit the utility of anti-VEGF therapy [10] and the fact that a percentage of patients do not respond [11] highlight the need to explore new target molecules for use in treatment of angiogenic-based diseases.

The oxygen induced retinopathy (OIR) model evaluates angiogenic responses to tissue hypoxia and is an established animal model of retinal diseases resulting from dysregulated angiogenesis of the eye [5]. Mice are normally born with an immature retinal vasculature that progressively develops until approximately 3 weeks of age. Experimental exposure of neonatal mice to high levels of oxygen (75%) arrests the normal retinal vessel development and causes regression of existing retinal vessels. Upon subsequent exposure to normal oxygen levels (room air, 21%), tissues sense the relatively lower oxygen levels as a state of 'relative hypoxia'. The retina is particularly sensitive to this change because of the initial loss of vessels during hyperoxia treatment and the normally well-regulated temporo-spatial signals that drive organized retinal vascular development are disrupted. In particular, the vessels in the periphery respond to this dysregulated hypoxic signaling by growing in a chaotic, disordered pattern while failing to revascularize the central retina, leaving an aberrant, avascular area (Figure 1A). The resulting retinal capillary network is tortuous, leaky and disorganized in the periphery while vessels of the central region are poorly perfused and largely nonfunctional, characteristic of the pathologic phenotype of retinal neovascular disease [12].

Prostate specific membrane antigen (PSMA) is a homodimeric type II transmembrane ectopeptidase with both folate hydrolase and N-acetylated, α-linked acidic dipeptidase or NAALADase activities [13–15]. In normal tissue, the expression of PSMA is predominantly restricted to prostatic epithelium, with low expression in kidney, salivary gland, duodenum and the central and peripheral nervous systems. As its name suggests, PSMA is highly over-expressed in prostate cancer where its increased expression correlates with advanced stages of prostate cancer and metastasis. Its function in the prostate remains unknown. Interestingly, PSMA has also been shown to be upregulated on the angiogenic vasculature of most solid tumors [16,17]. Previous investigations in our lab have shown that mice lacking PSMA are incapable of mounting a pathologic angiogenic response *in vivo* suggesting that PSMA induction at angiogenic sites is critical for endothelial function in angiogenesis [18]. Mechanistically, we found that inhibition of PSMA significantly decreased Beta-1 integrin activation and reduced the subsequent downstream signal transduction cascades involving PAK and FAK, thus impairing the endothelial cell functions of adhesion, motility and invasion that are fundamental to the angiogenic response [18].

While angiogenesis is an important component in the progression of a number of diseases, it is clear that all angiogenic processes are not regulated by the same signals and are often distinct pathologies [19]. To determine if PSMA also contributes to angiogenesis in the retina, we studied the development of the retinal vasculature in wild type and PSMA null mice under physiological (normal retina development) and pathophysiological conditions (hypoxia-driven retinopathy).

Results

In order to assess the role of PSMA in pathologic retinal angiogenesis, it was first necessary to verify that PSMA is expressed in the angiogenic neovasculature in wild type mice undergoing OIR. We initially evaluated retinal tissues from postnatal-day 17 mice (P17) when vasculoproliferative disease is maximal (Figures 1A and B). PSMA mRNA was detected in wild type P17 retinas as well as positive control kidney and the prostate tumor cell line TRAMP-C1 samples, but not in PSMA-null retinal tissue (Figure 1B). Subsequent qRT-PCR analysis showed that after an initial decrease, retinal PSMA mRNA expression is progressively induced over time, reaching maximum levels at P16 (Figure 1C). Immunohistochemical assessment confirmed that the angiogenic vasculature expressed PSMA protein where positive staining was detected on retinal angiogenic tufts (abnormal, glomerular-like, endothelial-rich capillary structures that extend beyond the inner limiting membrane into the vitreous of the eye, arrow, Figure 1D) in addition to the retinal neural tissue as previously reported [20]. No staining was observed on the extra-retinal vascular tufts in PSMA null OIR retinas (arrows, Figure 1E). Therefore, PSMA is expressed on the angiogenic neovasculature of wild-type mice undergoing OIR and may contribute to pathologic angiogenesis in the retina.

Examination of the retinas of wild type and PSMA null mice demonstrated that the lack of PSMA does not affect normal developmental retinal angiogenesis (Figure 2). Wild type and null mice raised in normoxia were perfused with FITC-labeled *Ricin communis* agglutinin 1 (RCA-1-FITC) at postnatal day 17 to assess vessel integrity. Whole mounts of wild type and PSMA null retinas showed an indistinguishably normal pattern of radial vessels with patent, non-leaky, perfused vessels detected throughout the entire retinal area of both genotypes. Further magnification of the mid-peripheral region revealed a characteristically normal branched pattern of vessels in the ganglion cell layer of wild type and PSMA null retinas (Figure 2 insets). Based on these data, loss of PSMA does not affect the development of normal retinal vasculature, in agreement with a pathologic angiogenesis-specific role for this protein in vessel growth.

In contrast to the normal developmental vascular patterns found in PSMA null retinas, analysis of retinas harvested from mice undergoing OIR showed a striking phenotypic difference between wild type and PSMA null animals. Wild type and PSMA null mice were subjected to OIR and perfused with RCA-1-FITC lectin on postnatal day 17. As expected, wild type retinas displayed few vessels in the central area accompanied by an overgrowth of perfused vessels in the periphery (Figure 3A). Similarly, the capillaries in the mid-periphery were highly abundant and formed a dense, honeycombed pattern with closely spaced vessels (Figure 3C), rather than the radial, branched vascular pattern seen in untreated animals (Figure 2). In contrast, retinas isolated from PSMA null animals after OIR show a vascular pattern that more closely resembles the normal structure, with a relative reduction in avascular area in the central retina and a less dense, more highly branched capillary bed in the periphery (Figures 3B and 3D). Quantification of the relative degree of central retinal vascularity showed that PSMA null retinas had a significantly lower total avascular area than those from wild type animals (approximately 40%, Figure 3E). In addition to the decrease in retinal avascular area, the number of extra-retinal vascular tufts is significantly decreased in PSMA null animals compared to wild type controls (Figure 3F) suggesting a less pathologic angiogenic response in the absence of PSMA.

While vessels formed in response to OIR in PSMA null retinas appear more 'normal' and less pathologic with regard to microvascular patterning and vessel coverage than their wild type counterparts, it is important that these vessels function normally as well. To measure the integrity of the wild type and PSMA null vessels, we perfused mice undergoing OIR at P17 with RCA-1-FITC and then stained the harvested retinas with Alexa594 labeled- *Griffonia simplicifolia* 1 isolectin B4 (GSl-B4-A594 that specifically binds to endothelial cells [21]) to distinguish perfused, functional vessels (dual FITC and Alexa594 labeled) from non-perfused, nonfunctional endothelial clusters (single Alexa594 labeled). In both wild type and PSMA null animals, the RCA-1-FITC signals colocalized with GSI-B4 A594 staining to a certain

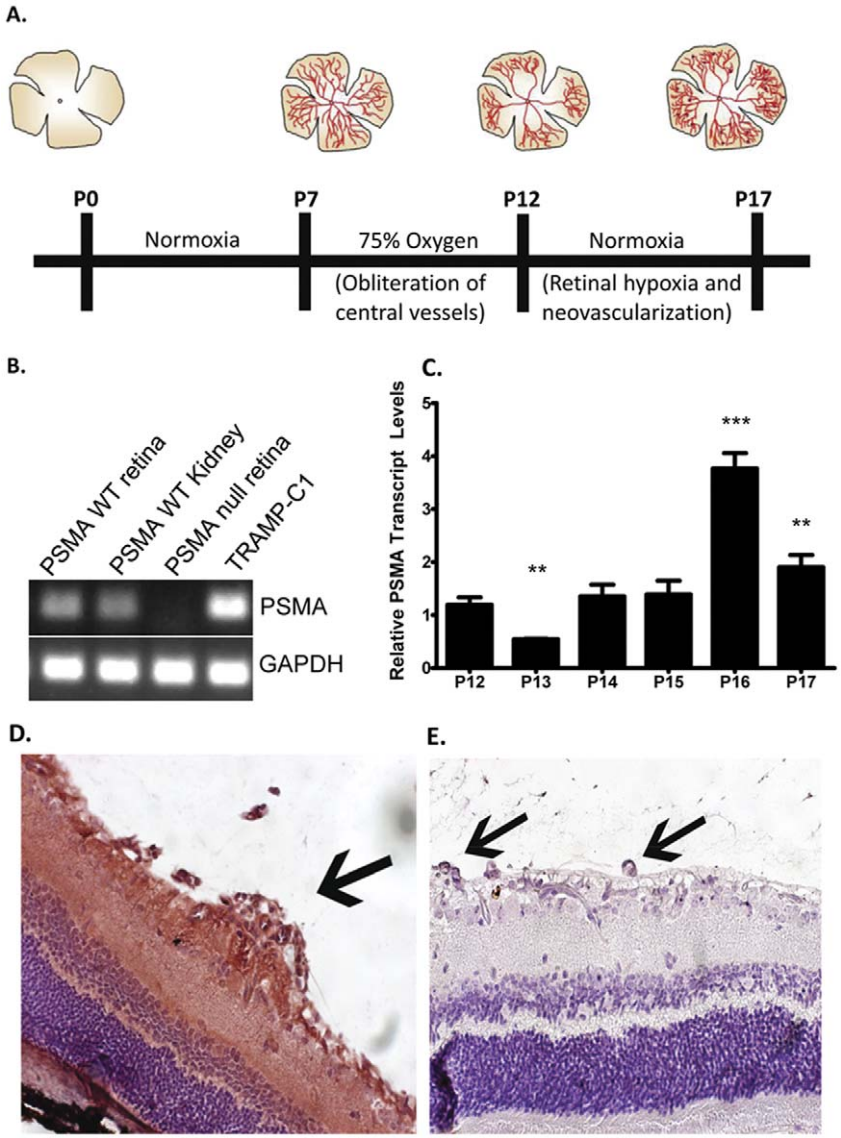

Figure 1. Retinal vasculature of wild type mice undergoing OIR expresses PSMA. A) A time line depicting the stages of retinal layer vascularization with diagrams of approximate vascular morphology of the retina at various time points. **B**) Conventional RT-PCR of RNA isolated from wild-type OIR retinas from P17 mice are positive for PSMA; PSMA wild-type kidney and TRAMP-C1 cells- PSMA positive controls, PSMA null retina-negative control. **C**) qRT-PCR for PSMA over time from retinal RNA isolated at the indicated time points relative to P12 levels. Paraffin embedded OIR retinas were immunostained for PSMA protein using the 3E2 antibody. Staining (red-brown) was observed on vascular tufts (arrows) of wild-type (**D**) but not PSMA-null (**E**) retinas. (n = 3 per group), **p,0.05, ***p,0.001.
doi:10.1371/journal.pone.0041285.g001

degree, indicating that both wild type and PSMA null animals are capable of forming patent and perfused vessels (Figure 4A). However, quantification of the total area of non-perfused endothelial cells in retinas from both genotypes (RCA-1-FITC-negative/GSI-B4- Alexa594 positive, pseudo colored white in Figure 4B) illustrates that PSMA null retinas show half the amount of non-perfused endothelium as the wild type and the vessels formed are clearly more functional (Figure 4C). Thus, in addition to affecting both vascular density and patterning, vessels formed in the absence of PSMA appear to be better perfused, patent and function as normal vessels.

During OIR, vessels initially regress in response to the relatively hypoxic conditions experienced upon exposure to room air after high oxygen levels (P12). This regression phase is followed by a robust pathologic angiogenic response, producing the vessel overgrowth characteristic of retinopathy (P15–17). In principle, the phenotype in PSMA null OIR retinas could be due either to a defect in initial vessel regression or, more consistent with PSMA in angiogenesis, a limited pathological angiogenic response during the retinal revascularization phase. Retinas harvested from wild type and PSMA null mice undergoing OIR at the peak of vascular regression immediately after hyperoxia (P12), at the initiation of retinal revascularization (P15) or at the point of the most severe angiogenic pathology in the model (P17, Figure 5A) showed no statistical difference in avascular area on P12 or P15 (Figure 5B). However, measurements of the central avascular areas in retinas of PSMA null mice on P17 were significantly lower than wild type indicating that the attenuated retinal pathology in the PSMA null mice is not due to retinal vessel persistence during the vascular

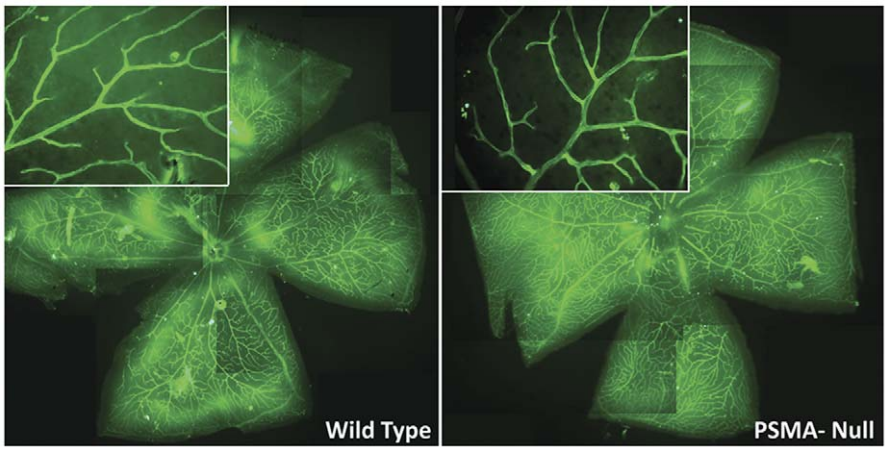

Figure 2. Retinal vasculature develops normally in PSMA null mice. Retinas from wild-type (**left**) and PSMA-null (**right**) mice (5X) raised in room air, harvested at P17 and perfused with FITC labeled *ricin communis* agglutinin 1 (RCA-1-FITC, green). Insets: higher (40X) magnification of the same retina and show normal radial branching pattern in animals of both genotypes. (Representative image, n = 3 per group).
doi:10.1371/journal.pone.0041285.g002

obliteration phase but rather to reduced pathological angiogenesis in response to relative hypoxia.

Retinopathy is most commonly the result of uncontrolled VEGF expression that induces overgrowth of blood vessels that are generally immature, leaky, obstructed and torturous [6]. Changes in hypoxia and pH as a result of disease activate critical angiogenic signaling pathways culminating in the upregulation of VEGF [22,23]. To establish if the decrease in angiogenic pathology observed in the OIR retinas of PSMA null mice was due to effects on hypoxic signaling, we examined the levels of VEGF and another hypoxia-induced angiogenesis promoting growth factor, angiopoietin 2 (Ang-2), over time using quantitative RT-PCR. In both wild type and PSMA null mice, VEGF levels increased in parallel by about 2.5-fold on P13 and remained elevated through P17 (Figure 6A). Similarly, lack of PSMA had no effect on Ang-2 levels which remained low until P16-17 and then increased by approximately 5–10 fold indicating that the blunted pathologic angiogenesis in the PSMA null mice is not due to deficiencies in production of pro-angiogenic factors in response to hypoxia (Figure 6B) and, consistent with our previous published data [18], is the result of an endothelial cell-intrinsic defect.

Finally, to determine the therapeutic potential of PSMA as a target in retinopathies, we treated wild type mice undergoing OIR with the small molecule PSMA inhibitor 2-PMPA in two dosing protocols, systemic administration of 100mg/kg 2-PMPA either once on P14 or daily from P14-P16 (Figures 7 A, B). Wild-type mice treated with a single dose of inhibitor showed a slight but not significant decrease in avascular area compared to vehicle control. However, daily administration of the inhibitor over three days decreased revascularization, as measured by a significant increase in avascular area compared to control and suggests that PSMA inhibition may be a viable therapy for slowing the progression of retinopathy. However, since PSMA is expressed in other tissues such as the brain where it regulates glutamate levels, systemic PSMA inhibition may potentially produce harmful side effects. To avoid this possibility we treated OIR mice with a single intravitreal injection of 2-PMPA on P14 and measured avascular area three days later. Indeed, retinas of inhibitor-treated mice showed improved vascular coverage and reduced avascular area than the retina from the vehicle control (Figure 7C). Although intravitreal injection is not as effective as systemic treatment in our experiments, it is likely that multiple doses would increase its effectiveness. While repeated injections in the mouse eye caused significant scarring, this regimen is well tolerated by humans and is the current method of anti-VEGF treatment and could be adapted for administration of PSMA inhibitors.

Discussion

Histological observations of high PSMA expression on the angiogenic neovasculature of solid tumors suggested that it may regulate endothelial function [24,25] and prompted our earlier investigation into the function of PSMA in angiogenesis [18]. In the previous study we demonstrated that tumor angiogenesis was significantly impaired in PSMA null mice due to diminished Beta-1 integrin activation and a subsequent decrease in endothelial cell invasion, thus affecting angiogenesis. In the current investigation we extended these observations to examine if PSMA may be a viable target for treatment of dysregulated angiogenesis that is the underlying cause of the majority of devastating retinopathies and may be of benefit to the large proportion of patients that are refractory to current anti-VEGF regimens [8]. To evaluate the role of PSMA in retinal neovascularization, we used a reliable model of retinal angiogenesis (oxygen induced retinopathy or OIR) that mimics many aspects of proliferative retinopathies [5]. We initially determined that PSMA expression is induced in the retinal vasculature undergoing OIR, indicating that it may indeed contribute to pathology in this model. We also observed that while the retinal vasculature develops normally in mice lacking PSMA, upon OIR challenge the lack of PSMA results in significant reduction of pathologic vascular angiogenesis when compared to wild type animals. The newly formed vessels in the PSMA null retinas were highly organized with regular microvascular patterning in contrast to the disorganized, chaotic and tortuous, characteristically angiogenic, vessels present in wild type retinas. Furthermore, lack of PSMA resulted in a reduction of avascular area and number of vascular tufts, indicating a diminished pathological response. Perfusion with fluorescent lectin showed that the retinal vessels in PSMA null animals were significantly more patent and well perfused than those of wild type mice, reinforcing the notion that PSMA regulates angiogenic vessel formation and its loss promotes more 'normal' vascular growth. Similarly, this response was not due to effects on angiogenic growth factor production or effects on vessel regression in response

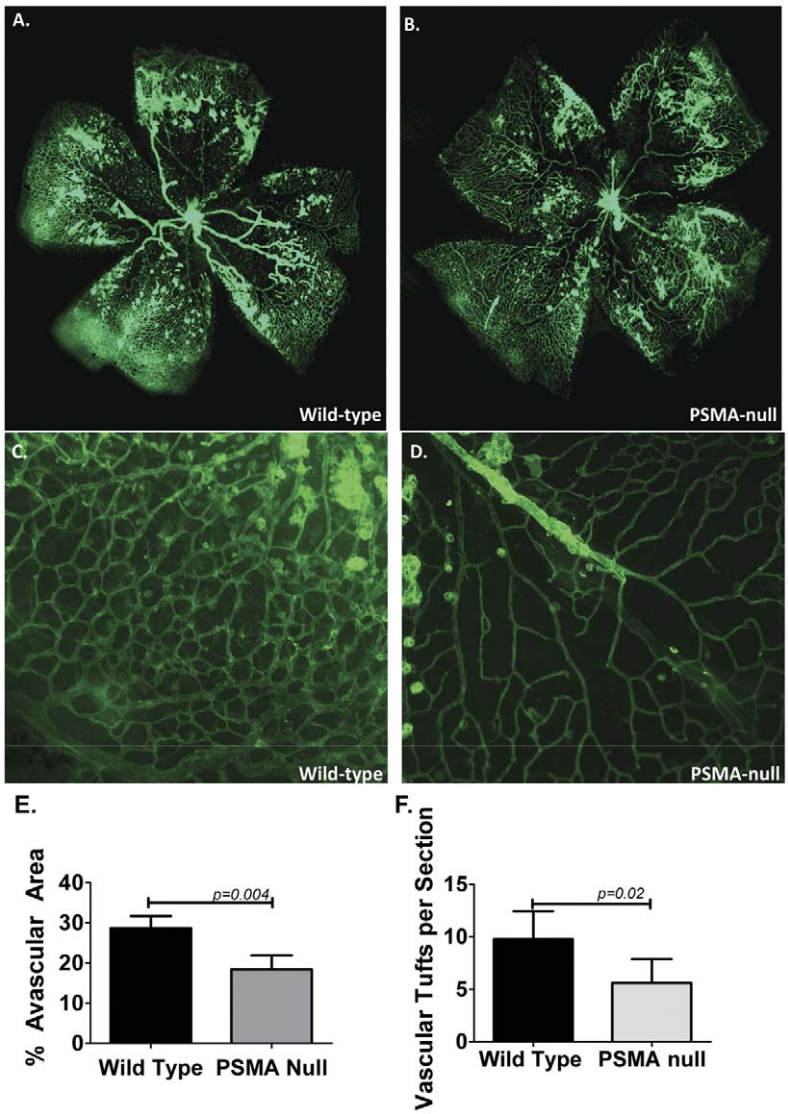

Figure 3. Pathologic angiogenesis is reduced in retinas of PSMA null mice. Whole-mount retinas from mice undergoing OIR were harvested at P17 and perfused with RCA-1-FITC. Wild type retinas (**A**) show a higher degree of central avascular area than retinas from PSMA null mice (**B**). Higher magnification (40x) of **BC** wild-type and **D**) PSMA-null capillary networks at the outer edge of the retina: Retinas isolated from wild-type mice **C**) show disorganized, tortuous vessels and vascular tufts while vessels of PSMA-null retinas **D**) are less tortuous and more closely resemble normal organization. **E**) Quantification of avascular area using Image J showed wild-type mice had an average avascular area of 28.7%, compared to 18.4% in the retinas isolated from PSMA null mice, (n = 4 per group, p = 0.004). **F**) Wild type animals had an average of 8.8 vascular tufts per histologic section, compared to an average of 5.2 tufts per section in PSMA-null (n = 8 per group, p = 0.017).
doi:10.1371/journal.pone.0041285.g003

to high oxygen levels. Finally, systemic or intra-ocular administration of an inhibitor of PSMA enzymatic activity phenocopied the response of null animals and resulted in a marked decrease in avascular area and increased vessel coverage in treated animals. Taken together, these results support a role for PSMA in retinal angiogenesis and thus may be a valuable therapeutic target.

The mouse model of OIR used in this study has been well characterized and has both strengths and limitations. The model lends itself well to genetic manipulation, either by deletion or overexpression, to test the contribution of specific genes on retinal neovascularization [26,27]. In addition, these models are quite reproducible, cost-effective and quantitative analysis is reliable with relatively low variability [28]. However, in human retinopathy of prematurity, the peripheral vessels are destroyed by exposure to high oxygen levels while the central vessels are affected in the mouse model [27]. However, despite this discrepancy the mouse OIR model recapitulates the pathology of progression resulting from ischemia-induced neovascularization to a remarkable degree, and thus is a reliable and robust model of this condition [26].

While numerous molecules and signaling pathways are responsible for developmental angiogenesis (reviewed in ref [29]), perhaps the best characterized system is that of VEGF, which through alternative splicing and proteolytic processing mechanisms, produces various VEGF isoforms that differ in their ability to bind heparan sulfate residues on extracellular matrix and cell surface proteins. Proper positioning of these isoforms creates precise gradients of matrix-bound and freely diffusible angiogenic factors that guide and control the endothelium of the developing vasculature. Perfusion of the vessels and pericyte coverage

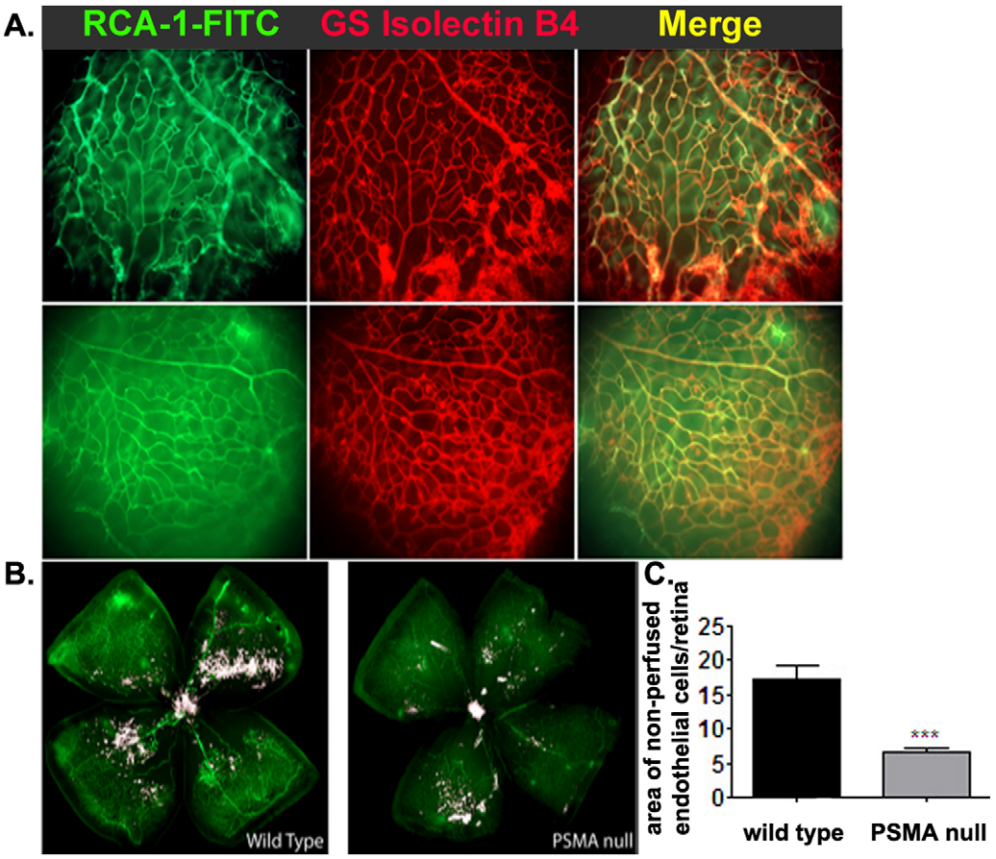

Figure 4. Perfusion of retinal vessels in PSMA null animals is increased. Following OIR, mice were perfused with RCA-1-FITC to detect perfused vessels immediately prior to sacrifice and harvest. Isolated retinas were then stained with Alexa 594 labeled *Griffonia simplicifolia* 1 isolectin B4 (GS Isolectin B4-A594) to stain all endothelial cells. **A**) RCA-1-FITC staining (**left, green**), GS Isolectin B4-A594 staining (**center, red**) and merged image (**right**) of representative wild type (**top**) and PSMA null (**bottom**) retinas. **B**) The double stained areas in the merged images (perfused vessels + endothelial cells) were pseudo-colored white to illustrate the area of non-perfused, GS Isolectin B4-A594 only staining endothelial cells (5X). **C**) Quantitative analysis of the relative extent of non-perfused endothelial cells per retina. (Representative image, n = 5 per group).
doi:10.1371/journal.pone.0041285.g004

contributes to cessation of angiogenesis, leading to normal, quiescent vasculature [30]. In contrast, while many of the same factors that regulate developmental angiogenesis are responsible for the blood vessel formation in pathologic states, under the pro-angiogenic conditions of sustained hypoxia, infiltrating immune cells and tissue damage the tight regulation of vessel growth is lost resulting in an asynchronous, leaky and immature vasculature and persistent angiogenesis. Clearly, additional unique mechanisms must regulate pathological angiogenesis since similar to PSMA, a number of pro-angiogenic molecules (such as PlGF [31], PECAM-1 [32], aminopeptidase A [33], CD13 [34]) have been shown to be dispensable for developmental angiogenesis. This suggests that they participate solely in the pathological response, making them particularly promising therapeutic targets.

Consistent with our previously published data linking PSMA regulation of angiogenesis to endothelial Beta-1 integrin signaling and adhesion [18], the decrease in pathologic angiogenesis in the retinas of PSMA null mice was not due to deficient VEGF or Ang-2 production in response to hypoxia. In fact, the retinas of PSMA null animals undergoing OIR displayed levels of VEGF and Ang-2 similar to those of the wild type, but angiogenesis was decreased in the absence of PSMA indicating that PSMA participates in endothelial cell functions downstream of angiogenic growth factor signaling.

While it is clear that VEGF-induced signals are critical for angiogenesis, proper interactions of endothelial cells with extracellular matrix proteins via the integrins are equally as important to promote migration and other cellular processes essential to the angiogenic response [35–37]. Numerous studies have implicated various integrin pairs in retinal vascular pathology [19,38–41], where blocking, disruption or lack of integrins generally impairs angiogenesis, supporting PSMA regulation of integrin signaling as the mechanistic basis for our findings. Importantly, the signals initiated by integrin/extracellular matrix and growth factor/receptor interactions are coordinated and transmitted to intracellular cytoskeletal and signaling proteins by the focal adhesion kinase FAK. Thus FAK controls essential cellular processes such as growth, survival, migration and differentiation [42]. Pertinent to this study, FAK has been previously demonstrated to be involved in pathological retinal angiogenesis [43]. In this study, over-expression of FAK by intra-ocular injection of an expression plasmid into mice undergoing OIR led to the formation of large retinal vascular tufts and pathologic neovascularization, whereas injection of a plasmid expressing the FAK inhibitor FRNK decreased new vessel formation [43]. Combined with our previous data [18], the current study suggests that PSMA likely regulates both retinal and tumor angiogenesis via the same or similar mechanisms, by enhancing adhesion and activation of Beta-1 integrin and increasing its associated FAK signaling, thus

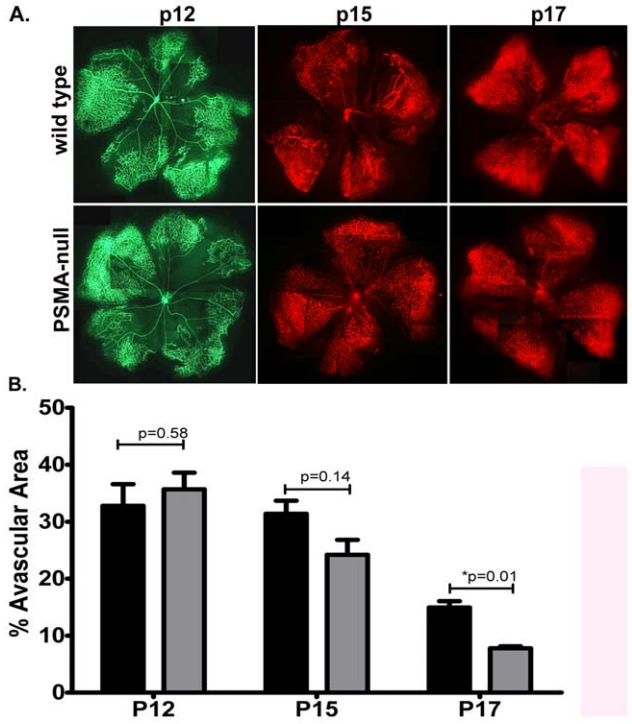

Figure 5. Vascular pathology is decreased in PSMA null animals undergoing OIR. A) Retinas were harvested from OIR mice at P12 (**left**), P15 (**center**) and P17 (**right**). Vasculature was stained using RCA-1-FITC (green, P12) or GS Isolectin B4-A594 (red, P15 and P17) and **B**) the central avascular area of each retina was measured using Image J. (n = 3 per group).
doi:10.1371/journal.pone.0041285.g005

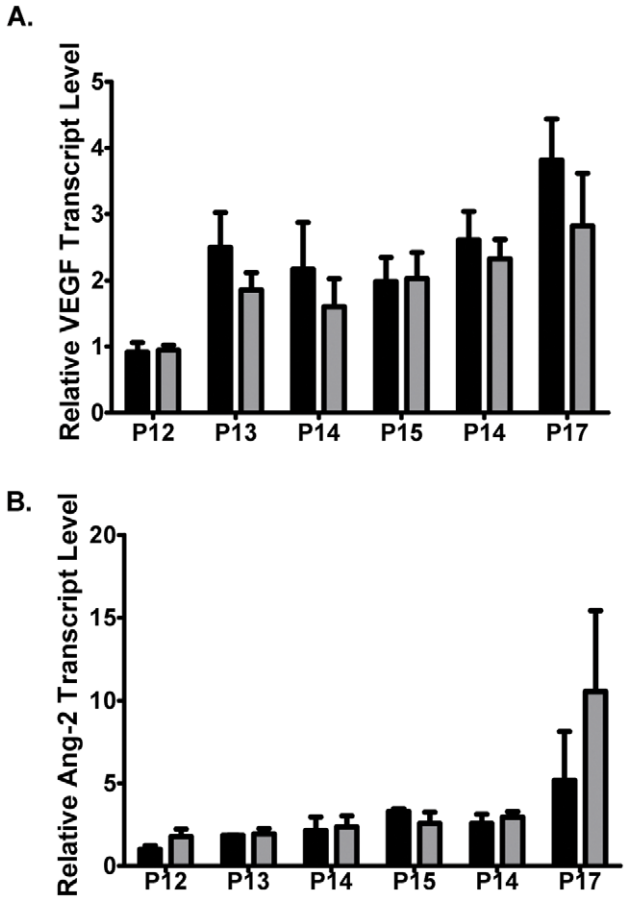

Figure 6. Angiogenic growth factor production is normal in response to hypoxia in PSMA null mice. PSMA expression was measured by qRT-PCR from RNA isolated from wild type and PSMA null retinas daily, beginning at the initiation of tissue hypoxia (P12 through P17). **A**) Wild type and PSMA mice produce similar VEGF expression levels during hypoxia treatment. **B**) PSMA null mice show similar Ang-2 levels to wild type mice over time. (n = 3 per time point).
doi:10.1371/journal.pone.0041285.g006

contributing to endothelial cell responses to angiogenic signals in a manner independent of VEGF signal transduction.

Due to its widespread contribution to many pathological disorders, early predictions were that angiogenesis would be a particularly effective therapeutic target. However, the results of clinical trials evaluating the efficacy of modulators of angiogenesis, primarily by blocking the VEGF pathway, in the treatment of cancer, diabetic retinopathy, rheumatoid arthritis, age-related macular degeneration and cardiovascular disease suggest that more precisely targeted therapies or therapies directed at multiple angiogenic pathways are needed to improve the treatment of angiogenesis-associated diseases [44]. Similarly, while recurrent intravitreal injections of the monoclonal anti-VEGF antibody ranibizumab (Lucentis) is the standard of care for age-related macular degeneration where the majority of patients show visual stabilization [8], isolated cases of macular ischemia and persistent elevation in intraocular pressure following treatment have been reported [45,46] and the long term effects of drug resistance, tolerance or ancillary effects in targeting this pathway have yet to be addressed. Furthermore, additional treatment modalities are clearly needed for those patients who do not respond to this therapy. In this regard, PSMA is also involved in the pathogenesis of neurodegenerative diseases by releasing free glutamate from N-acetyl-aspartyl-glutamate (NAAG) leading to neurotoxic levels of glutamate or 'glutamate excitotoxicity' [47,48]. Small molecule inhibitors of PSMA, including 2-PMPA, provide protection from glutamate excitotoxicity in animal models of stroke, amyotrophic lateral sclerosis, neuropathic pain and diabetic neuropathy [49,50]. While supportive of PSMA as a potential therapeutic target, 2-PMPA is a highly polar molecule, which limits its utility as a therapy. However, other more feasible PSMA inhibitors have been produced and one has been shown to be safe and well tolerated by humans at doses shown to be effective in animals [51]. These promising drugs are currently awaiting clinical trials [50,52]. Our finding that 2-PMPA decreased retinal vascular pathology in wild type mice undergoing OIR strongly suggests that PSMA inhibition may be a novel treatment that could be rapidly translated into therapeutic use for retinal diseases. In addition, due to poor drug permeability across the blood retinal barrier, intraocular injection is the preferred method of administration for age-related macular degeneration and so confounding variables such as long-term effects of PSMA inhibition on glutamate levels in the brain and bioavailability would be minimized. Therefore, our data indicate that inhibition of PSMA offers a VEGF-independent means of regulating retinal vascularization and perhaps in combination with other therapies may be a new and attractive target to improve the treatment of retinal neovascular diseases such as age-related macular degeneration.

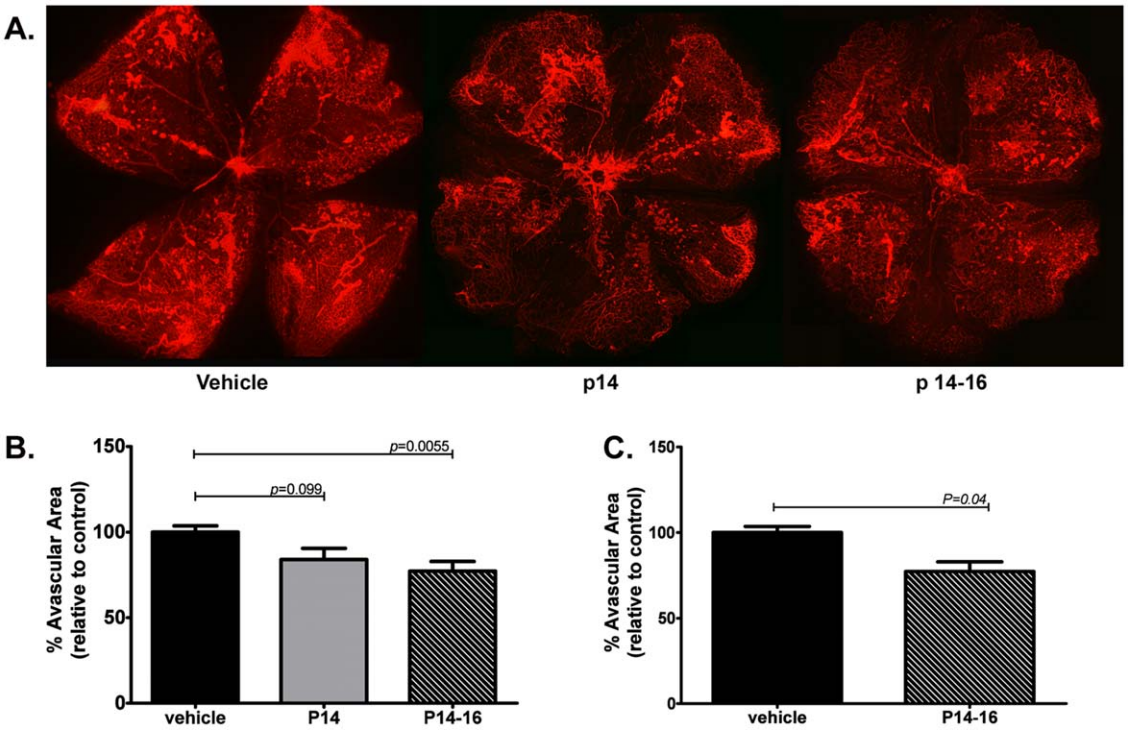

Figure 7. Inhibition of PSMA decreases pathologic angiogenesis in a mouse model of OIR. A) Wild type mice undergoing OIR were treated systemically with either a single dose of 100mg/kg 2-PMPA on P14 (n = 3, **center**) or three daily doses from P14 through P16 (n = 6, **right**), controls received vehicle (PBS, **left**). Retinas were isolated on P17, vasculature was stained using GS Isolectin B4–A594 and the avascular area calculated using Image J software. **B**) Mice receiving a single dose on P14 showed a slight but not statistically significant decrease in avascular area, whereas mice treated from P14–16 showed a significant decrease (23%) in avascular area compared to vehicle treated controls (p = 0.0055). **C**) Wild type mice on the OIR protocol were treated once on P14 with 10mg intravitreal 2-PMPA (10mg/ml, 1mL) in one eye and 1mL Vehicle (PBS) in the contralateral eye. Retinas treated with intravitreal 2-PMPA showed a significant decrease (16.66%) in avascular area compared to control retinas.
doi:10.1371/journal.pone.0041285.g007

Methods

Ethics Statement

The University of Connecticut Health Center has been fully accredited by the Association for the Assessment and Accreditation of Laboratory Animal Care International (AAALAC) since June 21, 1977. Most recent full accreditation: July 8, 2010. Animal Welfare Assurance number A3471–01; Valid Through: April 30, 2014. All animals were used according to specific animal protocols approved by the UCHC Institutional Animal Care Committee, UCHC.

Mice

C57/BL6 PSMA null mice were produced in 2005 (11) and have been backcrossed extensively to C57Bl/6. These were a generous donation from Warren Heston at Cleveland Clinic. Sibling heterozygotes were bred to produce the parents of (wild type × wild type) and (null × null) mating units and pups were no more than 3 generations removed from these units. Littermate progeny of the (het × het) crosses were used to breed the test animals in the UCHC animal facility and were provided food and water *ad libitum*. Littermates were compared in all experiments.

Oxygen Induced Retinopathy (OIR) Model

Seven day old mice weighing 6g or greater and their lactating mothers were maintained in 75% oxygen for five days. After 2.5 days in 75% oxygen, the lactating females were replaced with surrogate dames. Mice were then returned to room air (relative hypoxia) for up to 5 days. When indicated, mice were anesthetized with Tribromoethanol and perfused with FITC labeled *Ricin communis* agglutinin 1 (RCA-1-FITC) that binds preferentially to galactose containing oligosaccharides, to label perfused capillaries before enucleation. Eyes used for retinal whole mounts were pre-fixed in 4% paraformaldehyde (PFA) on ice 30 minutes, retinas isolated, then post-fixed 45 minutes in 4% PFA. After rinsing with PBS, retinas were blocked with 10% normal goat serum in PBS for 1 hour and stained overnight 4°C with the required marker or antibody. Retinas used for RNA isolation were stored in RNAlater on ice and the RNA was isolated using Qiagen RNA isolation kit according to manufacturer's instructions.

Quantitative analysis of retinal vascularization

Eyes used for histological sectioning were fixed overnight in 4% PFA at 4°C, stored in 70% ethanol, paraffin embedded, and 6μM sections cut. To analyze the number of extra-retinal vascular tufts, eyes were sagitally embedded in paraffin and sectioned 6μM apart. Each eye was analyzed using 5 H&E stained sections on either side of the optic nerve; vascular tufts, defined as endothelial cells on the vitreal side of the inner limiting membrane, were quantified under 40x by a blinded observer. To quantify avascular area, retinal whole mounts were blocked using 5% normal goat serum (Zymed), then stained overnight at 4°C with 1microgram/mL of endothelial cell specific Alexa594 conjugated *Griffonia simplicifolia* 1 isolectin B4 (Invitrogen I21413). After mounting whole mounts on slides, retinas were imaged using a 5× objective on a Zeiss LSM Confocal microscope and an image of the entire retina obtained

using the tile-scan feature. Central avascular area was outlined in NIH Image J using polygonal select tool by a blinded observer. Avascular area and total retina area were calculated using area measure tool and avascular area/total retinal area was calculated. Branch points were quantified in a 40× image of the outer edge of a retinal leaflet.

Immunohistochemistry

Slides were deparafinized and rehydrated. Antigen retrieval was conducted using 10mM sodium citrate (pH 6.0) in a pressure cooker. Endogenous peroxidase activity was quenched by incubating slides 15′ in 0.3% H_2O_2. Slides were blocked in 1% BSA for 30 minutes at room temperature in a humidified chamber then incubated under 1:50 3E2 antibody overnight in a humidified chamber. Slides were washed 3 times in PBS. 1:500 biotinylated secondary antibody (Vector Labs goat anti-mouse BA9200) in 1% BSA was applied and slides incubated for 1 hour at room temperature in a humidified chamber. Slides were washed 3 times, Vectastain Elite ABC Kit (Vector Labs SK-6100) was applied for 30 minutes. Slides were washed once in buffer, once in H_2O, then Novared (Sigma D-4293) was applied for 5 minutes. Slides were washed in H_2O, counterstained with hematoxylin (Vector Labs H-3404), washed in H_2O, dehydrated and mounted under Cytoseal 60.

Quantitative RT-PCR

RNA was isolated from retinas using Qiagen RNA isolation kit according to manufacturer's instructions. cDNA was generated using BioRad iScript reagent, including a reaction with no reverse transcriptase to control for DNA contamination. qPCR reactions were performed in triplicate using BioRad iQSupermix as indicated in manufacturer's directions and an Eppendorf thermocycler. Primers used in qPCR are as follows: **cyclophilin A** forward: 5′- ATGGCAAATGCTGGACCAAA-3′; reverse: 5′-TGCCATCCAGCCATTCAGT-3′; **VEGF** forward, 5′- CACGACAGAAGGAGAGCAGAAGT-3′, reverse, 5′-TTCGCTGGTAGACATCCATGAA -3′; **PSMA** forward: 5′-GATGTAGTGCCACCATACAGTG-3′, reverse: 5′-GCCAGTTGAGCATTTTTAACCAT 3′; **Ang-2** forward, 5′-TCAACAGCTTGCTGACCATGAT-3′, reverse, 5′-GGTTTGCTCTTCTTTACGGATAGC-3′. All experimental gene levels were normalized to a cyclophilin A internal loading control. Fold change calculations were performed using the wild-type P12 retina sample as control.

PSMA Inhibition Studies

On P15 mice were anesthetized using 12.5 mg/mL Avertin (250 mg/Kg). Using a dissecting microscope, the eyelids are opened using a sterile scalpel or by gently teasing eyelid apart using jewelers forceps. The tip of a 33 gauge needle attached to a Hamilton syringe was positioned adjacent to the pars plana, 2.5 mm posterior to the limbus, and 1uL or 10ug/uL or 1ug/uL 2-PMPA dissolved in PBS was injected into the vitreous cavity. The needle was kept in place for at least 20 seconds before being removed to prevent leakage. The eyelids were approximated over the eye and antibiotic ointment was applied. The contralateral eye was injected with sterile PBS as a control. Mice were monitored until regaining consciousness then returned to the home cage. For systemic inhibition studies, 100mg/kg or 50 mg/kg 2-PMPA (Alexis) in sterile PBS or PBS alone was injected intraperitoneally on days indicated.

Statistics

Statistical differences were assessed using the 2-tailed Student's t test. P values less than 0.05 were considered significant. All error bars represent standard deviation.

Author Contributions

Conceived and designed the experiments: CLG KPC GHF LHS. Performed the experiments: CLG KD MMR. Analyzed the data: CLG KD LAC MMR KPC GHF LHS. Contributed reagents/materials/analysis tools: MMR KPC GHF. Wrote the paper: CLG LAC LHS.

References

1. Nazimul H, Rohit K, Anjli H (2008) Trend of retinal diseases in developing countries. Expert Review of Ophthalmology 3: 43–50.
2. The Eye Diseases Prevalence Research Group (2004) Causes and Prevalence of Visual Impairment Among Adults in the United States. Arch Ophthalmol 122: 477–485.
3. Ellsbury DL, Ursprung R (2010) Comprehensive Oxygen Management for the Prevention of Retinopathy of Prematurity: the pediatrix experience. Clin Perinatol 37: 203–215.
4. Jefferies A (2010) Retinopathy of prematurity: Recommendations for screening. Paediatr Child Health 15: 667–674.
5. Stahl A, Connor KM, Sapieha P, Chen J, Dennison RJ, et al. (2010) The Mouse Retina as an Angiogenesis Model. Investigative Ophthalmology & Visual Science 51: 2813–2826.
6. David E Lederer SWC, Karl G Csaky (2009) Retina. In: Leonard A. Levin M, PhD, and Daniel M Albert, MD, MS, editor. Ocular Disease: Mechanisms and Management: Elsevier Ltd. 536–543.
7. Dhoot DS, Kaiser PK (2012) Ranibizumab for age-related macular degeneration. Expert Opin Biol Ther 12: 371–381.
8. Martin DF, Maguire MG, Ying GS, Grunwald JE, Fine SL, et al. (2011) Ranibizumab and bevacizumab for neovascular age-related macular degeneration. N Engl J Med 364: 1897–1908.
9. Nguyen QD, Brown DM, Marcus DM, Boyer DS, Patel S, et al. Ranibizumab for Diabetic Macular Edema: Results from 2 Phase III Randomized Trials: RISE and RIDE. Ophthalmology.
10. Zachary I (2005) Neuroprotective role of vascular endothelial growth factor: signalling mechanisms, biological function, and therapeutic potential. Neurosignals 14: 207–221.
11. Arsham Sheybani M, Arghavan Almony, MD, Kevin J. Blinder M, Gaurav K Shah, MD (2010) Anti-VEGF Non-Responders In Neovascular AMD. Review of Ophthamology 17: 52–54.
12. Grossniklaus HE, Kang SJ, Berglin L (2010) Animal models of choroidal and retinal neovascularization. Prog Retin Eye Res 29: 500–519.
13. Heston WD (1997) Characterization and glutamyl preferring carboxypeptidase function of prostate specific membrane antigen: a novel folate hydrolase. Urology 49: 104–112.
14. Israeli RS, Powell CT, Fair WR, Heston WD (1993) Molecular cloning of a complementary DNA encoding a prostate-specific membrane antigen. Cancer Res 53: 227–230.
15. Pinto JT, Suffoletto BP, Berzin TM, Qiao CH, Lin S, et al. (1996) Prostate-specific membrane antigen: a novel folate hydrolase in human prostatic carcinoma cells. Clin Cancer Res 2: 1445–1451.
16. Murphy GP, Elgamal AA, Su SL, Bostwick DG, Holmes EH (1998) Current evaluation of the tissue localization and diagnostic utility of prostate specific membrane antigen. Cancer 83: 2259–2269.
17. Lapidus RG, Tiffany CW, Isaacs JT, Slusher BS (2000) Prostate-specific membrane antigen (PSMA) enzyme activity is elevated in prostate cancer cells. Prostate 45: 350–354.
18. Conway RE, Petrovic N, Li Z, Heston W, Wu D, et al. (2006) Prostate-specific membrane antigen regulates angiogenesis by modulating integrin signal transduction. Mol Cell Biol 26: 5310–5324.
19. Friedlander M, Theesfeld CL, Sugita M, Fruttiger M, Thomas MA, et al. (1996) Involvement of integrins alpha v beta 3 and alpha v beta 5 in ocular neovascular diseases. Proceedings of the National Academy of Sciences 93: 9764–9769.
20. Carter RE, Feldman AR, Coyle JT (1996) Prostate-specific membrane antigen is a hydrolase with substrate and pharmacologic characteristics of a neuropeptidase. Proceedings of the National Academy of Sciences 93: 749–753.
21. Sahagun G, Moore SA, Fabry Z, Schelper RL, Hart MN (1989) Purification of murine endothelial cell cultures by flow cytometry using fluorescein-labeled griffonia simplicifolia agglutinin. Am J Pathol 134: 1227–1232.
22. Moeller BJ, Cao Y, Li CY, Dewhirst MW (2004) Radiation activates HIF-1 to regulate vascular radiosensitivity in tumors: role of reoxygenation, free radicals, and stress granules. Cancer Cell 5: 429–441.
23. Hanahan D, Folkman J (1996) Patterns and emerging mechanisms of the angiogenic switch during tumorigenesis. Cell 86: 353–364.

24. Chang SS, Reuter VE, Heston WD, Bander NH, Grauer LS, et al. (1999) Five different anti-prostate-specific membrane antigen (PSMA) antibodies confirm PSMA expression in tumor-associated neovasculature. Cancer Res 59: 3192–3198.
25. Liu H, Moy P, Kim S, Xia Y, Rajasekaran A, et al. (1997) Monoclonal antibodies to the extracellular domain of prostate-specific membrane antigen also react with tumor vascular endothelium. Cancer Res 57: 3629–3634.
26. Grossniklaus HE, Kang SJ, Berglin L (2010) Animal models of choroidal and retinal neovascularization. Prog Retin Eye Res 29: 500–519.
27. Aguilar E, Dorrell MI, Friedlander D, Jacobson RA, Johnson A, et al. (2008) Chapter 6. Ocular models of angiogenesis. Methods Enzymol 444: 115–158.
28. Smith LE, Wesolowski E, McLellan A, Kostyk SK, D'Amato R, et al. (1994) Oxygen-induced retinopathy in the mouse. Invest Ophthalmol Vis Sci 35: 101–111.
29. Chung AS, Ferrara N (2011) Developmental and Pathological Angiogenesis. Annual Review of Cell and Developmental Biology 27: 563–584.
30. Fuxe J, Tabruyn S, Colton K, Zaid H, Adams A, et al. (2011) Pericyte requirement for anti-leak action of angiopoietin-1 and vascular remodeling in sustained inflammation. Am J Pathol 178: 2897–2909.
31. Carmeliet P, Moons L, Luttun A, Vincenti V, Compernolle V, et al. (2001) Synergism between vascular endothelial growth factor and placental growth factor contributes to angiogenesis and plasma extravasation in pathological conditions. Nat Med 7: 575–583.
32. Duncan GS, Andrew DP, Takimoto H, Kaufman SA, Yoshida H, et al. (1999) Genetic Evidence for Functional Redundancy of Platelet/Endothelial Cell Adhesion Molecule-1 (PECAM-1): CD31-Deficient Mice Reveal PECAM-1-Dependent and PECAM-1-Independent Functions. J Immunol 162: 3022–3030.
33. Marchio S, Lahdenranta J, Schlingemann RO, Valdembri D, Wesseling P, et al. (2004) Aminopeptidase A is a functional target in angiogenic blood vessels. Cancer Cell 5: 151–162.
34. Rangel R, Sun Y, Guzman-Rojas L, Ozawa MG, Sun J, et al. (2007) Impaired angiogenesis in aminopeptidase N-null mice. Proc Natl Acad Sci U S A 104: 4588–4593.
35. Stupack DG, Cheresh DA (2003) Apoptotic cues from the extracellular matrix: regulators of angiogenesis. Oncogene 22: 9022–9029.
36. Hynes RO (1999) Cell adhesion: old and new questions. Trends Cell Biol 9: M33–37.
37. Rizzo MT (2004) Focal adhesion kinase and angiogenesis. Where do we go from here? Cardiovasc Res 64: 377–378.
38. da Silva RG, Tavora B, Robinson SD, Reynolds LE, Szekeres C, et al. (2010) Endothelial α3β1-Integrin Represses Pathological Angiogenesis and Sustains Endothelial-VEGF. The American Journal of Pathology 177: 1534–1548.
39. Kamisasanuki T, Tokushige S, Terasaki H, Khai NC, Wang Y, et al. (2011) Targeting CD9 produces stimulus-independent antiangiogenic effects predominantly in activated endothelial cells during angiogenesis: A novel antiangiogenic therapy. Biochemical and Biophysical Research Communications 413: 128–135.
40. Wilkinson-Berka JL, Jones D, Taylor G, Jaworski K, Kelly DJ, et al. (2006) SB-267268, a Nonpeptidic Antagonist of αvβ3 and αvβ5 Integrins, Reduces Angiogenesis and VEGF Expression in a Mouse Model of Retinopathy of Prematurity. Investigative Ophthalmology & Visual Science 47: 1600–1605.
41. Reynolds LE, Wyder L, Lively JC, Taverna D, Robinson SD, et al. (2002) Enhanced pathological angiogenesis in mice lacking [beta] 3 integrin or [beta] 3 and [beta] 5 integrins. Nat Med 8: 27–34.
42. Parsons JT (2003) Focal adhesion kinase: the first ten years. J Cell Sci 116: 1409–1416.
43. Kornberg LJ, Shaw LC, Spoerri PE, Caballero S, Grant MB (2004) Focal adhesion kinase overexpression induces enhanced pathological retinal angiogenesis. Invest Ophthalmol Vis Sci 45: 4463–4469.
44. Sivakumar B, Harry LE, Paleolog EM (2004) Modulating angiogenesis: more vs less. JAMA 292: 972–977.
45. Kahook MY, Kimura AE, Wong LJ, Ammar DA, Maycotte MA, et al. (2009) Sustained elevation in intraocular pressure associated with intravitreal bevacizumab injections. Ophthalmic Surgery Lasers and Imaging 40: 293–295.
46. E. Jason Sabet-Peyman MFMAH, MD; Jennifer E Thorne, MD, PhD; Heather Casparis, MD; Sayjal J Patel, MD; Diana V Do, MD (2009) Progression of Macular Ischemia Following Intravitreal Bevacizumab. Ophthalmic Surgery, Lasers & Imaging 40: 316–318.
47. Rojas C, Frazier ST, Flanary J, Slusher BS (2002) Kinetics and inhibition of glutamate carboxypeptidase II using a microplate assay. Anal Biochem 310: 50–54.
48. Mesters JR, Barinka C, Li W, Tsukamoto T, Majer P, et al. (2006) Structure of glutamate carboxypeptidase II, a drug target in neuronal damage and prostate cancer. EMBO J 25: 1375–1384.
49. Zhou J, Neale JH, Pomper MG, Kozikowski AP (2005) NAAG peptidase inhibitors and their potential for diagnosis and therapy. Nat Rev Drug Discov 4: 1015–1026.
50. Tsukamoto T, Wozniak KM, Slusher BS (2007) Progress in the discovery and development of glutamate carboxypeptidase II inhibitors. Drug Discovery Today 12: 767–776.
51. Van Der Post JP, De Visser SJ, De Kam ML, Woelfler M, Hilt DC, et al. (2005) The central nervous system effects, pharmacokinetics and safety of the NAALADase-inhibitor GPI 5693. British Journal of Clinical Pharmacology 60: 128–136.
52. Rojas C, Stathis M, Polydefkis M, Rudek MA, Zhao M, et al. (2011) Glutamate carboxypeptidase activity in human skin biopsies as a pharmacodynamic marker for clinical studies. J Transl Med 9: 27.